

THE UNIVERSITY OF MICHIGAN

COLLEGE OF ENGINEERING

DEPARTMENT OF NUCLEAR ENGINEERING
LABORATORY FOR FLUID FLOW AND HEAT TRANSPORT PHENOMENA

Technical Report No. 14

Cavitation Damage Correlations for Various Fluid-Material Combinations

FREDERICK G. HAMMITT
M. JOHN ROBINSON
CLARENCE A. SIEBERT
FAZIL A. AYDINMAKINE

GPO PRICE \$ _____
OTS PRICE(S) \$ _____
Hard copy (HC) \$4.00
Microfiche (MF) 0.25

Under contract with:

National Aeronautics and Space Administration
Grant No. NsG-39-60
Washington, D. C.

FACILITY FORM 602

Accession Number: N65 129413
(NASA CR OR TMX OR AD NUMBER) 114
(CATEGORY) 12
(THRU)
(CODE)

Administered through:

October, 1964

OFFICE OF RESEARCH ADMINISTRATION • ANN ARBOR

THE UNIVERSITY OF MICHIGAN

COLLEGE OF ENGINEERING
Department of Nuclear Engineering
Laboratory for Fluid Flow and Heat Transport Phenomena

Technical Report No. 14

CAVITATION DAMAGE CORRELATIONS FOR VARIOUS FLUID-
MATERIAL COMBINATIONS

Frederick G. Hammitt
M. John Robinson
Clarence A. Siebert
Fazil A. Aydinmakine

ORA Project 03424

Under Contract with:

National Aeronautics and Space Administration
Grant No. NsG-39-60
Washington 25, D.C.

Office of Research Administration
Ann Arbor

October, 1964

ACKNOWLEDGMENTS

The authors would like to acknowledge the assistance of the following faculty and research personnel of The University of Michigan: Messrs. D. Sundberg, R. Haupt, E. D. Shippey, Prof. R. D. Pehlke, Y. A. Sozusen, R. A. Schaedel, J. Hoo, D. M. Ericson, Jr., and H. G. Olson.

ABSTRACT

12412
Cavitation damage tests on a variety of materials in water and mercury have been carried out during this reporting period. Although the data is not complete at this stage of the tests, this report summarizes the quantitative data available to date, and various significant conclusions are reached.

Cavitation damage data on stainless steel, refractory materials, carbon steel, aluminum, plexiglas, and a series of copper and nickel alloys of varying heat-treats, is presented. An attempt to correlate this data with material properties, degree of cavitation, and velocity effects shows that a single material property is not sufficient. Rather, a suitable grouping of material properties remains to be determined. Velocity effects are shown and explained in relation to changes in local flow conditions. Pressure profiles for the various cavitation conditions, including three pressure tap locations on the surface of the test specimens, are also shown and related to the damage.

A more comprehensive report will be issued at a later date after the presently envisioned test program has been completed.

Auth

TABLE OF CONTENTS

	Page
ACKNOWLEDGMENTS	ii
ABSTRACT	iii
LIST OF TABLES	v
LIST OF FIGURES	vi
1.0 INTRODUCTION	1
2.0 EXPERIMENTAL ARRANGEMENTS	2
2.1 Venturis and Specimens	2
2.2 Fluid Conditions	7
3.0 EXPERIMENTAL DATA	8
3.1 Measurements and Data Reduction	8
3.1.1 Quantities Measured	
3.1.2 Numerical Data Reduction	
3.2 Materials Tested	10
3.3 Flow Conditions	11
3.4 Experimental Results	17
3.4.1 Summarization of Numerical Data	
3.4.2 Mean Depth of Penetration vs. Duration	
3.4.3 Mean Depth of Penetration Rate vs. Time	
3.4.4 "Wet" vs. "Dry" and "Hot" vs. "Cold" Mercury	
3.4.5 Flow Pattern Changes (Pin-Type Specimen Tests)	
4.0 NORMALIZED DAMAGE RESULTS	48
4.1 Numerical Procedures	48
4.2 Material Effects	49
4.2.1 General Expectations	
4.2.2 Copper and Nickel Series	
4.3 Velocity Effects	59
4.3.1 General Anticipation	
4.3.2 Experimental Results	
4.4 Degree of Cavitation Effects	81
4.4.1 General Anticipation	
4.4.2 Experimental Results	
5.0 CONCLUSIONS	97
6.0 APPENDIX	102

LIST OF TABLES

Table	Page
1. Mechanical Properties of Materials Used	12
2. Mean Depth of Penetration for Specimens at Selected Durations for Mercury	18
3. Mean Depth of Penetration for Specimens at Selected Durations for Water	21
4. Consolidated Data for Mean Depth of Penetration for Mercury	26
5. Consolidated Data for Mean Depth of Penetration for Water	27
6. Surface Tension and Viscosity for Mercury	43
7. Actual Pressure Above Vapor Pressure on Test Specimen Surface For Standard Cavitation in Mercury and Water	77

LIST OF FIGURES

Figure	Page
1. Drawing of 2-Specimen Damage Venturi	3
2. Specimen Holder and Specimen Assembly	4
3. Drawing of Damage Specimen	5
4. Photograph of Damage Specimen	5
5. Drawing of Tubular Test Specimen (pin)	6
6. Typical Mean Depth of Penetration versus Duration Curves for Mercury	29
7. Typical Mean Depth of Penetration versus Duration Curves for Water	31
8. (a) Front Side, Polished Surface, and Back of Specimen 47-3, (b) Front Side, Polished Surface, and Back of Specimen 48-3, Cavitated in Mercury at 34 Ft./Sec., Standard Cavitation, for a Duration of 800 Hours	33
9. Metallographic Cross-Section through Stainless Steel Pin Specimen Wall, (a) Magnification 50X, (b) Magnification 100X, Marbles Etch	46
10. Photomicrographs of OHFC Copper Grain Structure at 100X, (a) As Received, (b) Recrystallized at 900°F, Small Grain Size, (c) Recrystallized at 1500°F, Large Grain Size	52
11. $(MDP_{ss})/(MDP)$ versus Strain Energy to Failure for Various Combinations of Materials, Cavitation Conditions and Velocities in Mercury and Water	57
12. $(MDP_{ss})/(MDP)$ versus Tensile Strength for Various Combina- tions of Materials, Cavitation Conditions and Velocities in Mercury and Water	58
13. Normalized Pressure Profile for Visible Initiation, 3 Specimens in Mercury at Various Velocities	62
14. Normalized Pressure Profile for Standard Cavitation, 3 Specimens in Mercury at Various Velocities	63
15. Normalized Pressure Profile for Velocity of 22.9 ft./sec., in Mercury, 3 Specimens, at Various Cavitation Conditions	64

LIST OF FIGURES (cont.)

Figure		Page
16.	Normalized Pressure Profile for Velocity of 33.1 ft./sec., 3 Specimens, in Mercury, at Various Cavitation Conditions	65
17.	Normalized Pressure Profile for Visible Initiation, 3 Specimens, in Water, at Various Velocities	66
18.	Normalized Pressure Profile for Cavitation to Nose, 3 Specimens, in Water, at Various Velocities	67
19.	Normalized Pressure Profile for Standard Cavitation, 3 Specimens, in Water, at Various Velocities	68
20.	Normalized Pressure Profile for 64.5 ft./sec., 3 Specimens, in Water, at Various Cavitation Conditions	69
21.	Normalized Pressure Profile for 96.4 ft./sec., 3 Specimens, in Water, at Various Cavitation Conditions	70
22.	Normalized Pressure Profile for 199.5 ft./sec., 3 Specimens, in Water, at Various Cavitation Conditions	71
23.	Drawing of Plexiglas Holder-Specimen Combination for Measuring Pressures on the Specimen Face	72
24.	$(MDP)/(MDP_{max})$ versus Velocity for Standard Cavitation in Water for Copper and Brasses	75
25.	$(MDP)/(MDP_{max})$ versus Velocity for Standard Cavitation in Water for Stainless and Carbon Steel	76
26.	$(MDP)/(MDP_{max})$ versus Velocity for Standard and Back Cavi- tation in Mercury for Stainless Steel and Columbium-1% Zirconium	80
27.	$(MDP)/(MDP_{max})$ versus Velocity for Visible and Nose Cavi- tation in Mercury for Stainless and Carbon Steel	82
28.	Hypothesized Bubble Energy Spectra for Various Cavitation Conditions at a Constant Velocity for a Given Material	84
29.	$(MDP)/MDP_{max}$ versus Cavitation Condition for Various Materials in Mercury and Water	85
30.	Normalized Pressure Profile for Velocity of 64.5 ft./sec., for Standard Cavitation in Water, 1, 2 and 3 Specimens	87

LIST OF FIGURES (cont.)

Figure		Page
31.	Normalized Pressure Profile for Velocity of 96.4 ft./sec., for Standard Cavitation in Water, 1, 2 and 3 Specimens	88
32.	Normalized Pressure Profile for Velocity of 199.5 ft./sec., for Standard Cavitation in Water, 1, 2 and 3 Specimens	89
33.	Normalized Pressure Profile for Velocity of 22.9 ft./sec., for Visible Initiation in Mercury, 1, 2 and 3 Specimens	91
34.	Normalized Pressure Profile for Velocity of 33.1 ft./sec., for Visible Initiation in Mercury, 1, 2 and 3 Specimens	92
35.	Normalized Pressure Profile for Velocity of 22.9 ft./sec., for Standard Cavitation in Mercury, 1, 2 and 3 Specimens	93
36.	Normalized Pressure Profile for Velocity of 33.1 ft./sec., for Standard Cavitation in Mercury, 1, 2 and 3 Specimens	94

1.0 INTRODUCTION

This report covers some aspects of the continuing investigation of cavitation damage induced by mercury and water flowing in cavitating venturis, at The University of Michigan. Although the investigation is not complete, some of the points from the presently available data seem sufficiently significant to justify an interim report of this nature.

More comprehensive data, considering those aspects covered in the present report, as well as others, will be reported at a later date.

2.0 EXPERIMENTAL ARRANGEMENTS

2.1 Venturis and Specimens

The data has been taken in The University of Michigan mercury and water cavitating venturi facilities described in previous papers.^{1, 2, etc.} The basic venturi design used is shown in Figure 1. However, this has appeared in two versions: that shown in Figure 1 which provides space for two plate-type test specimens with an angle of separation of 90° ; and a second version (used only in the water loop) which holds three plate-type specimens, located symmetrically with 120° separation. The venturi flow-paths are identical except for the test specimens.

The plate-type specimens used, aligned to the flow, are shown in Figures 2, 3, and 4, with their holders. While the great majority of the tests have utilized this type of specimen, some tests have been conducted with 1/4" diameter pin-type specimen held with its axis normal to the flow at the same axial location as the plate-type specimens. Figure 5 is a drawing of a specimen of this type. While the plate-type specimens and specimen holders are contoured to match the venturi wall profile, it will be noted that the shoulders on the pin are not so contoured so that a slight discontinuity with the venturi wall exists at this point.

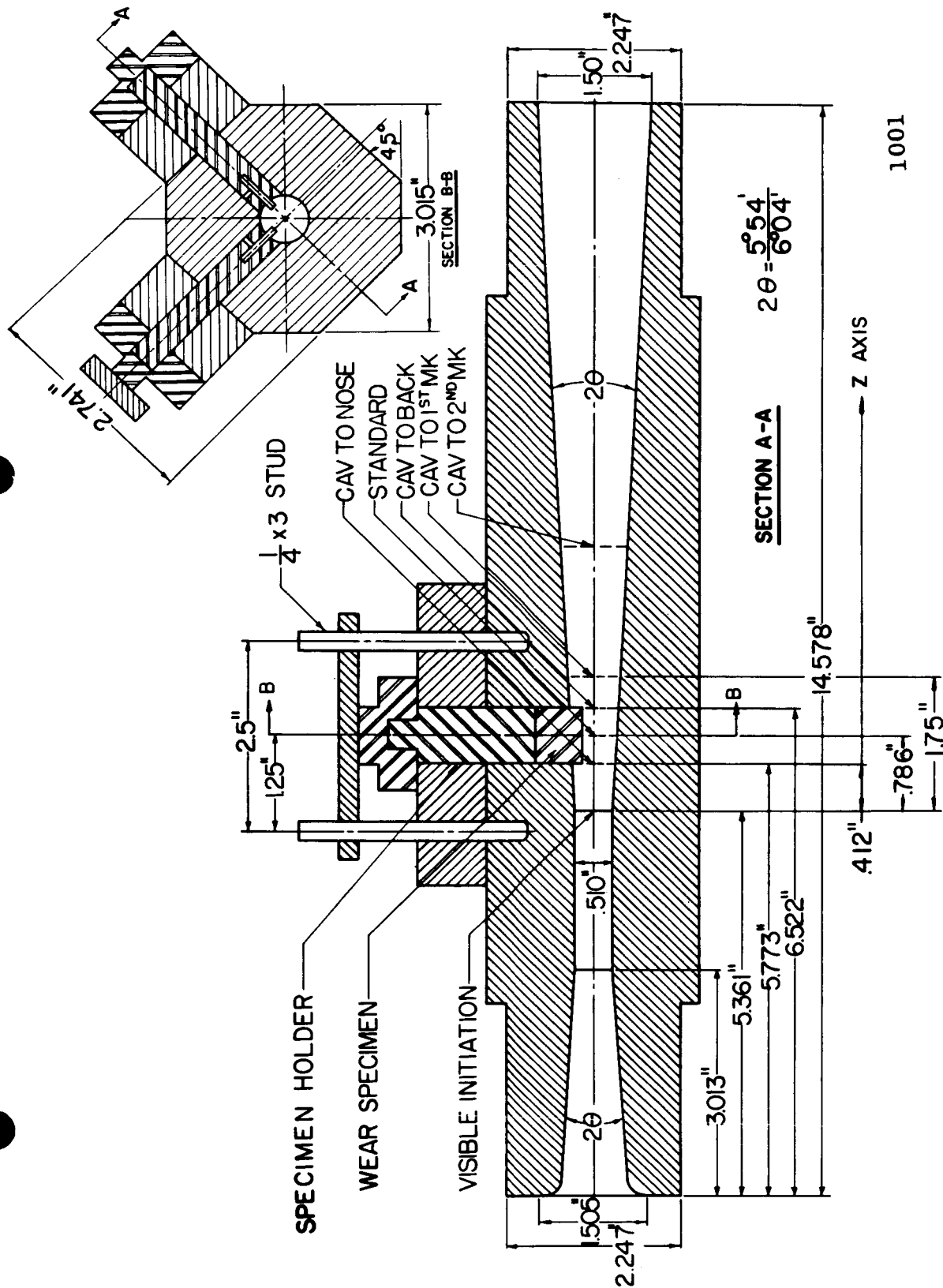


Figure 1. Drawing of the Damage Test Venturi Showing Location of Specimens, Specimen Holders and Cavitation Termination Points.

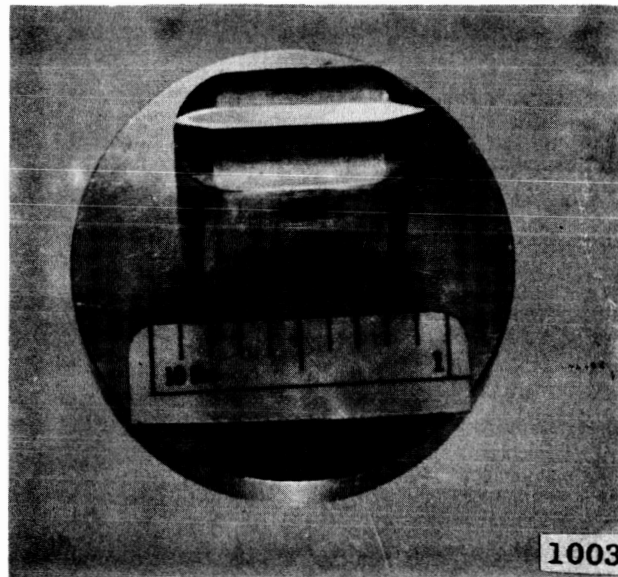


Figure 2. Photograph of Specimen Holder With Test Specimen in Place.

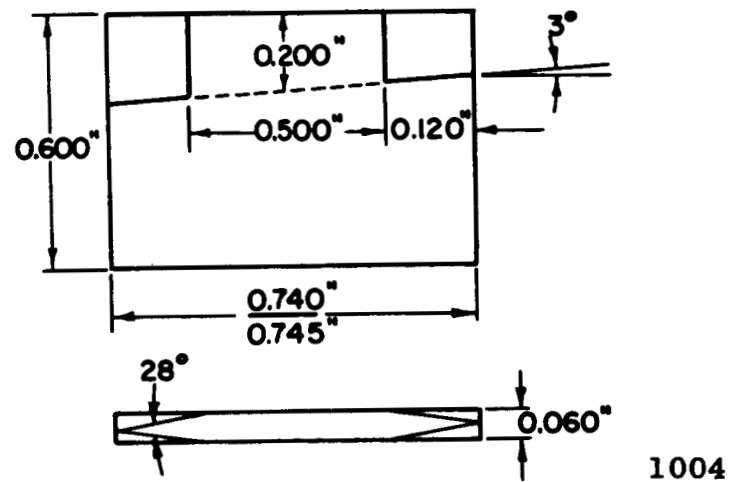
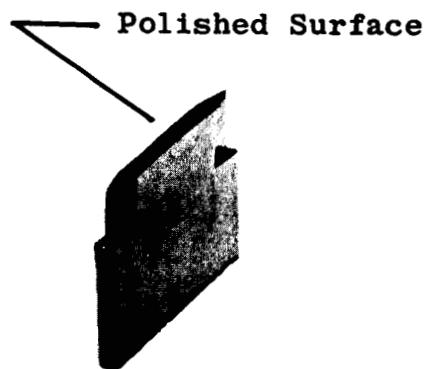


Fig. 3. Drawing of Damage Specimen.



1005

Fig. 4. Photograph of Damage Specimen.

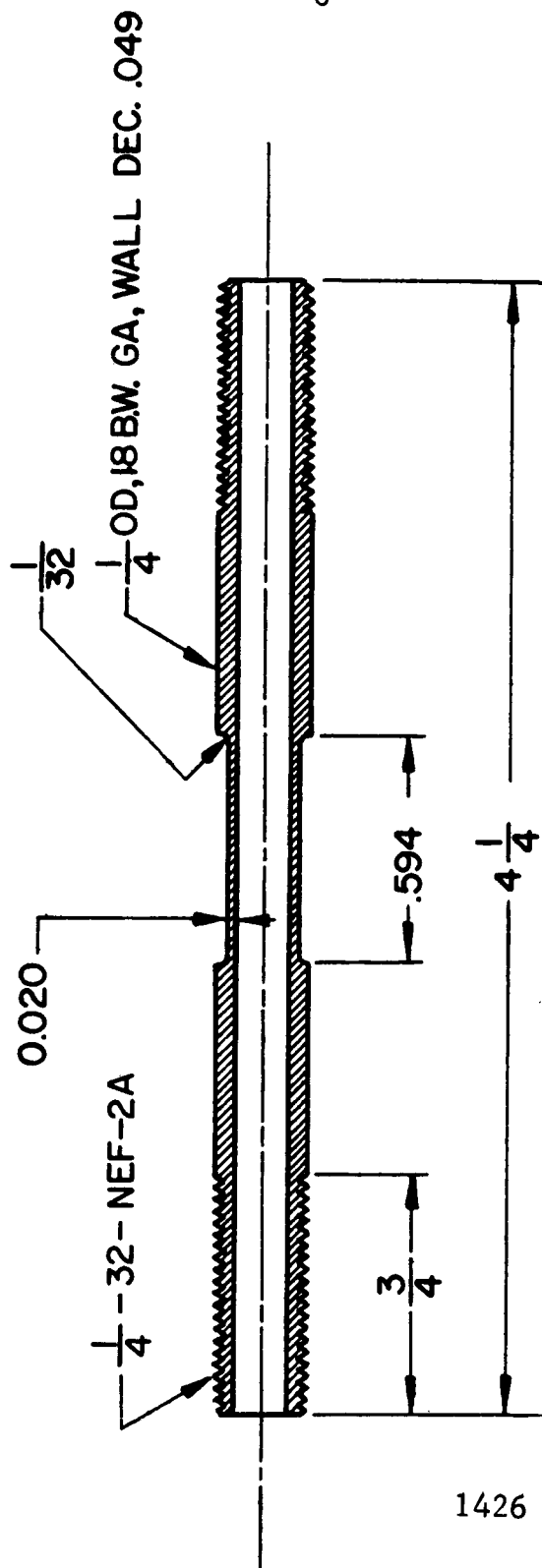


Fig. 5. Drawing of Tubular Test Specimen (pin).

2.2 Fluid Conditions

The fluids used to the present have been water and mercury. In substantially all cases the water has been at approximately room temperature, and with air content near saturation for STP. The solid impurity content of the water is about that of tap water (about 200 ppm in the present case) and the pH about 9.7.

The mercury temperature has also been approximately ambient for almost all the runs, although a single 50 hour run at 500° has been completed. In most of the runs it has been found that trace contents of water and air were entrained. Measurements have shown that the quantity of water for these runs is on the order of 0.5 to 1.0% by volume. However, a single run with "dry"* mercury at room temperature of 400 hours to the present is available, and the mercury as used in the high temperature run was "dry." As explained later the "dry" mercury has been found to be much less damaging than the "wet." This rather unexpected result emphasized the sensitivity of damage to apparently minor effects, and also the necessity of obtaining accurate information in a cavitation damage experiment on the fluid purity.

* Measurements indicate that the water content of "dry" mercury as used herein is less than 15 ppm, and the gas content 0.2 to 0.5 ppm of air.

3.0 EXPERIMENTAL DATA

3.1 Measurements and Data Reduction

3.1.1 Quantities Measured

For all damage runs, the following quantities have been observed and recorded.³

- i) Weight loss
- ii) Pit tabulation according to number and size (four size categories)
- iii) Unusual pit formations recorded by photomicrographs. Composite photomicrograph (and sometimes "macros") of entire polished surface made in some cases. Metallographic cross-section pictures taken through damaged areas in some instances.

3.1.2 Numerical Data Reduction

The present report is concerned primarily with the numerical (quantitative) data. The qualitative pictorial aspects of the damage have been discussed at length in a previous report³ and paper to be presented.⁴ New information related to these subjects will be covered in future reports.

All the numerical damage data has been processed by an IBM 7090 program. The following items are listed in the numerical output:

- i) Specimen number and material,
- ii) Throat velocity and degree of cavitation,

- iii) Cumulative duration to time of specimen examination,
- iv) Number of pits in all size categories,
- v) Mean depth of penetration* as calculated from pit count,
- vi) Percent of area damaged (i.e., total pit surface area divided by total surface area), as calculated from pit count,
- vii) Mean depth of penetration rate from pit count,
- viii) As item (v), but calculated from measured weight loss and density,
- ix) As item (vi), but calculated from weight loss and density,
- x) As item (vii), but calculated from weight loss and density,
- xi) Measured weight loss.

In addition, the program has generated plots of mean depth of penetration, and its rate (i.e., time derivative), versus duration for all samples tested. Items (iv) through (vii) are not included in those cases where some portion of the polished surface has become too pitted to allow individual pits to be distinguished. This situation generally occurs rather early in the mercury tests where the damage is quite rapid, and only much later, if at all, in the water tests.

In general, the water tests are conducted to a cumulative duration of 100 hours, although longer and shorter durations have been used in some cases. For the mercury tests 50 hours has been standard for most cases, although some much longer and shorter durations have been used. The samples are inspected generally after the following cumulative durations: 1, 4, 7, 10, 20, 30, 40, 50, 75, and 100 hours, both in

*Based on weight loss, density, and total exposed area.

water and mercury. If the run is continued after 100 hours the interval for inspection generally remains at 25 hours up to several hundred hours, and then may be increased to 50 hours.

Since the venturi design used in the mercury facility has two specimen locations, pairs of specimens of a given material are run together. In the water facility, three locations are available in each venturi, and three venturis are operated together in parallel.² Hence, there are nine specimen locations available in a given run, i.e., at the same velocity and degree of cavitation, so that for each material and operating condition there are generally three hopefully identical specimens.

3.2 Materials Tested

The materials to be tested have been chosen in some cases because of their present technological importance and in others because of their range of physical and mechanical properties, desired to give the necessary scope and breadth to the investigation to assist in improving the understanding of the cavitation-erosion phenomena.

The materials tested to date in mercury are:

- i) Type 302 stainless steel (annealed)
- ii) 1010* carbon steel (annealed)
- iii) Plexiglas
- iv) Cb - 1% Zr alloy
- v) Ta - 10W
- vi) Ta - 8W - 2Hf

*Actual analysis shows 0.08% carbon.

whereas the materials tested to the present in water, and for which data is available, include all those tested in mercury, and in addition:

- i) Pure copper in three different heat-treats--cold-worked, high temperature anneal, and low temperature anneal,
- ii) 70/30 Brass in three different heat-treats as above,
- iii) Aluminum - type 6061-T6

The materials yet to be tested in water include:

- i) Copper-nickel alloy in three heat-treats as above,
- ii) Pure nickel in three heat-treats as above,
- iii) Three aluminum alloys including pure aluminum fully-annealed, and also two wrought alloys of differing mechanical properties.

The applicable mechanical properties of all the materials involved, as far as they are known to the present, are listed in Table 1. A program to measure certain required additional mechanical properties is continuing.

3.3 Flow Conditions

The flow conditions capable of variation are: geometry, degree of cavitation (extent of cavitating region), and throat velocity. All the damage tests to the present have been conducted in venturis with contour, as shown in Figure 1, and with nominal 1/2 inch throat diameter. As previously mentioned, the water venturis used in the present water facility have three specimen positions whereas those used in the mercury facility, only two. However, the earliest water tests, some of the data from which are included, were conducted in the present mercury

PHYSICAL PROPERTY DATA FOR MATERIALS RUN IN LABO

Material	Condition	Density (g/cm ³)	Tensile Strength (psi)	0.2% Yield Strength (psi)
Stainless Steel (3) 300 Series	As Received	7.85 ^a	95,200	37,000 ^b 44,000
Carbon Steel (1) 1010	As Received	7.85	50,000 ^b	30,000 ^b
Aluminum (2) 1100-0	Annealed	2.77	14,300 13,000 ^b	10,500 5,000 ^b
Aluminum (2) 2024-T3		2.77	70,300 70,000 ^b	56,000 50,000 ^b
Aluminum (2) 6061-T6	Age Hardened	2.77	45,000 45,000 ^b	41,000 40,000 ^b
Ta-10w (A)		17.655	88,100 ^d 80,900	84,300 ^d 72,790
Ta-8w-2Hf (B)		17.655	123,200 ^d 89,250	123,200 ^d 80,350
Columbium (C) -1% Zirconium	Annealed	8.72	29,300 ^d	14,600 ^d
Columbium-1% Zirconium(C)	20% Cold-Worked	8.72		
Molybdenum- 1/2% Titanium(E)		10.215	94,700 ^d	89,600 ^d
Tenelon (F)		7.810	131,750	82,000
Titanium (G)		4.52	117,300	102,000
Plexiglas (P)		1.23	10,445 ^b	1,600 ^b
70/30 Brass (cz)	60% C.W.(As Rec'd.)	8.610	93,850	82,000
70/30 Brass	850°F. Anneal.* Small Grain Size	8.617	47,550	20,000

E 1

RATORY FOR FLUID FLOW AND HEAT TRANSFER PHENOMENA

% Elong. in 2 in.	% Red Area	Hardness	Strain Energy to Failure (lb-in/in ³)	Bending Fatigue Strength	Elastic Modulus
54.4	50.9	76 ^b Roc. B 140 BHN ^c 135 BHN(5)	44,750	35,000 ^b 10 ⁷ cycles	28 ^b x10 ⁶
40 ^b	71 ^b	48 ^b Roc. B 85 BHN ^c 91.5 BHN(5)		25,000 ^b 10 cycles	28 ^b x10 ⁶
36.3 35 ^b	89.3	23 BHN ^b	7,500	5,000 ^b	10 ^b x10 ⁶
21.3 18 ^b	35.1	120 BHN ^b	14,400	20,000 ^b	10 ^b x10 ⁶
19.0 12 ^b	48.1	95 BHN ^b	10,300	14,000 ^b	10 ^b x10 ⁶
20.6 ^d 21.0	69.1 ^d 63.3	93.1 R _B 163 BHN(5)	16,750	61,500 ^d	129x10 ⁶
10.9 ^d 22.0	63.0 ^d 59.55	175 BHN(5) 93.9 R _B	20,800		129x10 ⁶
42.5 ^d	92.8 ^d	90-120 BHN ^d	6,000 ^b	21,000 ^d	12x10 ⁶
			2,910 ^e		12x10 ⁶
30.7 ^d	54.7 ^d			73,200 ^s	
44.2	46.6	262 BHN(3)	54,500		28x10 ⁶
15.5	32.6	328 BHN(3)	16,170		
4.0 ^b			320 ^e		4 ^b x10 ⁵
5.32	40.7	168 BHN(5)	4,700		16 x10 ⁶
62.6	60.9	65 BHN(5)	28,750		16 x10 ⁶

TABLE 1--

Material	Condition	Density (g/cm ³)	Tensile Strength (psi)	0.2% Yield Strength (psi)
70/30 Brass	1400°F. Anneal.* Large Grain Size	8.622	40,390	11,000
OFHC Copper ^(cu)	60% C.W. (As Rec'd)	8.974	53,400	49,500
OFHC Copper	900°F. Anneal.* Small Grain Size	9.043	31,500	9,500
OFHC Copper	1500°F. Anneal.* Large Grain Size	9.057	30,650	5,000
70/30 Copper -Nickel (cn)	60% C.W. (As Rec'd)	9.046	87,285	77,000
70/30 Copper -Nickel	1300°F. Anneal.* Small Grain Size	9.051	57,900	20,000
70/30 Copper -Nickel	1800°F. Anneal.* Large Grain Size	9.024	53,300	18,000
Pure Nickel(ni)	75% C.W. (As Rec'd)	8.973	93,100	82,000
Pure Nickel	1100°F. Anneal.* Small Grain Size	8.999	50,470	13,000
Pure Nickel	1600°F. Anneal.* Large Grain Size	9.001	48,700	7,000

^aUnless otherwise noted the values in this table have been meas-

^bTypical Handbook values.

^cConverted Value.

^dPersonal communication from G. M. Wood, Pratt & Whitney Air-

^eCalculated from handbook data by C. A. Siebert, University of

BHN(5)--equivalent to BHN-500 kg

BHN(3)--equivalent to BHN-300 kg

* 1 hour duration at this temperature.

(Continued)

% Elong. in 2 in.	% Red Area	Hardness	Strain Energy to Failure	Bending Fatigue Strength	Elastic Modulus
58.9	51.7	67.4 R_H	15,250		16 $\times 10^6$
6.17	19.8	104 BHN(5) 58.6 R_B	3,125		17 $\times 10^6$
51.3	48.5	71.2 R_H 28.3 R_B	13,900		17 $\times 10^6$
32.5	33.2	55.7 R_H 6.4 R_E	6,080		17 $\times 10^6$
4.5	15.4	162 BHN(5)	3,060		22 $\times 10^6$
34.9	43.5	76 BHN(5)	16,300		22 $\times 10^6$
34.4	34.4	56 BHN(5)	13,750		22 $\times 10^6$
3.9	10.2	173 BHN(5)	3,200		30 $\times 10^6$
43.8	51.6	55 BHN(5)	18,300		30 $\times 10^6$
41.8	49.7	80.3 R_H	16,125		30 $\times 10^6$

ured in this laboratory.

craft Company.

Michigan.

facility using a two-specimen venturi. Static pressure profiles, measured along the venturi wall and along the polished face of a specially instrumented damage specimen,¹² indicate that the change in channel-blockage caused by the addition of a third damage specimen alters the flow significantly. This difference has also been noted from visual observation of the cavitating region, so that although the same names are used to describe the cavitation conditions in the two types of venturis, their significance in terms of pressure profiles and visual appearance is different. This situation is described in greater detail in the section discussing the normalized damage results, where typical pressure profiles are included. The definitions of the cavitation conditions (degrees of cavitation) for both types of venturi are listed in the Appendix.

Aside from the number of test specimens, the geometry for all tests using the plate-type specimens has been the same. For the few tests using a pin-type specimen, there is the obviously substantial change in flow pattern due to that type of obstruction. This will be described in greater detail in a later section.

The final flow variable is the throat velocity. In the mercury tests this has been varied over the approximate range between 24 and 64 ft./sec. The lower limit is set by the requirement, dictated by facility design,² of a minimum pressure recovery in the venturi diffuser of about one atmosphere. The upper limit is set by available pump head.

In the water facility the velocity range is from about 64 to 200 ft./sec. Again, the lower limit is set by minimum required pressure recovery in the diffuser, and the upper limit by available pump head and

pressure capability of the equipment. Thus there is a slight overlap in velocity between the mercury and water tests.

3.4 Experimental Results

3.4.1 Summarization of Numerical Data

The full detailed tabulated IBM results, to the present, previously described, are not included herein. However, they are available and will be eventually included in a report when the full test program as presently envisioned is completed. All specimens are listed in Tables 2 and 3 for mercury and water respectively, showing the mean depths of penetration at 50 and 100 hours, and for selected longer durations when available. In addition, an approximate sketch of the mean depth of penetration rate versus duration curves (taken from the IBM-generated curves) are included to show the general trends. The amplitudes shown on these curves are approximately to scale for a given curve, but no scaling of amplitudes between curves has been attempted. The numerical data is averaged and consolidated for each material in Tables 4 and 5.

3.4.2 Mean Depth of Penetration vs. Duration

a. Mercury Tests

The mean depth of penetration for all the "Standard Cavitation" mercury tests to date are plotted in Figure 6 as a function of test duration. Each curve represents averaged data from the two specimens run together. As noted, the longest duration achieved to date is 800 hours. There are single runs at 300 and 250 hours also, but the majority are in the 50 to 100 hour range. The total of the specimen hours represented

TABLE 2

MEAN DEPTH OF PENETRATION FOR SPECIMENS AT
SELECTED DURATIONS FOR MERCURY

Spec. No.	Mat'l.	Hg Cond.	Vel. ft/ sec	Cav. Cond.	MDP After X Hours					Sketch Of Rate Curve
					50	100	200	500	800	
1-3	SS	Cold -Wet	24	Std.	55	70	145			
2-3	"	"	"	"	65	85	180			
11-3	"	"	34	Zero	0					
12-3	"	"	"	"	0					
53-3	"	"	"	"	0(10 hr)					
55-3	"	"	"	"	0(10 hr)					
49-3	"	"	"	Vis.	3	6				
50-3	"	"	"	"	2	3.5				
84-3	"	"	"	"	3.5(25 hr)					
99-3	"	"	"	"	0.5(25 hr)					
63-3	"	"	"	Nose	4	5				
64-3	"	"	"	"	6	6				
107-3	"	"	"	"	0.4(25 hr)					
113-3	"	"	"	"	3 (25 hr)					
64-1	CS	"	"	"	130	300				
65-1	"	"	"	"	80	280				
22	CbZr	"	"	"	42					
23	"	"	"	"	67					
6-3	SS	"	"	Std.	55					
7-3	"	"	"	"	55					
47-3	"	"	"	"	40	100	130	650	730	
48-3	"	"	"	"	60	150	180	530	600	
71-3	"	"	"	"	17(10 hr)					
78-3	"	"	"	"	78					
112-3	"	"	"	"	47					
81-3	"	"	"	"	36					
82-3	"	"	"	"	47					
87-3	"	Dry- Cold	"	"	3.0					No data

TABLE 2--(Continued)












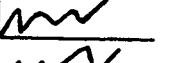
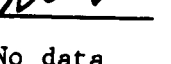

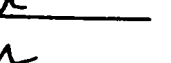
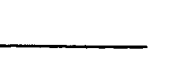
Spec. No.	Mat'l.	Hg Cond.	Vel. ft/ sec.	Cav. Cond.	MDP After X Hours					Sketch Of Rate Curve
					50	100	200	500	800	
102-3	SS	Dry- Cold	34	Std.	2.8					No data
89-3	"	500°F	"	"	24.5					"
90-3	"	500°F	"	"	24.5					"
114-3	"	Cold -Dry	"	"	4.7	8.0	11.5	12.0		Insuffi- cient Data
118-3	"	"	"	"	4.7	5.5	7.3	8.7		"
61-1	C/S	Wet- Cold	"	"	160	195				
68-1	"	"	"	"	140	215				
69-1	"	?	"	"	77					No data
70-1	"	?	"	"	47					"
3	Plex.	Wet- Cold	"	"	270 (7 hr)					
4	"	"	"	"	400 (7 hr)	500 (10 hr)	2100 (25 hr)			
5	"	"	"	"	200 (7 hr)	450 (10 hr)	2400 (25 hr)			
1	CBZR C.W.	"	"	"	330	760				
8	CBZR Annealed	"	"	"	100	520				
5	CBZR Annealed	"	"	"	100	200				
6	CBZR Annealed	"	"	"	120	290				
4	A	"	"	"	35	90				
5	"	"	"	"	26	68				
4	B	"	"	"	35	83				
5	"	"	"	"	27	49				
66-3	SS	"	"	Back	20	66				No data
67-3	"	"	"	"	40	125				
115-3	"	"	"	"	3.7 (10 hr)					
116-3	"	"	"	"	1.3 (10 hr)					

TABLE 2--(Continued)



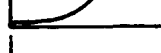
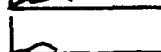


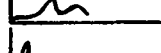



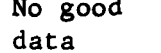
Spec. No.	Mat'l.	Hg Cond.	Vel. ft/ sec.	Cav. Cond.	MDP After X Hours					Sketch Of Rate Curve
					50	100	200	500	800	
69-3	SS	Wet- Cold	34	1st M	0(4 hr)					No data
70-3	"	"	"	"	0(4 hr)					"
71-1	C/S	"	48	Nose	420					
11	CBZR	"	"	"	15	22				
20	"	"	"	"	115					
14	"	"	"	Std.	320					
25	"	"	"	"	84					
60-3	SS	"	64	Zero	0(1.0 hr)					
62-3	"	"	"	"	0(1.0 hr)					
43-3	"	"	"	Vis.	3.0					
54-3	"	"	"	"	3.5					
56-3	"	"	"	Nose	15	26				
57-3	"	"	"	"	15	22				
51-3	"	"	"	Std.	9.4	7.6				
52-3	"	"	"	"	110	160	374	786(300 hr)		
58-3	"	"	"	Back	13	13	106	602(300 hr)		No good data
59-3	"	"	"	"	4					"

TABLE 3

MEAN DEPTH OF PENETRATION FOR SPECIMENS AT
SELECTED DURATIONS FOR WATER

Spec. No.	Mat'l.	Heat Treat	Vel. ft/sec	Cav. Cond.	MDP After X Hours			Rate Curve
					50	100	200	
4-3	SS	As Recd.	65	Std.	.35	.60	2.6	Typical*
5-3	"	"	"	"	.35	.80	1.8	"
9-3	"	"	"	"	1.7	2.3		"
10-3	"	"	"	"	.9	0	0	
14-3	"	"	"	"	3.2	4.0	7.0	"
15-3	"	"	"	"	2.0	2.0	5.0	"
17-1	CS	"	"	"	17.0	30.0	48.0	Typical except 30 hr incubation. 10 hr incu- bation.
19-1	"	"	"	"	23.0	35.0	65.0	
31-1	"	"	"	"	30.0	35.0	70.0	
16	cz	"	"	"	13.0	14(75 Hr)		"
17	"	"	"	"	9.0	12(75 Hr)		"
18	"	"	"	"	4.0	9(75 Hr)		"
88	"	Low- Small Grain	"	"	4.8	5.0(75 Hr)		"
89	"		"	"	4.8	5.0(75 Hr)		"
90	"		"	"	3.5	5.8(75 Hr)		"
238	"	High- Large Grain	"	"	8.5	10.5(75 Hr)		"
239	"		"	"	6.5	9.5(75 Hr)		"
240	"		"	"	9.0	12.0(75 Hr)		"
1	cu	As Recd.	"	"	13.0			"
2	"	"	"	"	9.5			"
3	"	"	"	"	10.0			"
76	"	Low- Small Grain	"	"	19			"
77	"		"	"	10			"
78	"		"	"	5.5			"
151	"	High- Large Grain	"	"	7.0			"
152	"		"	"	4.5			"
153	"		"	"	15.0			

TABLE 3--(Continued)

Spec. No.	Mat'l.	Heat Treat	Vel. ft/sec	Cav. Cond.	MDP After X Hours			Rate Curve
					50	100	200	
12-3	SS		97	Std.	7.0	7.5	10.0	Typical
23-3	"		"	"	1.0	1.5	4.0	None given
46-3	"		"	"	22	22	30	Typical
14-1	C/S		"	"	80	110	150	Double Early Max.
18-1	"		"	"	80	100	130	Some Incuba.
22-1	"		"	"	100	125	145	" "
85	cz	Low-	"	"	4.5			" "
86	"	Small	"	"	4.0			Typical
87	"	Grain	"	"	5.0			"
235	"	"	"	"	6.7			"
236	"	High-	"	"	8.5			"
237	"	Large	"	"	8.5			"
4	cu	Grain	"	"	8.5			"
5	"	As Recd.	"	"	10**			"
6	"	"	"	"	7.5			"
79	"	"	"	"	12.0			"
80	"	Small	"	"	12			"
81	"	Grain	"	"	10			"
154	"	"	"	"	9			"
155	"	Large	"	"	6.5			None
156	"	Grain	"	"	11.0			Typical
2-2	Al	"	"	"	10.0			"
8-2	"		"	"	65	70	85	Typical- Some Incub.
9-2	"		"	"	50	60	75	"
13	cz	As Recd.	"	"	60	70	85	"
14	"	"	"	"	18	22		"
15	"	"	"	"	12	15		"
72-3	SS		200	"	11	14		"
73-3	"		"	"	2.0	3.0		None
108-3	"		"	"	3.0	4.5		Typical
					1.5	2.5		"

TABLE 3--(Continued)

Spec. No.	Mat'l.	Heat Treat	Vel. ft/sec	Cav. Cond.	MDP After X Hours			Rate Curve
					50	100	200	
45-1	CS		200	Std.	400	900		Typical-Incu. for 30 hrs.
63-1	"		"	"	400	900		
66-1	"		"	"	400	750		
1	cz	As Recd.	"	"	45	50		Big jump at 40 hrs.
2	"	"	"	"	45	50		
3	"	"	"	"	30	55		
4	"	"	"	"	32	38		Typical
5	"	"	"	"	38	42		"
6	"	"	"	"	30	35		"
76	"	Low-	"	"	27	31		"
77	"	Small	"	"	28	33		"
78	"	Grains	"	"	22	28		"
226	"	High-	"	"	25	29		"
227	"	Large	"	"	23	28		"
228	"	Grains	"	"	28	42		"
7	cu	As Recd.	"	"	30			"
8	"	"	"	"	24			"
9	"	"	"	"	18			"
82	"	Low-	"	"	18			"
83	"	Small	"	"	27			"
84	"	Grains	"	"	25			"
157	"	High-	"	"	22			"
158	"	Large	"	"	20			"
159	"	Grains	"	"	39			"
1	Alloy		"	"	6.0	6.5***		"
2	A		"	"	4.0	4.7		"
3	"		"	"	23.	23.		"
1	Alloy		"	"	3.6	4.5		"
2	B		"	"	7.0	9.0		"
3	"		"	"	8.0	11.0		"

TABLE 3--(Continued)

Spec. No.	Mat'l.	Heat Treat	Vel. ft/sec	Cav. Cond.	MDP After X Hours			Rate Curve
					50	100	200	
15	CBZR	Annealed	200	Std.	8.5	9.0		Typical
17	"	"	"	"	11	14		"
21	"	"	"	"	41	49		Double Hump
7	cz	As Recd.	"	Nose	27	31		Typical
8	"	"	"	"	27	34		"
9	"	"	"	"	27	32		"
79	"	Low-	"	"	16	23		"
80	"	Small	"	"	18	23		"
81	"	Grains	"	"	14	17		"
229	"	"	"	"	16	22		"
230	"	High-	"	"	16	22		"
231	"	Large	"	"	16	19		"
10	cu	Grains	"	"	32			Double Hump
11	"	As Recd.	"	"	25			****
12	"	"	"	"	32			"
85	"	"	"	"	34			"
86	"	Low-	"	"	29			"
87	"	Small	"	"	37			"
160	"	Grains	"	"	30			"
161	"	"	"	"	21			Typical
162	"	High-	"	"	32			"
10	cz	Large	"	Vis.	10	15		"
11	"	Grains	"	"	18	22		"
12	"	"	"	"	18	22		"
82	"	"	"	"	8	11		Double Hump
83	"	Low-	"	"	9	11		****
84	"	Small	"	"	10	13		Typical
232	"	Grains	"	"	11	16		"
233	"	High-	"	"	12	15		"
234	"	Large	"	"	14	20		Double Hump
		Grains						****

TABLE 3--(Continued)

Spec. No.	Mat'l.	Heat Treat	Vel. ft/sec	Cav. Cond.	MDP After X Hours			Rate Curve
					50	100	200	
13	cu	As Recd.	200	Vis.	18			Typical
14	"	"	"	"	30			Double Hump *****
15	"	"	"	"	18			Typical
88	"	Low-	"	"	18			"
89	"	Small	"	"	12			"
90	"	Grains	"	"	11			"
163	"	"	"	"	16			"
164	"	High-	"	"	11			"
166	"	Large	"	"	13			"
		Grains	"	"				
		"	"	"				

*Means very early maximum and then decrease and no appreciable incubation period unless so stated.

**Extrapolated from 30 hours to 50 hours.

***Extrapolated from 75 hours to 100 hours.

*****Second hump nearly as big as first.

TABLE 4

CONSOLIDATED DATA FOR MEAN DEPTH OF PENETRATION FOR MERCURY

Specimen Numbers	Mat'l.	Hg Cond.	Vel. ft/sec	Cav. Cond.	MDP (Avg.)		
					50	100	200
1,2	SS	Wet-Cold	24	Std.	60.0	78.0	162.0
49,50,84,99	"	"	34	Vis.	2.5	4.8	
63,64,107,113	"	"	"	Nose	4.0	5.5	
11,12,53,55	"	"	"	Zero	0.0)	10	
64,65	CS	"	"	Nose	105.0	290.0	
22,23	CbZr(CW)	"	"	"	105.0		
6,7,47,48,71, 78,112,81,82	SS	"	"	Std.	52.0	125.0	155.0
47,48	"	"	"	"	590.0)	500	665.0)
87,102,114,118	"	Dry-Cold	"	"	3.8	6.8	9.4
89,90	"	Hot-Dry	"	"	24.5		
61,68	CS	Wet-Cold	"	"	150.0	205.0	
3,4,5	Plex.	"	"	"	290)	7	475)
1,8	CbZr(CW)	"	"	"	290.0	640.0	
5,6	CbZr(Anneal.)	"	"	"	110.0	245.0	
4,5	Ta-10W	"	"	"	26.0	79.0	
4,5	Ta-10W-2Hf	"	"	"	31.0	66.0	
66,67	SS	"	"	Back	30.0	96.0	
69,70	"	"	"	1st M.	0)	4	
71	CS	"	48	Nose	420.0		
11,20	CbZr	"	"	"	65.0		
14,25	"	"	"	Std.	202.0		
60,62	SS	"	64	Zero	0)	1	
43,54	"	"	"	Vis.	3.3		
56,57	"	"	"	Nose	15.0	24.0	
51,52	"	"	"	Std.	60.0	84.0	
58,59	"	"	"	Back	8.5		

TABLE 5

CONSOLIDATED DATA FOR MEAN DEPTH OF PENETRATION FOR WATER

Specimen Numbers	Mat'l.	Heat Treat	Vel. ft/sec	Cav. Cond.	MDP (avg.)		
					50	100	200
4,5,9,10, 14,15	SS	Annealed	65	Std.	1.4	1.6	2.7
17,19,31	CS	"	"	"	23.0	33.3	61.0
16,17,18	cz	As Rec'd.	"	"	8.7	11.7)	75
88,89,90	"	Sm.Grain	"	"	4.9	6.1)	75
238,239,240	"	Lg.Grain	"	"	8.0	10.7)	75
1,2,3	cu	As Rec'd.	"	"	11.0		
76,77,78	"	Sm.Grain	"	"	11.5		
151,152,153	"	Lg.Grain	"	"	9.0		
12,23,46	SS	Annealed	97	"	10.0	10.3	14.7
14,18,22	C/S	"	"	"	87.0	112	142
13,14,15	cz	As Rec'd.	"	"	14	17	
85,86,87	"	Sm.Grain	"	"	4.5		
235,236,237	"	Lg.Grain	"	"	8.0		
4,5,6	cu	As Rec'd.	"	"	10.0		
79,80,81	"	Sm.Grain			10.3		
154,155,156	"	Lg.Grain			9.2		
2,8,9	Al	As Rec'd.	"	"	58	67	82
72,73,108	SS	Annealed	200	"	2.2	3.3	
45,63,66	C/S	"	"	"	400	850	
1,2,3,4,5,6	cz	As Rec'd.	"	"	37	45	
76,77,78	"	Sm.Grain	"	"	26	31	
226,227,228	"	Lg.Grain	"	"	25	33	
7,8,9	cu	As Rec'd.	"	"	24		
82,83,84	"	Sm.Grain	"	"	23		
157,158,159	"	Lg.Grain	"	"	27		
1,2,3	Alloy A	Annealed	"	"	11	14	
1,2,3	Alloy B	"	"	"	6.7	8.3	
15,17,21	CbZr	"	"	"	20	24	

TABLE 5--(Continued)

Specimen Numbers	Mt'l.	Heat Treat	Vel. ft/sec	Cav. Cond.	MDP (avg.)		
					50	100	200
7,8,9	cz	As Rec'd.	200	Nose	27	32	
79,80,81	"	Sm.Grain	"	"	16	21	
229,230,231	"	Lg.Grain	"	"	17	22	
10,11,12	cu	As Rec'd.	"	"	30		
85,86,87	"	Sm.Grain	"	"	33		
160,161,162	"	Lg.Grain	"	"	28		
10,11,12	cz	As Rec'd.	"	Vis.	16	20	
82,83,84	"	Sm.Grain	"	"	9	11	
232,233,234	"	Lg.Grain	"	"	12	17	
13,14,15	cu	As Rec'd.	"	"	22		
88,89,90	"	Sm.Grain	"	"	14		
163,164,166	"	Lg.Grain	"	"	13		

Nomenclature

SS = stainless steel
 C/S = carbon steel
 cz = brass
 cu = copper
 Al = aluminum
 Alloy A = Refractory alloy "A" = Ta-10W
 Alloy B = " " "B" = Ta-8W-2Hf
 CbZr = Columbium - 1% Zirconium

As Rec'd. = Intermediate grain size, "as received."

Sm. Grain = Low heat treat (annealed at 850°F)

Lg. Grain = High " " (" " 1400°F)

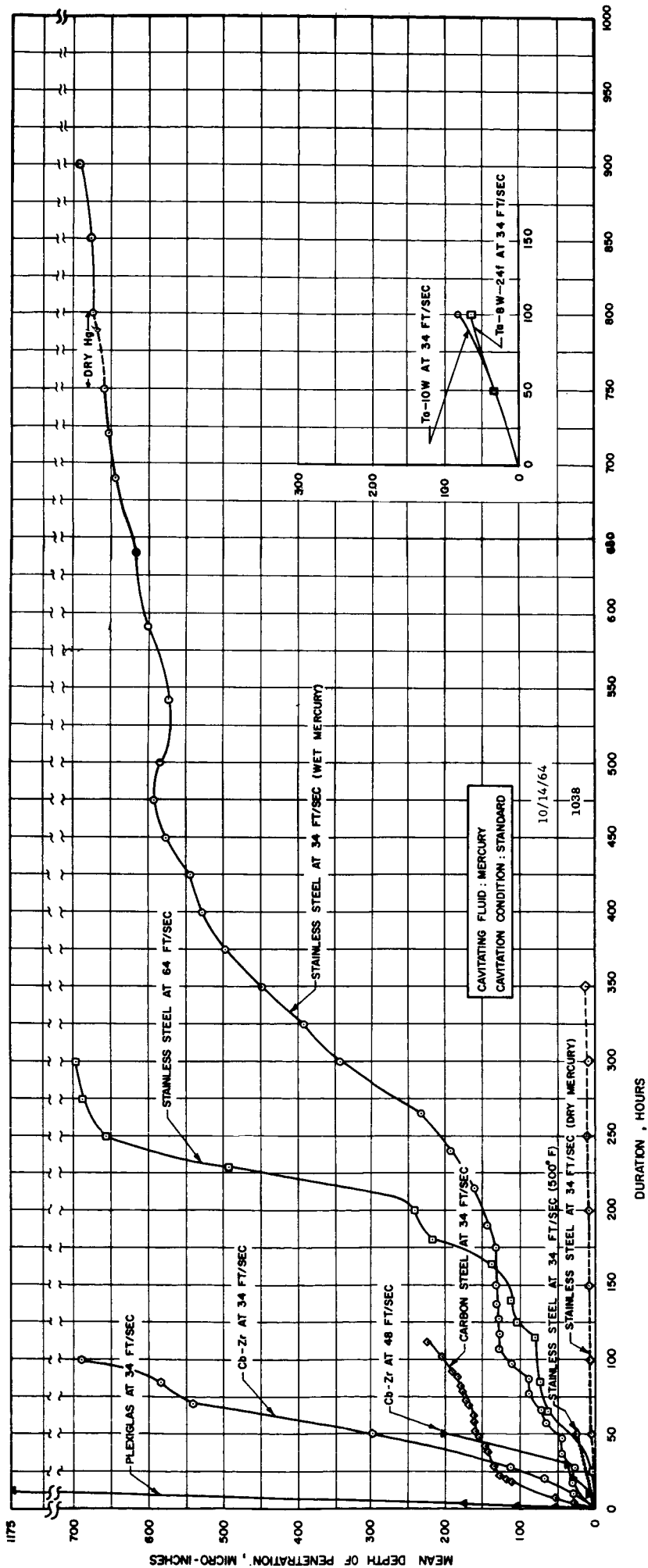


Fig. 6. Typical Mean Depth of Penetration versus Duration Curves for Mercury.

on the curve is about 3500, and substantial additional test hours have been accrued in mercury for the other degrees of cavitation.

Figure 6 shows the effects of material, velocity, fluid condition (temperature and water content) and duration for a given degree of cavitation. It is noted in general that the damage rate for a given material, condition, etc. is not uniform with time, but rather shows a high rate initially,* followed by a reduced rate** and again an increasing rate. The longest duration test shows six or seven different high-rate regions. It is noted that the last fifty hours of this test are for "dry mercury," and yet the increase in damage during this interval is somewhat greater than that for the preceding interval of the same duration. Since in other tests it has been found that "dry" mercury is only about 1/10th as damaging as "wet," it may be that this last test increment represents another high rate of damage period for these specimens. The continuation of the long duration test with "dry" rather than "wet" mercury, as used for the remainder of the test, was an error made before it was realized that there was a significant difference between the behavior of the fluid in these two conditions.

The different damage intensities resulting from the various tests are discussed in detail in later sections.

b. Water Tests

Figure 7 shows typical mean depth of penetration vs. duration data for the water tests. The curves correspond to the three different

*In general, no measurable "incubation period" exists for either water or mercury tests. This is made particularly evident by an examination of the pit count records.

**The negative rate sometimes shown may be due to surface adsorption of either mercury or water or other impurities.

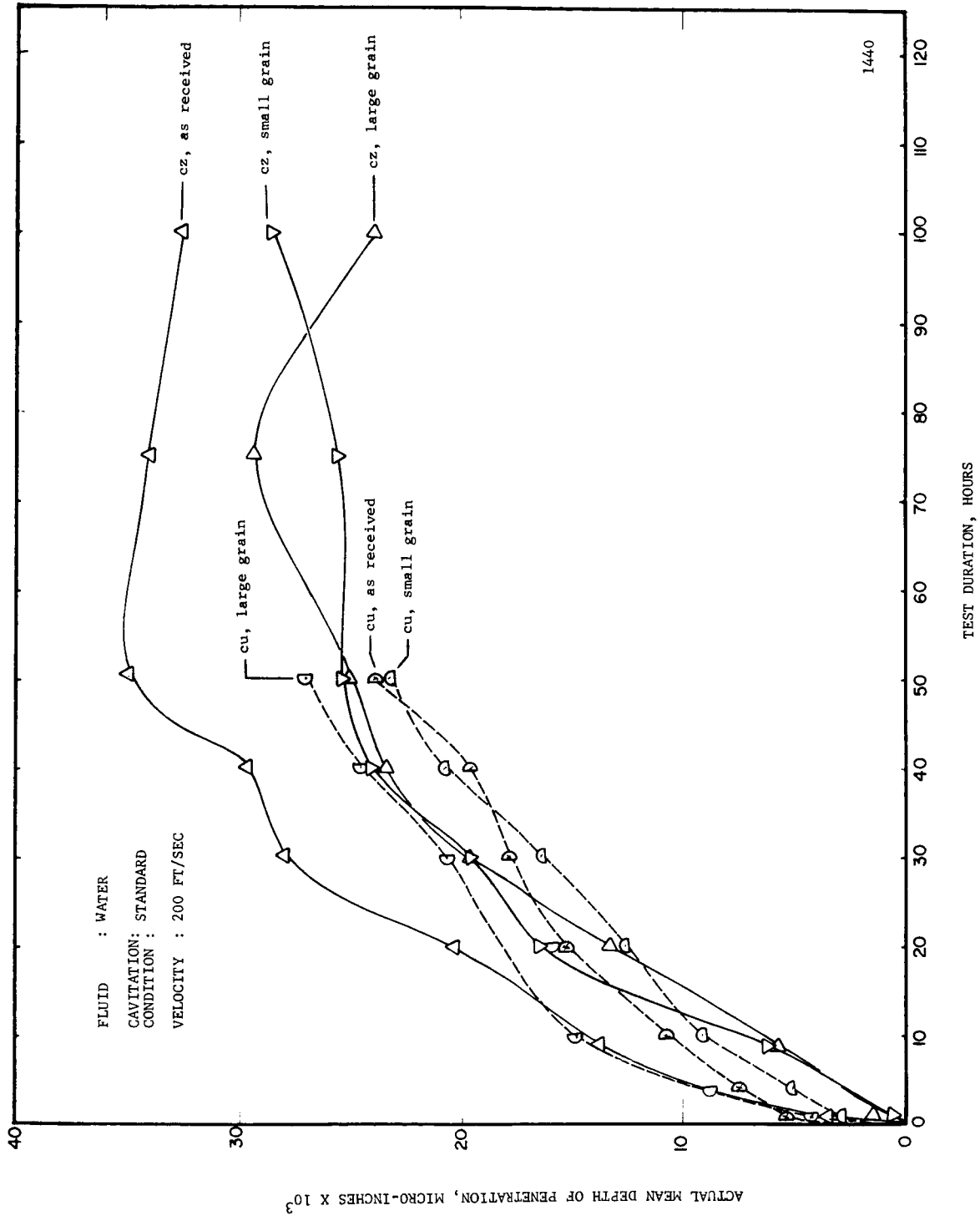


Fig. 7. Typical Mean Depth of Penetration versus Duration Curves for Water.

heat-treat conditions of pure copper and of brass respectively, so that there are a total of six curves. They apply only to the tests for 200 ft./sec. and "Standard Cavitation." All these tests have been completed to 100 hours, the standard duration adopted for the water tests. Eventually similar curves for the entire series of water tests will be presented in this fashion.

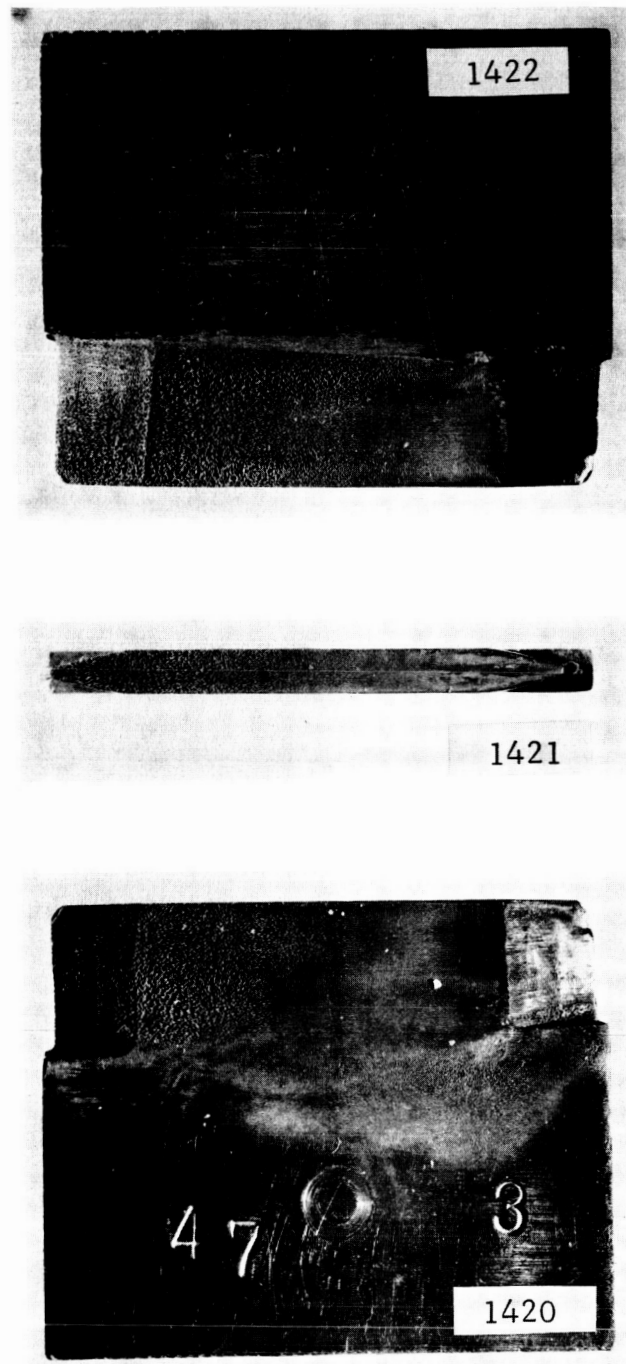
The present water curves illustrate, as do the mercury curves, that the damage rate is highly non-linear showing a very high rate at the start, which decreases substantially for the remainder of the test with water. It is believed that the secondary "humps" are not present, as they were for mercury, because the damage is not sufficient. (Note comparison of vertical scales.) Because of the much smaller volume losses encountered in the water tests (even though the velocity is the order of 6 times that in the mercury tests), the proportionate precision of the data is much less and the scatter greater.

Further detailed results will be discussed in a later section.

3.4.3 Mean Depth of Penetration Rate Vs. Time

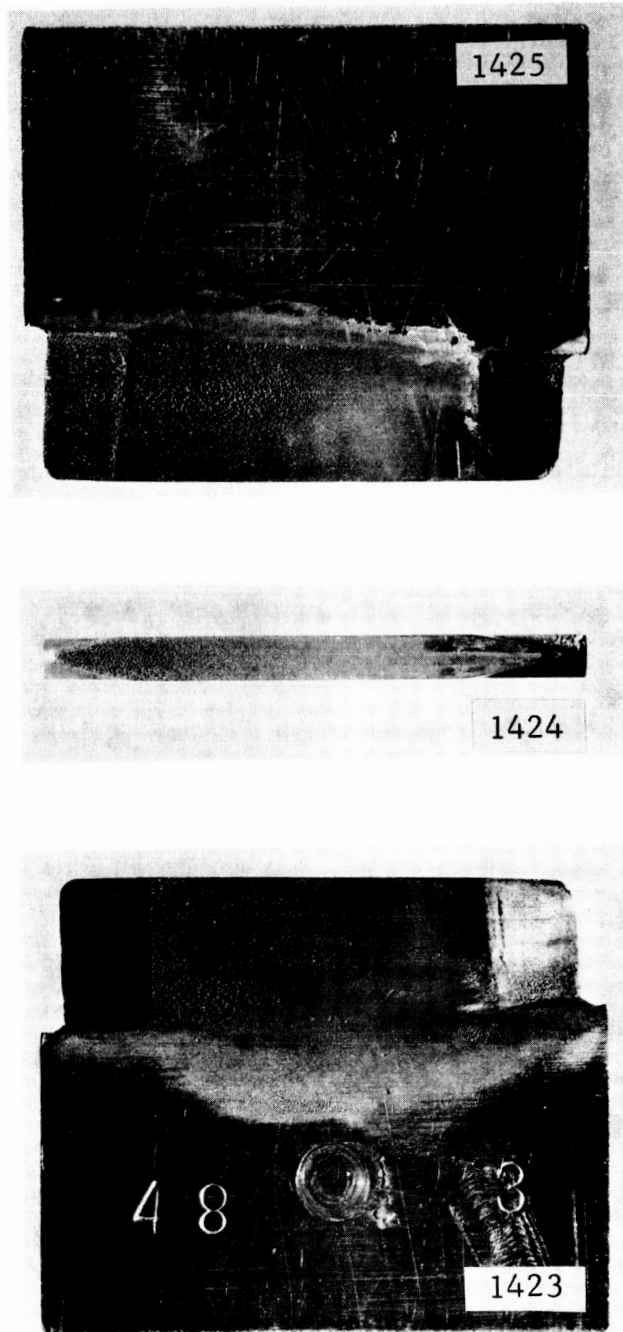
a. Present Observations

It has been noted above that for both mercury and water, the rate of damage is not uniform throughout the test, but rather reaches a very high value almost immediately (without any observable incubation period). After this initial high-rate period, the damage rate falls very substantially and remains at a low level, increasing gradually, over an extended period. If the test is carried to high enough levels of accumulated damage (as for many of the mercury samples--see Figure 8



(a)

Figure 8. (a) Back Side, Polished Surface and Front Side of Specimen No. 47-3 (SS) After 800 Hours Exposure to Cavitation in Mercury at a Throat Velocity of 34 Ft./Sec., for "Standard Cavitation".



(b)

Figure 8. (b) Back Side, Polished Surface and Front Side of Specimen No. 48-3 (SS) After 800 Hours Exposure to Cavitation in Mercury at a Throat Velocity of 34 Ft./Sec., For "Standard Cavitation".

for a photomicrograph of the previously discussed long duration mercury specimens*), the rate again increases to a high value. Subsequently, there may be numerous peaks and valleys in the rate curve, and it does not appear to level off at any fixed value.

The rate-curve sketches for all specimens, presented in Tables 2 and 3, show the greatest portion of the experimental evidence for the above statements. In addition, the existence of the early hump and the lack of a nucleation period was further illustrated very clearly by a previously reported⁵ test carried out in water at this laboratory using stainless steel irradiated test specimens. Finally, the mean depths of penetration computed from the tabulated pit counts show the same shape of rate curves, although there is a substantial error in amplitude which is presently unexplained (i.e., the pit count data shows a much smaller mean depth of penetration than the actual weight measurements).

b. Proposed Explanation of Experimental Observations (Here and Elsewhere)

On the basis of the present evidence it is believed that an initial hump in the damage rate vs. duration curve, followed by a diminution of rate which is in turn followed by a gradual increase to one or several subsequent humps may be a fairly common form of cavitation damage.

It is believed that the initial hump has been unnoticed by various previous investigators since the total accrued damage in this phase

*From the viewpoint of precision machinery as e.g., pumps of a SNAP system, behavior of materials for such damage levels may be academic in that "failure" for that particular application has already occurred, i.e., the resistance of materials to initial damage is of primary importance.

is small. It was called to our attention in the present tests both by the observation of increasing numbers of pits (for weight losses too small for precise direct determination) in the very early portions of the tests, and by the aforementioned tests with irradiated specimens. The initial hump cannot be due to flow perturbation by a roughened surface, since the surface is almost undamaged during this portion of the test. Hence, it must be due as stated in an earlier paper¹ to the characteristics of the initial surface as, for example, the existence of inclusions or other irregularities or "weak spots" which are easily removed.* The cause of the early rate decrease may also be a work-hardening of the surface which has been shown to occur very early in cavitation tests by X-ray diffraction techniques.⁶ However, if this is the case, it is only a very shallow layer which is affected, since tests conducted in this laboratory with the brass and copper specimens using a microhardness indenter showed no consistent change in hardness.

Later non-linearities in the damage rate curve are believed almost entirely due to flow perturbation caused by the damage itself. It has been recently noted, for example, in magnetostriction tests⁷ that a hump in the rate curve occurs after substantial damage (which roughly corresponds in damage magnitude to the later humps in the mercury specimen curves), and then that the rate decreases to an eventually constant value (as opposed to the present tests). It is believed that

*An initial rounding of sharp corners may also be involved. However, this is not the complete explanation since both pit counts on the polished surface and weight measurements show the initial hump.

the change in surface roughness as the test proceeds initially results in an increase in damage rate by increasing the area exposed, and in building up sufficient coldwork that fatigue failure becomes imminent across the specimen face. Later on, the increased surface area and fatigue mechanisms become "saturated," but a degree of protection to the surface is realized by the roughness itself, so that bubble collapses generally are held at a distance. Thus the rate decreases until all operative mechanisms become "saturated," and the rate becomes uniform. However, the magnetostriction test differs from flowing systems generally in that:

- i) The damage is essentially uniform across an area fixed by the apparatus
- ii) The bubbles are of relatively uniform size and collapse violence, apparently being incapable of creating relatively large, single-blow craters as sometimes observed, e.g., in present venturi tests on materials ranging from aluminum to stainless steels,¹ and in water tunnel tests on aluminum by Knapp,⁷ but instead causing a fairly uniform very fine pitting.*

Somewhat different but fairly similar arguments can be advanced to explain the rate curves from a rotating disc apparatus, which are rather similar in form to those from the magnetostriction facility. After substantial damage is incurred, the flow pattern is perturbed in

*Preliminary tests in this laboratory to observe pitting from magnetostriction-type tests on foils of very soft material so far tend to substantiate these statements.¹⁴

such a manner that local cavitation is induced by the roughened surface so that new area is exposed to attack, and the rate of damage increases. However, the "new" areas become further and further removed from the inducer hole, so that the attack per unit area is likely to be less severe as the region spreads (i.e., it is "out-of-range" from the inducer hole), and the rate will presumably eventually decrease. Whether or not it will eventually reach a relatively constant value as for the magnetostriction tests where the exposed area is fixed is not evident nor experimentally demonstrated, to the author's knowledge.

The present venturi tests with the "conventional" specimens obviously differ in detail from the rotating disc apparatus tests in the interrelations between the exposed area and the cavitation field. However, high-speed motion picture studies of the flow and detailed examination of the damage patterns³ show that local cavitation created by the specimens themselves, rather than the overall cavitating field, is probably very important in the production of damage. Hence, the rate of damage becomes dependent upon the flow perturbation due to previous damage, once that damage has become substantial (as opposed to the initial hump), much as in the rotating disc apparatus. However, the situation is more complicated in that the major site of cavitation initiation is not so well known or localized, so that the resultant rate vs. duration curves could be expected to be (and apparently are) more complex and less predictable.

3.4.4 "Wet" vs. "Dry" and "Hot" vs. "Cold" Mercury

a. Experimental Observations

As previously indicated, the mercury used in the majority of the damage tests contained trace quantities of water (estimated at 100 to

1000 ppm), and was at approximately room temperature. However, when heaters had been installed on the loop, it became possible to operate with mercury temperatures on the order of 500°F. Since lighter components as gas or water are disentrained in the strong centrifugal field of the pump, operation at high temperature removed the water almost entirely from the mercury. Methods of measuring entrained water and gas quantities in mercury have been developed in this laboratory in connection with the study of their effect on cavitation number. Hence, it has become possible to verify that in the "dry" condition the water content of the mercury is less than about 15 ppm.* Unfortunately no corresponding measurements are available for the majority of the runs with "wet" mercury** since the method of measurement had not been conceived at that time. However, measurements taken recently have shown that the water content ranges from approximately 250 ppm to 750 ppm and is velocity dependent, because of the nature of the pump design. A "dry" mercury damage run for a pair of "conventional" stainless steel specimens has so far been carried to 400 hours. Examination of Figure 6 indicates that the damage for the "dry" mercury appears to be about a factor of 10 less than for "wet" mercury, other test conditions being the same. Two

*Upon "drying" it was noted that the mercury wet the stainless steel damage specimens much more effectively than before so that it was necessary to boil-out the specimens under vacuum to attain true weight measurements. This is taken as further evidence of the almost complete removal of water.

** If it turns out that mercury damage rate is very sensitive to the quantity of water in the mercury, then it may be that minor variations in this quantity are partly responsible for some of the nonlinearities in the damage vs. duration curves for "wet" mercury. No conclusions in this regard can be drawn without further data on the effect of water content.

additional 50 hour "dry" runs with stainless steel have also been completed. Weight losses from all three sets agree closely at the 50 hour point. This very substantial increase in damage capability to a non-corrodible material caused by the addition of a small quantity of water to the mercury is further confirmed by observations on pin-type specimens (to be described later). As noted in Table 7, to be discussed later, the pressure recovery on the downstream end of the specimens is much greater for the "wet" mercury and this may partially explain the damage results.

A single high-temperature (500°F) damage run has been carried to 50 hours with a pair of stainless steel (type 302) specimens. Again, the mercury was necessarily "dry." Examination of Figure 6 shows that the damage attained by this "dry-hot" run is of the same order of magnitude as for the corresponding "wet-cold" run (the 800 hour run), i.e., it is much greater than for the "dry-cold" specimens previously discussed. It is of course planned to explore the effects of high-temperature in a more comprehensive manner using longer durations and different specimens. However, this has not been accomplished as yet.

b. Proposed Explanations of Observations

The experimental observation is that "wet-cold" and "dry-hot" mercury are approximately equally damaging to a material (austenitic stainless steel) whose mechanical properties do not differ very greatly over the temperature range involved (~ 80 to 500°F),* and which is

*According to data published by U.S. Steel,¹³ the ultimate strength decreases by 0.76 over this range, the yield strength by 0.6 and the elongation by 0.62. Thus, very roughly, the strain energy decreases by about $0.76 \times 0.62 = 0.5$ over this temperature range.

essentially non-corrodible by water for the temperatures and durations involved. However, "dry-cold" mercury is very much less damaging to the same material. The only difference between these various fluid-material combinations which seems likely to be sufficiently substantial to explain the observed effects is that of vapor pressures.

The "hot-dry" mercury has presumably a vapor pressure characteristic of pure mercury at the existing temperature, i.e., ~ 1.9 psia. The effective vapor pressure of the "cold-wet" mercury is presumably about that of water at the existing temperature, i.e., about 1 psia.* Hence, these are of the same order of magnitude, while the vapor pressure of "cold-dry" mercury is only a few microns. Thus, it appears that a decrease in vapor pressure (even though the degree of cavitation and all other flow parameters are held constant) results in a substantial decrease in cavitation damage.

A consideration of the dynamics of bubble growth and collapse indicates that the influence of vapor pressure might be two-fold. A higher vapor pressure would promote nucleation and growth, but inhibit collapse, in that the vapor would behave as a perfect gas under adiabatic compression toward the end of collapse. In a given flow and pressure regime, a higher vapor pressure might result in an earlier nucleation and more rapid growth of bubbles, leading to a larger maximum diameter, and, aside from the inhibition of final collapse as mentioned above, a more energetic and damaging collapse. In the present instance, it

*Confirmed by the fact that the loop centrifugal pump cavitates when the mixture temperature approached the saturation temperature for water at pump inlet pressure.

appears that the second mechanism is the more important in that the high vapor pressure fluid is the more damaging.

Damage tests with entrained gas rather than water would be of interest in that the collapse-inhibiting mechanism would be presumably stronger than with a vapor, since the gas would be a non-condensable. On the other hand, the effect upon growth would be less than that of a vapor, since the gas quantity could not be increased by evaporation from the surrounding liquid (and presumably gas diffusion effects would be relatively negligible). Consequently, it would be expected that the effect of entrained gas would definitely be to inhibit damage, and in fact it is known that the injection of gas into cavitating water upstream of a turbomachine will indeed substantially reduce damage. In the same connection, it has been noted in the experiments in this laboratory that injection of gas into the water loop will reduce the sound level from cavitation very substantially and also produce a much steadier cavitation cloud.

While the vapor pressure mechanisms are believed of primary importance, other parameters affected significantly by the fluid changes in these tests are surface tension, interfacial tension, i.e., the degree of wetting between mercury and steel, and viscosity. The influence of these parameter changes is not known at present. However, the surface tension and viscosity values at the applicable temperatures are shown in Table 6. Moreover, it may be that tests of this type will result in the possibility of damage inhibition in closed systems by suitable trace additives to the fluid.

TABLE 6
SURFACE TENSION AND VISCOSITY FOR MERCURY*

Temperature	Surface Tension	Viscosity
80°F	0.03185 lb/ft.	3.66 lb/ft-hr
500°F	0.02875 lb/ft.	2.32 lb/ft-hr

*WADD TR-6196

3.4.5 Flow Pattern Changes (Pin-Type Specimen Tests)

The flow pattern resulting from the insertion of the "conventional" plate-type specimens (Figures 2, 3, and 4) into the cavitating region of a venturi is somewhat similar to cavitating flow over the leading edge of a pump blade, i.e., a substantially translatory cavitating flow with a significant axial pressure gradient. As has become evident from pump tests and from the present venturi tests, this is not an extremely damaging type of flow.

If a strong vorticity is superimposed upon a translatory flow of the type discussed above, so that the vortex impinges in a suitable fashion upon a structural member or test specimen, the damage intensity may be increased by orders of magnitude. This has become evident in tests with open-shrouded centrifugal or mixed-flow impellers, where the leakage flow over the blade tips, having a strong vorticity and also being in a substantial pressure gradient, may impinge on the following blade of the impeller itself, and cause very substantial damage. The rotating disc facility produces a somewhat similar and very damaging flow. It has been found in recent tests in this laboratory that a similar situation can be created in a cavitating venturi by the insertion of a pin or cylinder with axis normal to the flow direction across the venturi diffuser.

In the present instance, experiments were started with such pin-type specimens (Figure 5), which were actually thin-walled tubes, to develop a specimen capable of high degrees of precompression during a cavitation test without buckling. However, it was soon discovered that

the rate of damage on such a specimen was orders of magnitude greater than for the "conventional" specimens. Also, the damage rate is very sensitive to the degree of cavitation.

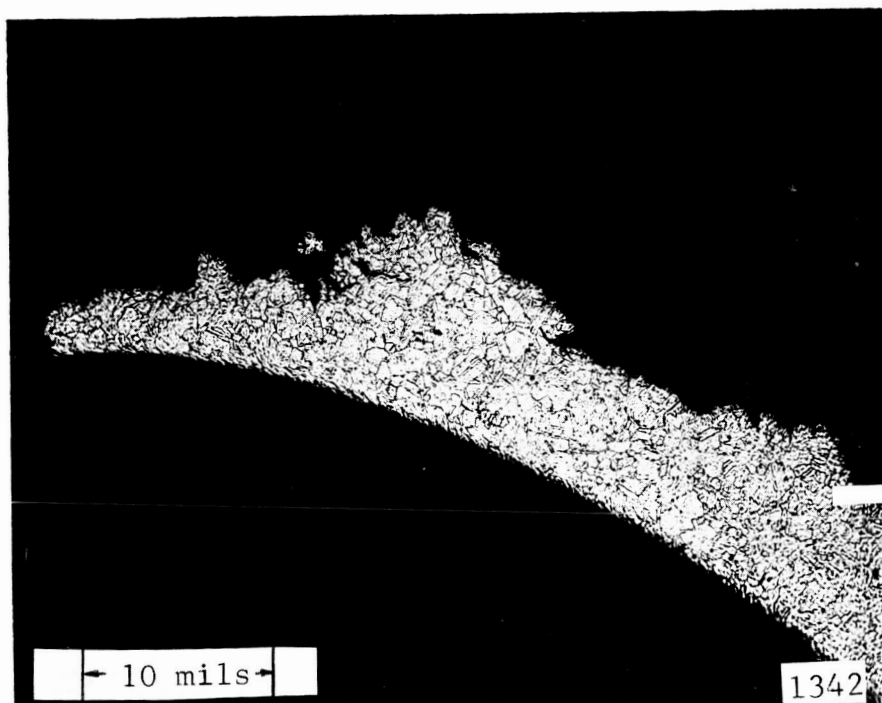
It is presumed that there exists an unsteady vaporous wake region behind the pin in the region of the trailing vortices, consisting perhaps of more or less discreet vapor bubbles. By a suitable adjustment of velocity and downstream pressure, these bubbles can be caused to collapse on the downstream portion of the cylinder, in which case very intense damage is caused. For a given velocity, the damage rate is very dependent upon the pressure differential across the pin, as this controls the location of bubble collapse, and the driving pressures for collapse, i.e., at low back pressure the trailing vortices collapse well into the fluid downstream of the pin, causing little damage.

The first pin tests were made with "wet" mercury. It was found that with a 34 ft./sec. throat velocity and a suitable setting of the venturi pressure differential, a hole completely through the \sim 20 mil pin wall was created in 5 hours. Figure 9 shows a metallographic cross-section through this region. Thus, the mean depth of penetration in this particular area was of the order of 4000 micro-inches per hour, whereas the maximum rate for a "conventional" specimen at the same velocity and with the same fluid is of the order of 1 - 5 micro-inches/hour (Figure 6).

Subsequent tests with "dry" mercury showed a much smaller damage rate, although still large as compared to "conventional" specimens. The previously discussed large difference in damage capability between "wet"



(a)



(b)

Figure 9. Metallographic Cross-section through Stainless Steel Pin Specimen Wall, (a) Magnification 50X; (b) Magnification 100X, Marbles Etch.

and "dry" mercury is thus confirmed also for the pin-type specimens.

No further quantitative results for the pins are yet available. However, it is apparent from the preliminary tests discussed above that a very accelerated cavitation device could be made with such specimens, particularly if "wet" mercury were used as the fluid. It is also apparent that the combined translatory-vortex flow pattern created by a test specimen of this type is very damaging, an observation consistent with turbomachinery tests.

It is believed that a suitable specimen or obstruction inserted into a cavitating venturi could create a flow pattern closely analogous to that found to be damaging in turbomachines, and the desired combination of velocity, vorticity, and pressure gradient could be obtained. Thus a valuable tool for the realistic study of prototype damage would be created.

4.0 NORMALIZED DAMAGE RESULTS

4.1 Numerical Procedures

The presently available data regarding mean depth of penetration (and its rate) for all runs in water and mercury are listed in Tables 2 and 3 for various fixed durations. Tables 4 and 5 summarize this data for the various distinct fluid, material, and flow parameters, again at the fixed durations of 50, 100, 200, etc. hours where data is available. A more comprehensive analysis and reduction of the data will be reported at a later date when the series of runs has been completed. At the present, it is only desired to obtain a first look at the results in such a way that the effects of material, velocity and cavitation condition can be evaluated.

For each distinct fluid, material, and flow regime combination, the average mean depth of penetration has been computed at 50 and 100 hours.* These averages are then normalized by dividing by the corresponding average mean depth of penetration for stainless steel.

For example, to obtain the effect of material, the mean depths of penetration are averaged over all velocities and degrees of cavitation for mercury or water. The data for the two fluids are kept distinct, and only the "cold-wet" mercury points are considered for the mercury contribution in the present comparisons.

*The detailed numerical calculations are filed with O.R.A. Project 03424 calculations files under Damage Program, 1964, F. G. Hammitt calc. of 6/64 and 7/64.

To obtain the effect of velocity, the averages should be taken over all materials and cavitation conditions for which a set of comparative velocity data exists. At present, comparative data exists for only a relatively limited number of material and degree of cavitation combinations both for water and mercury.

The procedure for degree of cavitation comparisons is similar, and again only a rather limited number of points exist at present for either fluid.

4.2 Material Effects

4.2.1 General Expectations

The ability to predict with reasonable precision the comparative resistance of different materials to damage from an arbitrary cavitation flow-field remains a major unattained objective. The difficulties involved in overcoming this obstacle are largely a result of the fact that the damage is caused in most cases by a variety of mechanisms whose relative importance depends on the particular flow condition, fluid, material, etc. In most cases, at least the following mechanisms are involved:

- i) Fatigue from repeated blows of relatively small magnitude,
- ii) Single-blow failure (individual craters),
- iii) Corrosion or other chemical effects.

The material properties associated with resistance to (iii) above are, of course, in no way related to (i) and (ii), resistance to which are normally associated with various mechanical properties of materials.

Three categories of mechanical properties of materials seem associated with resistance to mechanically-caused cavitation damage:

- i) Strength or hardness properties as ultimate and yield strengths, endurance limit, hardness, etc. The resistance to fatigue failure, (i) above, certainly must involve properties of this type;
- ii) Properties associated with failure energy as strain energy to failure, impact resistance, the combination of strength and ductility, etc. These certainly seem intimately involved with failures of the type (ii) above.
- iii) In addition, time-response and other miscellaneous effects may be significantly involved in some cases. For example, the various gross mechanical properties listed above depend significantly upon rate-of-loading, if the rate is high. Also, the duration of the blow from a collapsing bubble, delivered either as a shock wave or jet, is very short and also short-range in space so that highly transient effects become important, as well as the possible ability of the material to deflect "out-of-range" of the load during that brief instant it is applied without incurring permanent effects.

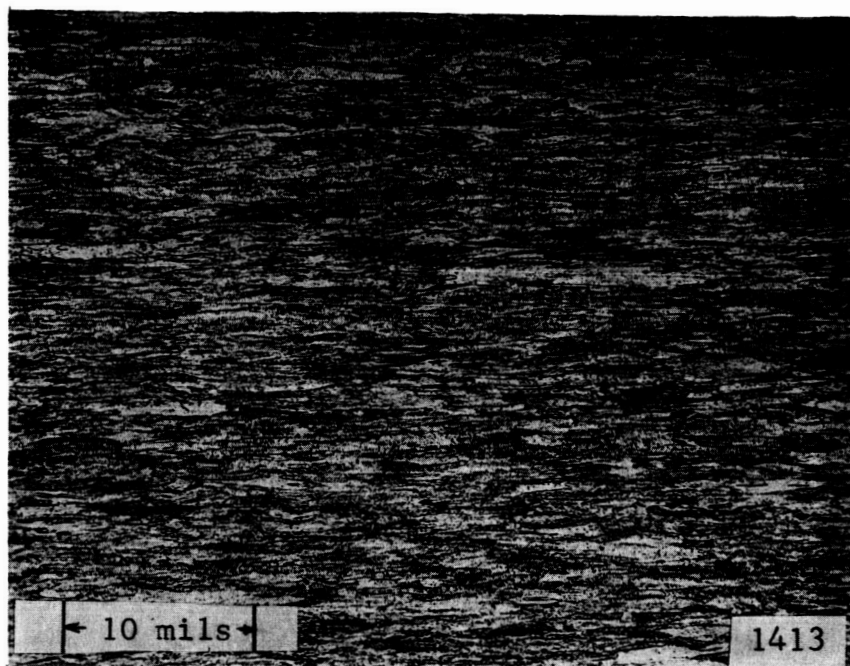
While the effects discussed under (iii) above are perhaps of considerable importance in many actual cases, they are comparatively very difficult to describe and measure with the present state of knowledge in the materials field. The properties discussed under (i) and (ii) above are at least easier to measure and are perhaps of the greatest importance. It seems likely that some combination of properties, representing both of these groups, i.e., (i) and (ii), would give the desired

figure of merit regarding resistance to mechanical cavitation damage. However, the relative weight to be given the two groups may well depend on the particular type of test, fluid, and material involved, so that more than one empirical constant may be required. It is hoped that some such "figure of merit" may result from the present investigation when the test series is completed. The attempt to form such a combined property grouping has not yet been made on the basis of the preliminary data available. However, this data is sufficient to show that no single mechanical property will suffice to provide a reasonable correlation.

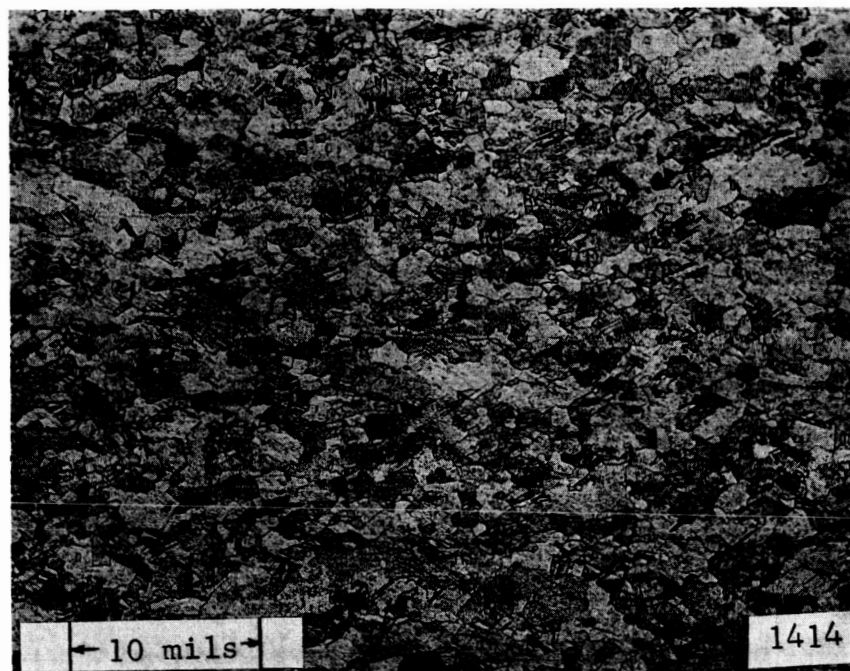
4.2.2 Copper and Nickel Series

Pure copper, copper-zinc (brass), copper-nickel, and pure nickel were selected as materials, relatively non-corrodible in water, each of which could be heat-treated to give a broad range of mechanical properties with considerable overlap between the materials. In addition, the microstructure of the materials is clean and simple, properties conducive to easy metallographic examination. Of these four materials, tests have been completed only on pure copper and brass, each in three heat-treat conditions:

- i) As received sheet material (Figure 10a)--fairly extensive cold-work with the grains elongated in a direction parallel to the polished face of the specimens (Figures 2, 3, and 4), i.e., parallel to the flow;
- ii) Low heat-treat (Figure 10b)--relatively small grains in an isotropic structure;
- iii) High heat-treat (Figure 10c)--relatively large grains in an isotropic structure.

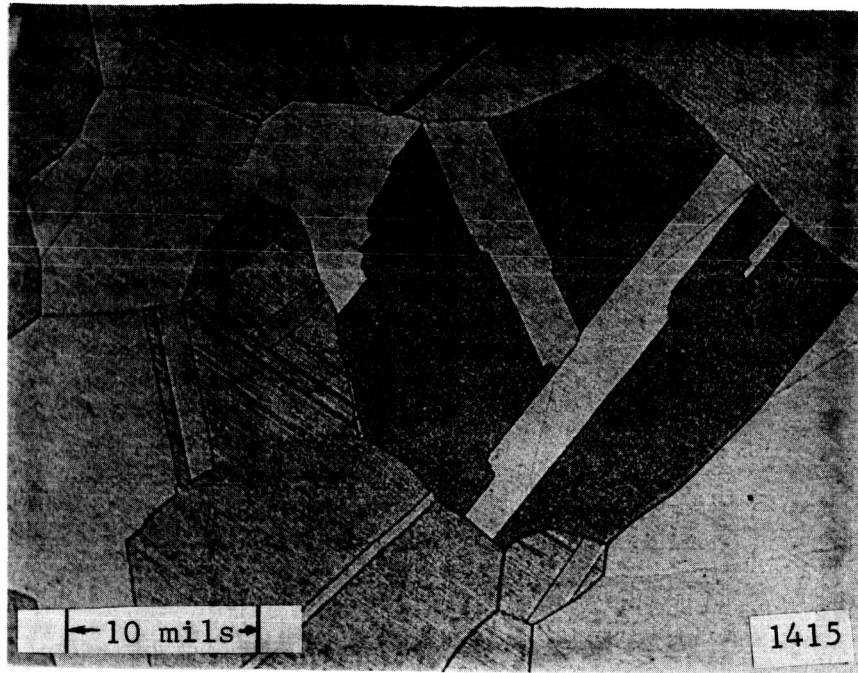


(a)

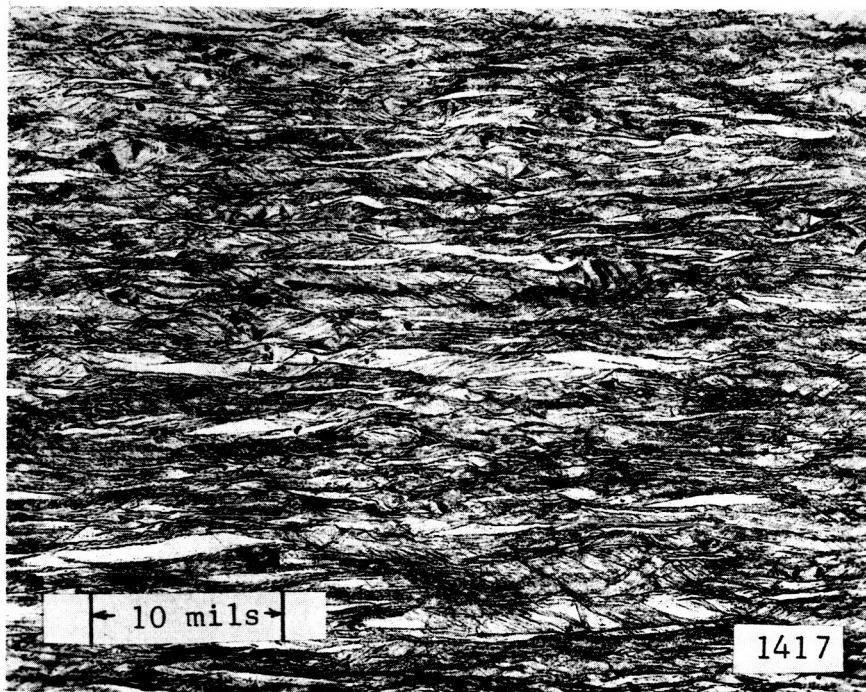


(b)

Figure 10. Photomicrographs of Grain Structure of OHFC Copper at 100X, (a) As Received; (b) Recrystallized at 900°F.

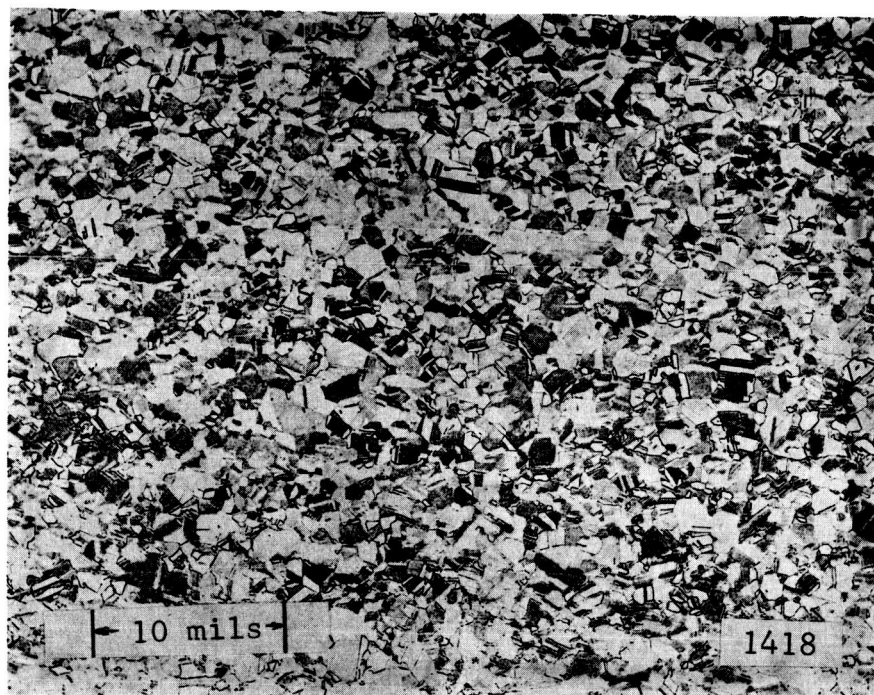


(c)

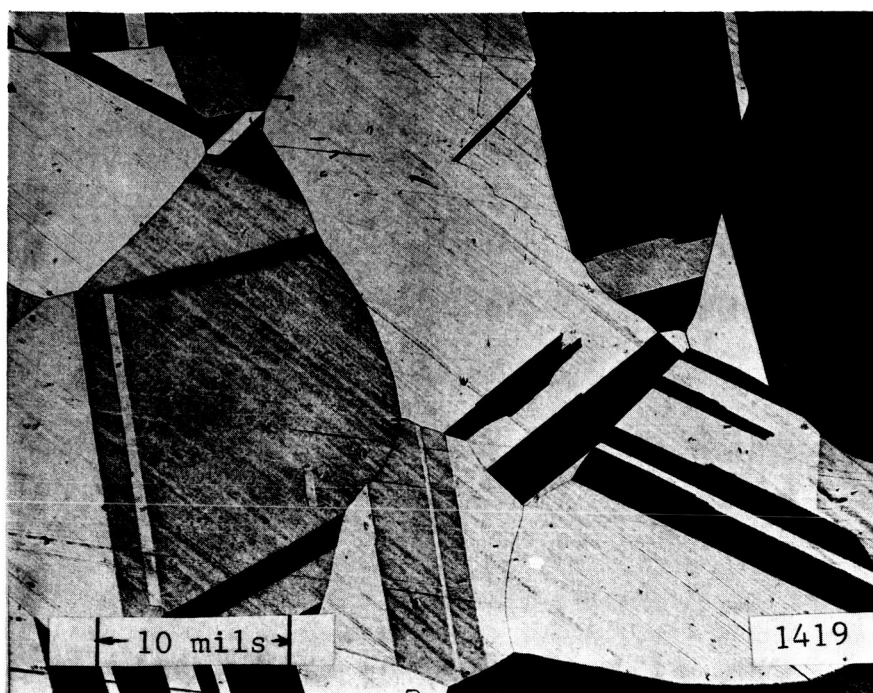


(d)

Figure 10. Photomicrographs of Grain Structure of OHFC Copper at 100X, Recrystallized at 1500°F, (c), and Brass, 100X, As Received, (d).



(e)



(f)

Figure 10. Photomicrographs of Brass, (e) Recrystallized at 850°F, 100X, and (f) Recrystallized at 1400°F, 100X.

The mechanical properties of these materials (measured after heat-treat) as part of the present investigation are listed fully in Table 1. It is noted that for these materials the "as received" condition is characterized by very high tensile strength and hence low ductility and strain energy to failure. The low heat-treat condition shows the highest strain energy, slightly more than the minimum tensile strength, and hence maximum ductility, whereas the high heat-treat condition is characterized by minimum tensile strength and moderate strain energy. It is further noted that there is an overall factor of about 4 in strain energy for a given material from maximum to minimum, and a corresponding factor of about 2 in tensile strength.

Examination of Table 4 shows that the mean depths of penetration at 50 hours (or 100 hours for the cases where it is available) for a given velocity and degree of cavitation differ only slightly between the materials or the heat-treat conditions, i.e., over a total factor of more than 9 in strain energy and 3 in tensile strength. This may be explained partially by the fact that as the tensile strength for these materials increases the strain energy decreases, i.e., merit in one of these properties can apparently counter weakness in another, which seems intuitively reasonable. Since the mean depths of penetration in these cases are about the same for both materials and all heat treats, whether the comparison is made at 50 or 100 hours, it is clear that it can make no difference whether rates or total values are compared, since all the damage vs. duration curves are essentially parallel, and in fact almost identical within the precision of the data.* The averaged normalized

*As previously explained, no eventual constant rate condition has been observed in any of the venturi tests so that this condition also cannot be used as a reference.

(as previously explained) mean depths of penetration for copper and brass at 50 and 100 hours for "Standard Cavitation" and 200 ft./sec. are plotted in Figure 11, against strain energy to failure. The corresponding curve for three refractory alloys and stainless steel covering an approximately similar range of strain energy is also included, and is noted to be quite distinct from the curves for the coppers and the brasses. Apparently damage for these materials is much more sensitive to strain energy than for the coppers and brasses, presumably because (Table 1) tensile strength and strain energy increase together, so that the previously discussed counterbalancing effect between these properties does not exist. Also included for comparison are single points for carbon steel (presumably not directly comparable with the others because of its relatively high corrodibility), aluminum (6061-T6), and plexiglas. It is felt that the apparent relative immunity of this material from cavitation damage in water is at least partially the result of a very low elastic modulus combined with relatively high strength properties, so that it may distort, without incurring permanent deformation, out of the effective range of the bubble collapse forces.

Also included in Figure 11 is the corresponding data for mercury. However, only the steels and refractories are available*, and these are connected by a single curve, which is distinct from the other curves. However, it is noted that its region of maximum sensitivity to either strain or tensile strength (Figure 12) is for lower values of these properties in the water tests than in the mercury tests. A differentiation might be expected since the stresses created by cavitation in water are less than for mercury, but the actual shape of the curves

*Damage rate similar to water on coppers and brasses.

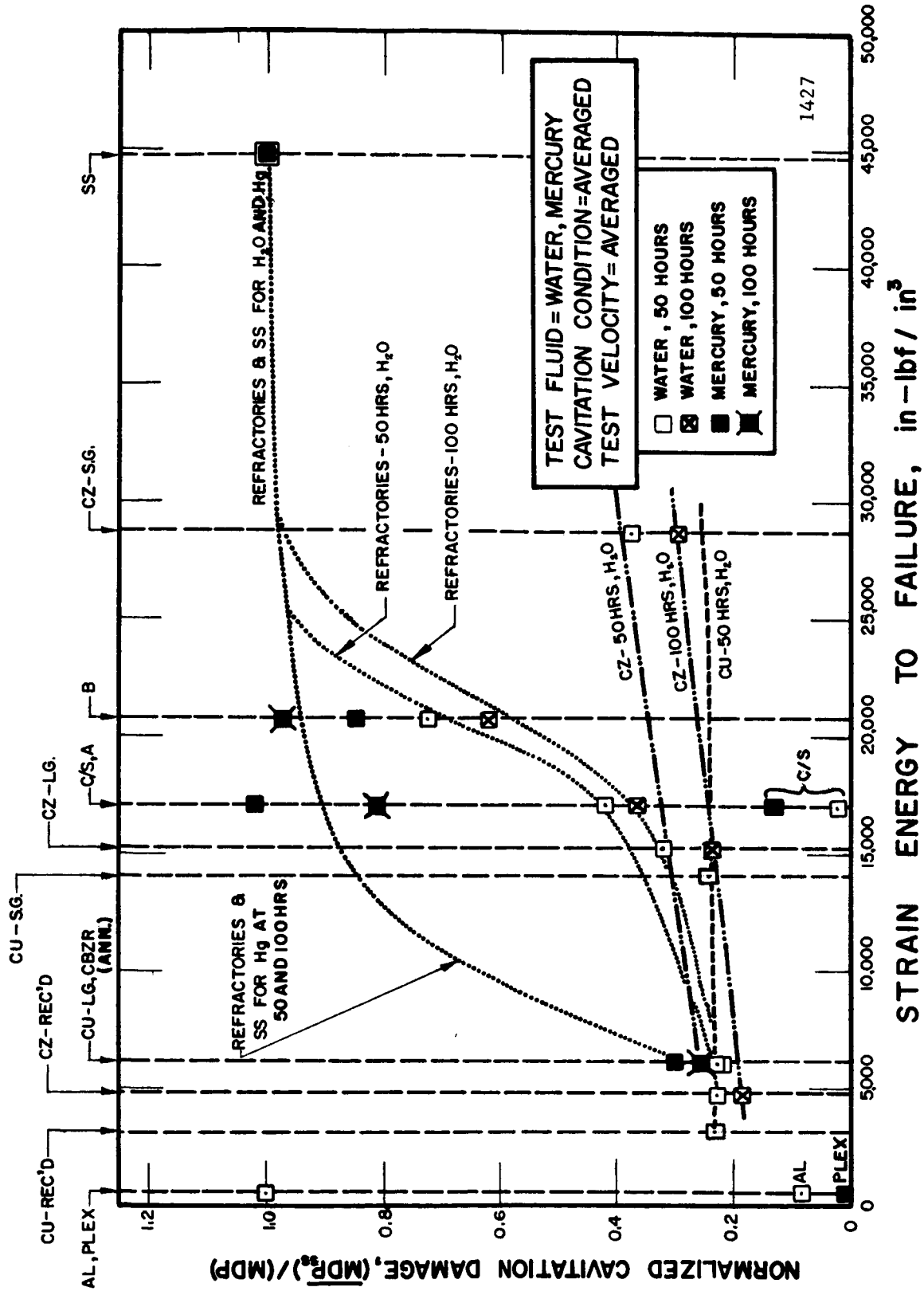


Fig. 11. $(MDP_{ss})/(MDP)$ versus Strain Energy to Failure for Various Combinations of Materials, Cavitation Conditions and Velocities in Mercury and Water.

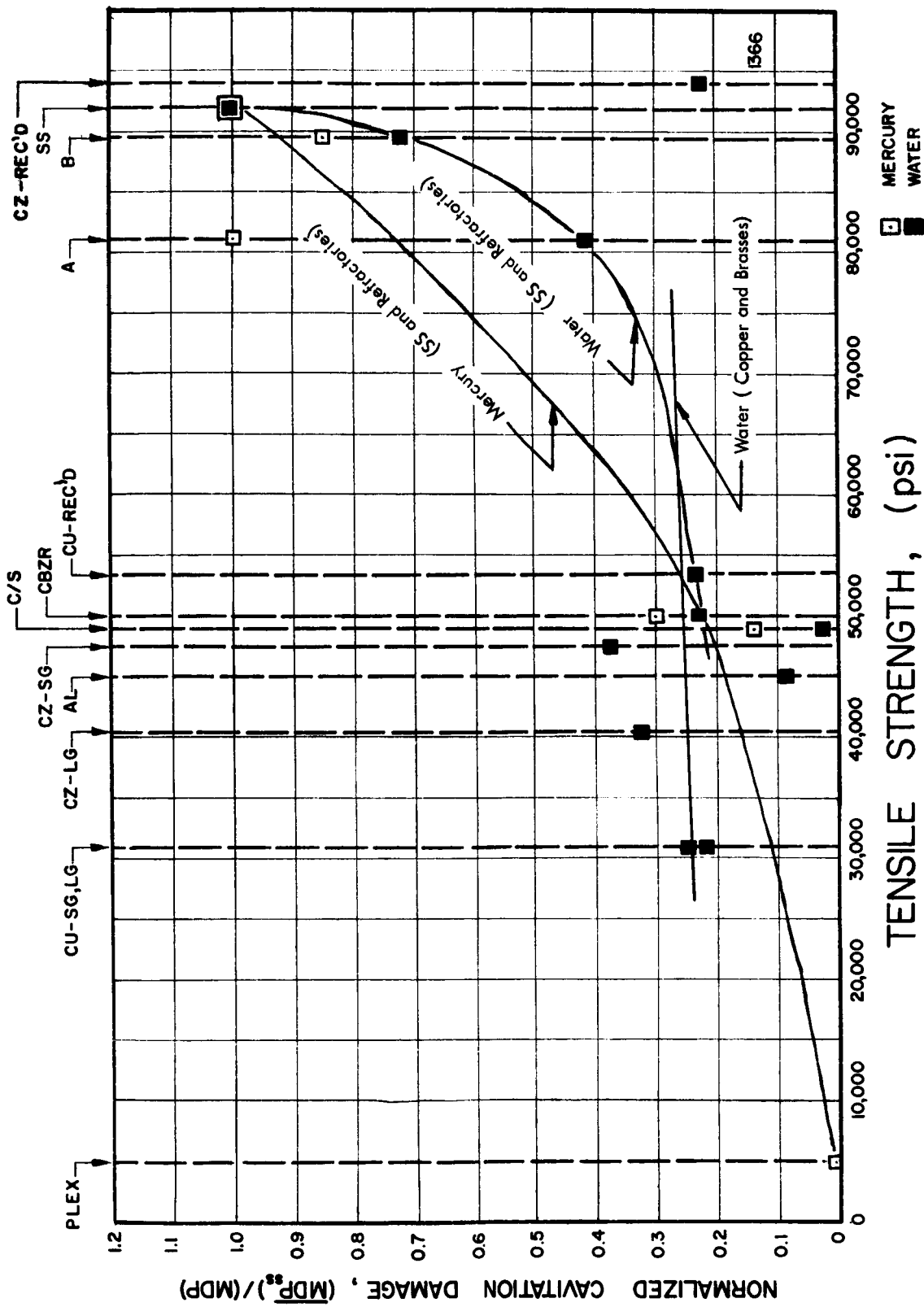


Fig. 12. $(MDP_{ss})/(MDP)$ versus Tensile Strength for Various Combinations of Materials, Cavitation Conditions and Velocities in Mercury and Water.

could not be foreseen. For either fluid the curve appears to be "saturated" for the higher values of strain energy or tensile strength. Figure 12 is a corresponding plot against tensile strength.

It is apparent from Figures 11 and 12 that:

- i) In general, no single mechanical property is adequate to correlate cavitation damage data,
- ii) At least a strength property and an energy property must be considered,*
- iii) In some cases, a combined property as suggested under (ii) above would not be adequate. For example, note the difference in behavior of plexiglas and the refractories between water and mercury, and also the fact that plexiglas is roughly as resistant to cavitation damage as stainless steel in water, although its strength and failure energy are much less.

4.3 Velocity Effects

4.3.1 General Anticipation

Many past investigators, in most cases using devices such as a rotating disc type facility,⁸ jet or droplet impacting facilities,⁹ and in the case of Knapp¹⁰ an ogive in a water tunnel have found that damage increases very rapidly with velocity. In some cases it has been reported that there was a threshold velocity below which there was no damage. It was often found that the damage was proportional to the velocity increment above the threshold velocity raised to a power ranging between 5

*A combined parameter so arranged that it increased with either energy or strength could be promising, and experimentation with various such parameters is planned.

and 7.* However, it is clear from a detailed examination of the flow in any of these cases that there is no reason to expect such a "law" to be general, but rather that the operative relation be a function of the type of flow, and perhaps also of the materials tested (influencing the relative importance of different failure mechanisms).

In the present case, the damage has been much less dependent upon the velocity than is usually reported. However, a detailed consideration of the flow in the cavitating venturi in the vicinity of the test specimens indicates several possible mechanisms whereby velocity might be expected to influence damage:

- i) Effect upon pressure in the collapse region, thus affecting driving force for collapse.
- ii) "Scale effects" altering the detailed flow structure in presently unpredictable ways. For example, the cavitation "cloud" in the water tunnel of the present investigation appears "thinner" (or more transparent) at high velocity than at low. The explanation is not presently known, but it is clear that departures from the classical scaling laws involving various "real fluid" properties, can also affect the damage.
- iii) Increased velocity means added conventional erosion. However, "zero cavitation" tests indicate that the contribution of such erosion, at least in the absence of cavitation, is relatively negligible in the present tests.

* Depending upon the choice of a threshold velocity, which is quite arbitrary in many cases. The higher is the selected threshold value, the higher the apparent exponent.

In the present case, it is believed that the major effect of velocity upon damage is the possible increase in collapsing pressures with an increase in velocity. It is apparent that this effect is less pronounced for the well-developed cavitation conditions, where the test specimens are under pressures near vapor pressure for all velocities, than for the less-developed conditions where a substantial portion of the test specimens are downstream of the collapse region for the "cloud," and hence under substantially higher pressure because of the action of the diffuser. It is noted that these relations are peculiar to this type of facility and would not be the same for other flow geometries.

Actual static pressure profiles, approximately applicable for any velocity since they are normalized by dividing by the kinetic pressure, from venturis with both water and mercury¹² are shown in Figures 13 through 22, for various degrees of cavitation and velocities in both fluids to illustrate the above statements.

All pressure profiles in this report differ from those of previous reports,^{1,3} in that test specimens were present and data from three pressure taps in the polished surface of one of the test specimens is included. The device used to measure these pressures consists of a specimen and holder combination machined out of two pieces of plexiglas and glued together to form the device shown in Figure 23. Taps identical to the wall taps in the venturi were drilled into the face of the specimens in order to measure the pressures at three locations on the surface.

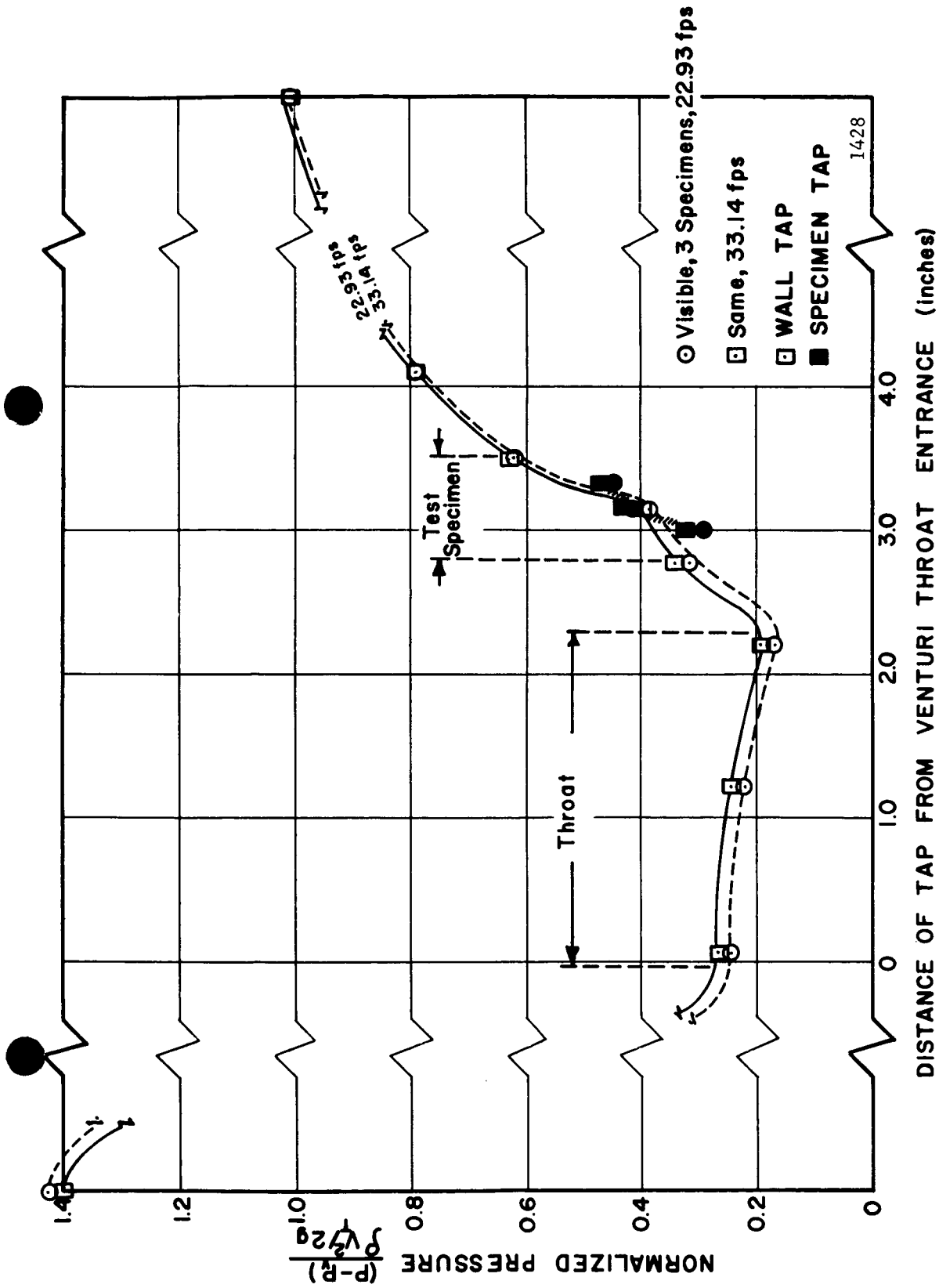


Fig. 13. Normalized Pressure Profile for Visible Initiation, 3 Specimens in Mercury at Various Velocities.

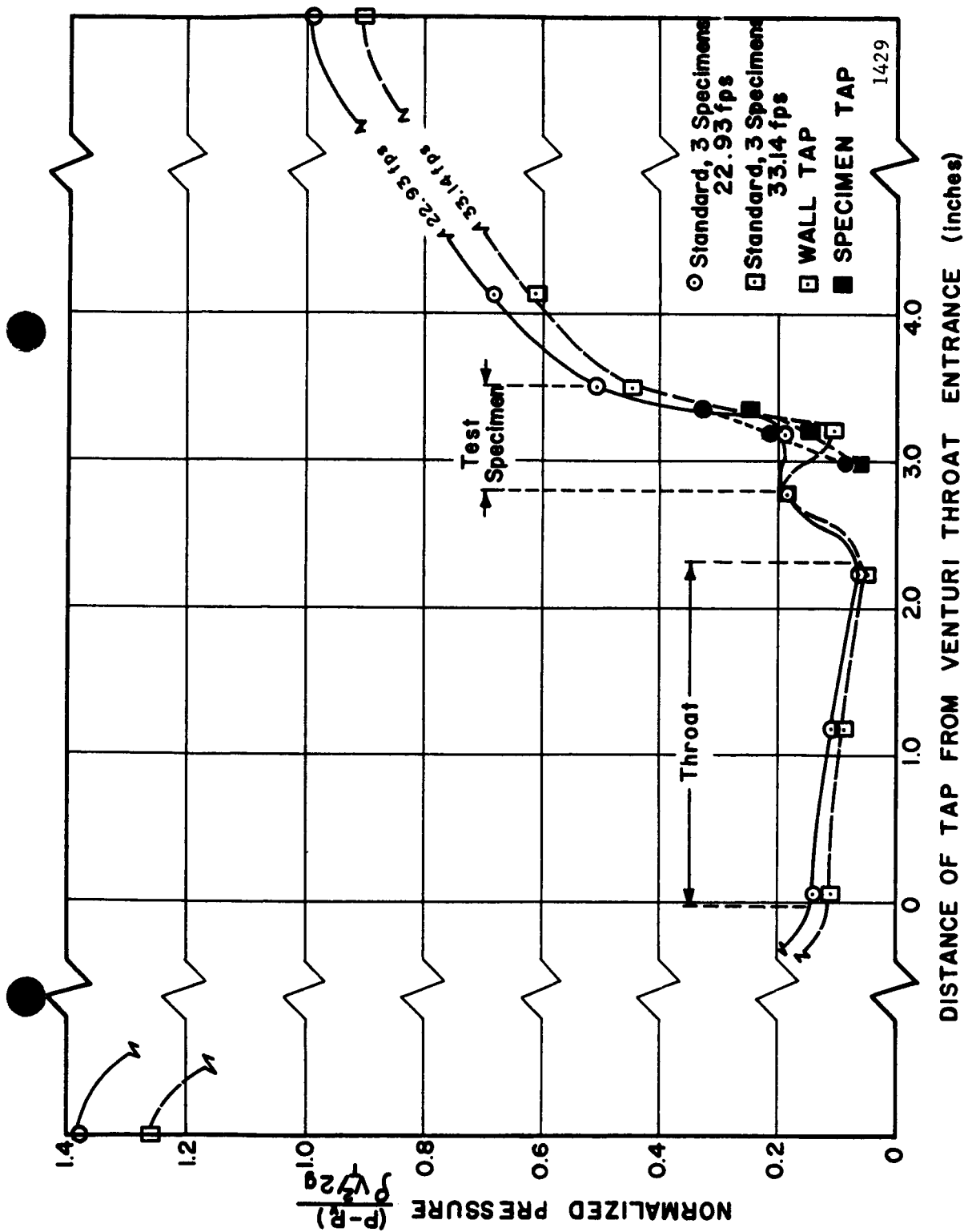


Fig. 14. Normalized Pressure Profile for Standard Cavitation, 3 Specimens in Mercury at Various Velocities.

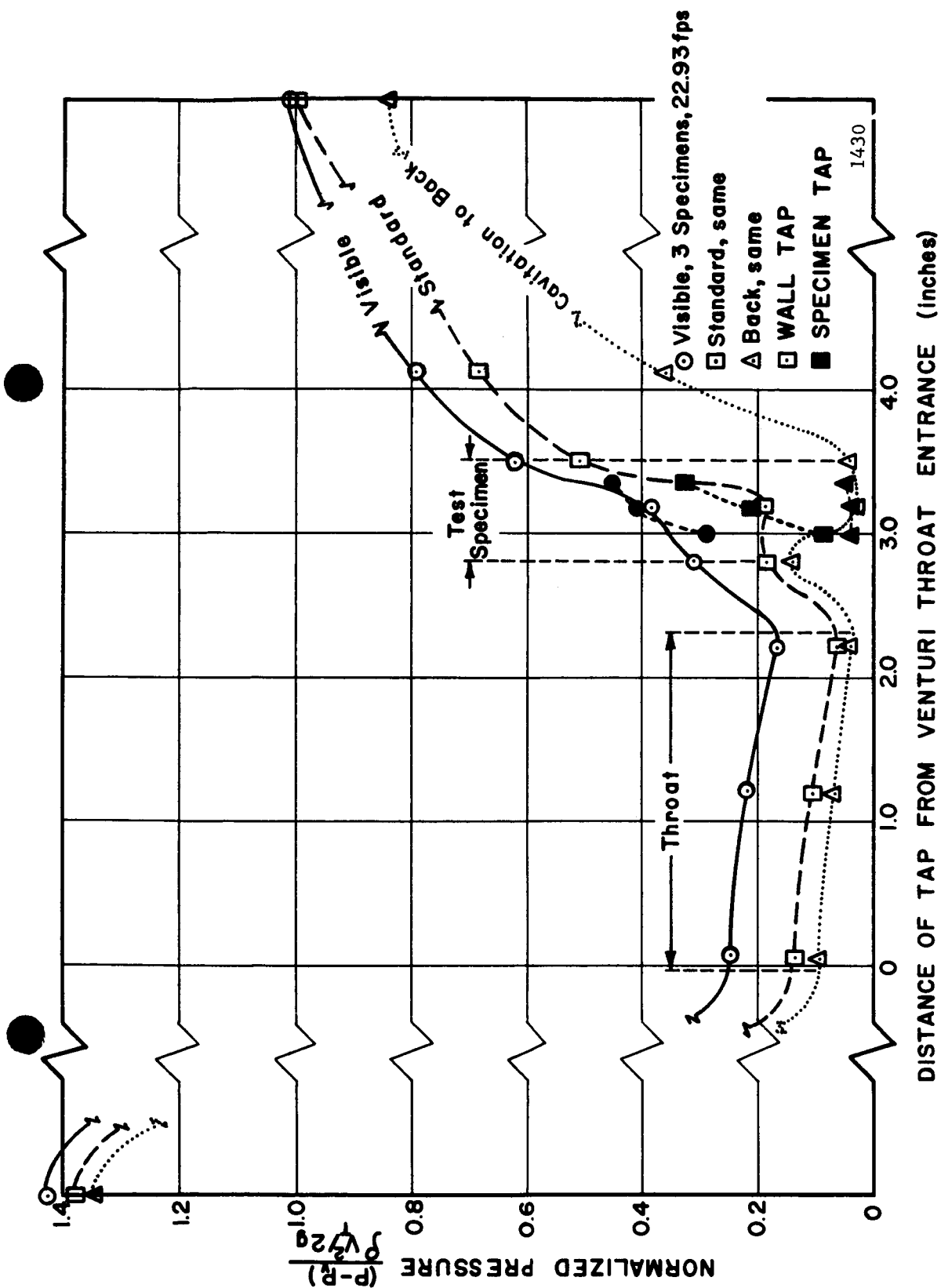


Fig. 15. Normalized Pressure Profile for Velocity of 22.9 ft/sec. in Mercury, 3 Specimens, at Various Cavitation Conditions.

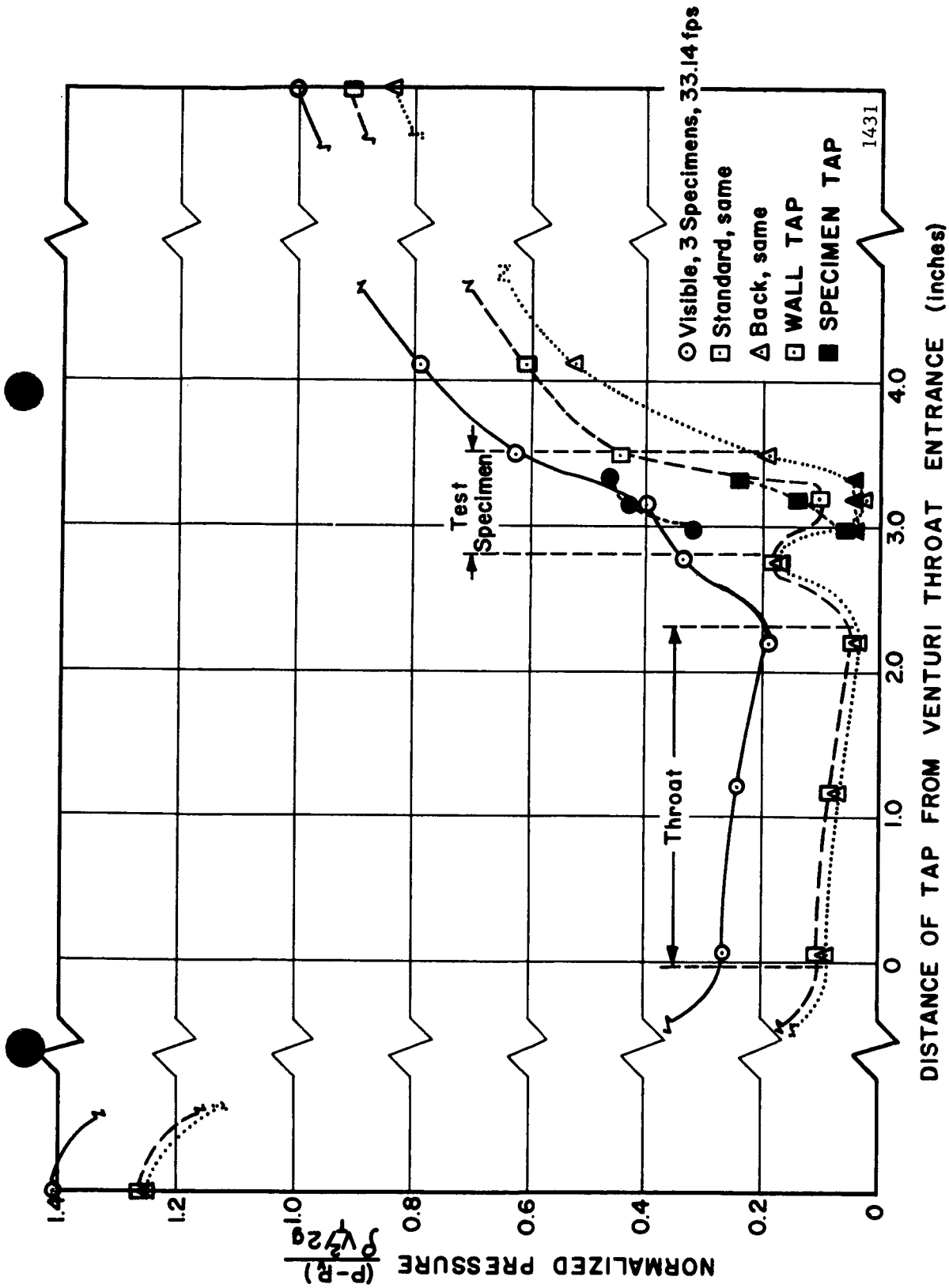


Fig. 16. Normalized Pressure Profile for Velocity of 33.1 ft/sec.,
3 Specimens, in Mercury, at Various Cavitation Conditions.

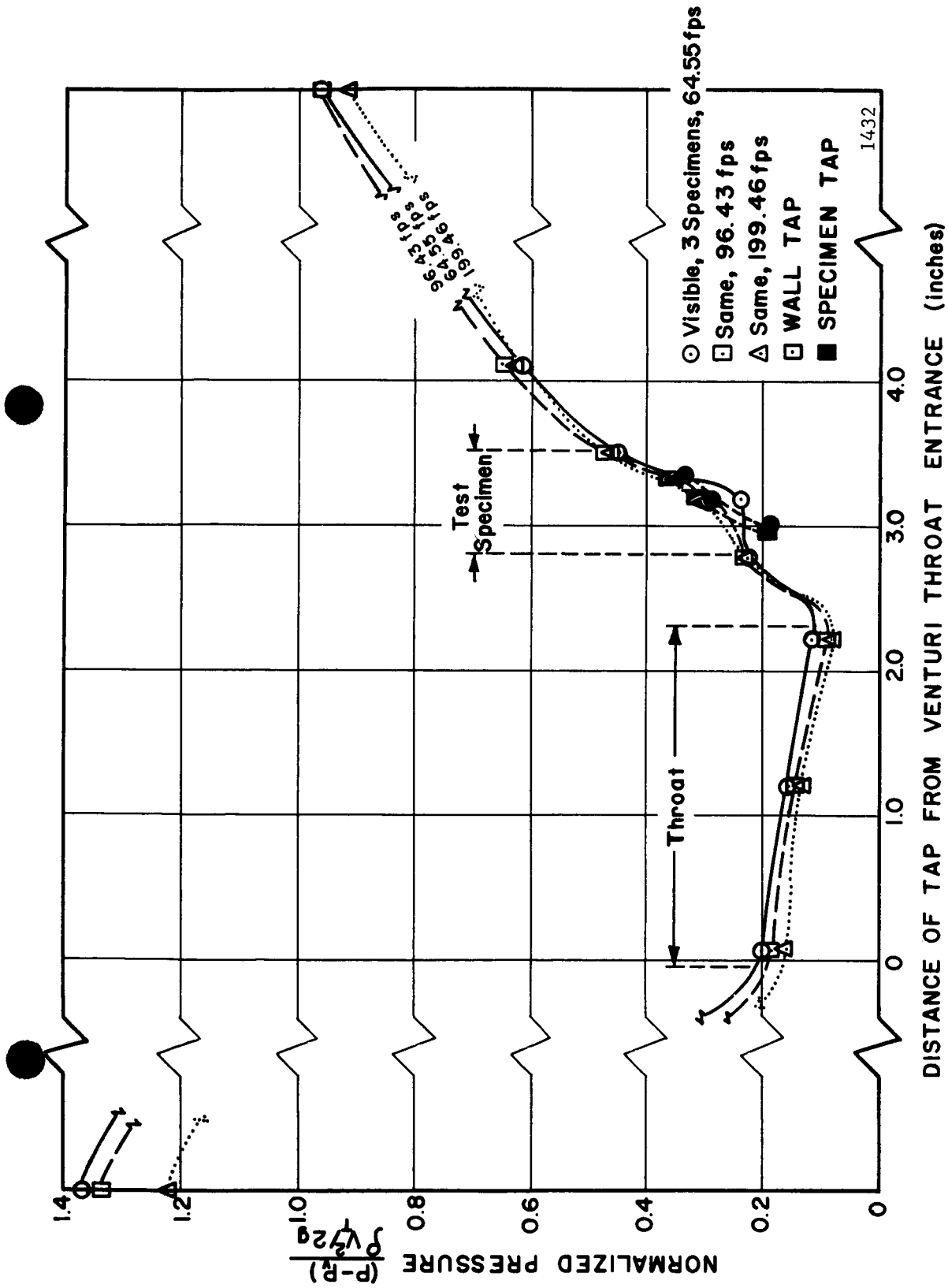


Fig. 17. Normalized Pressure Profile for Visible Initiation,
3 Specimens, in Water, at Various Velocities.

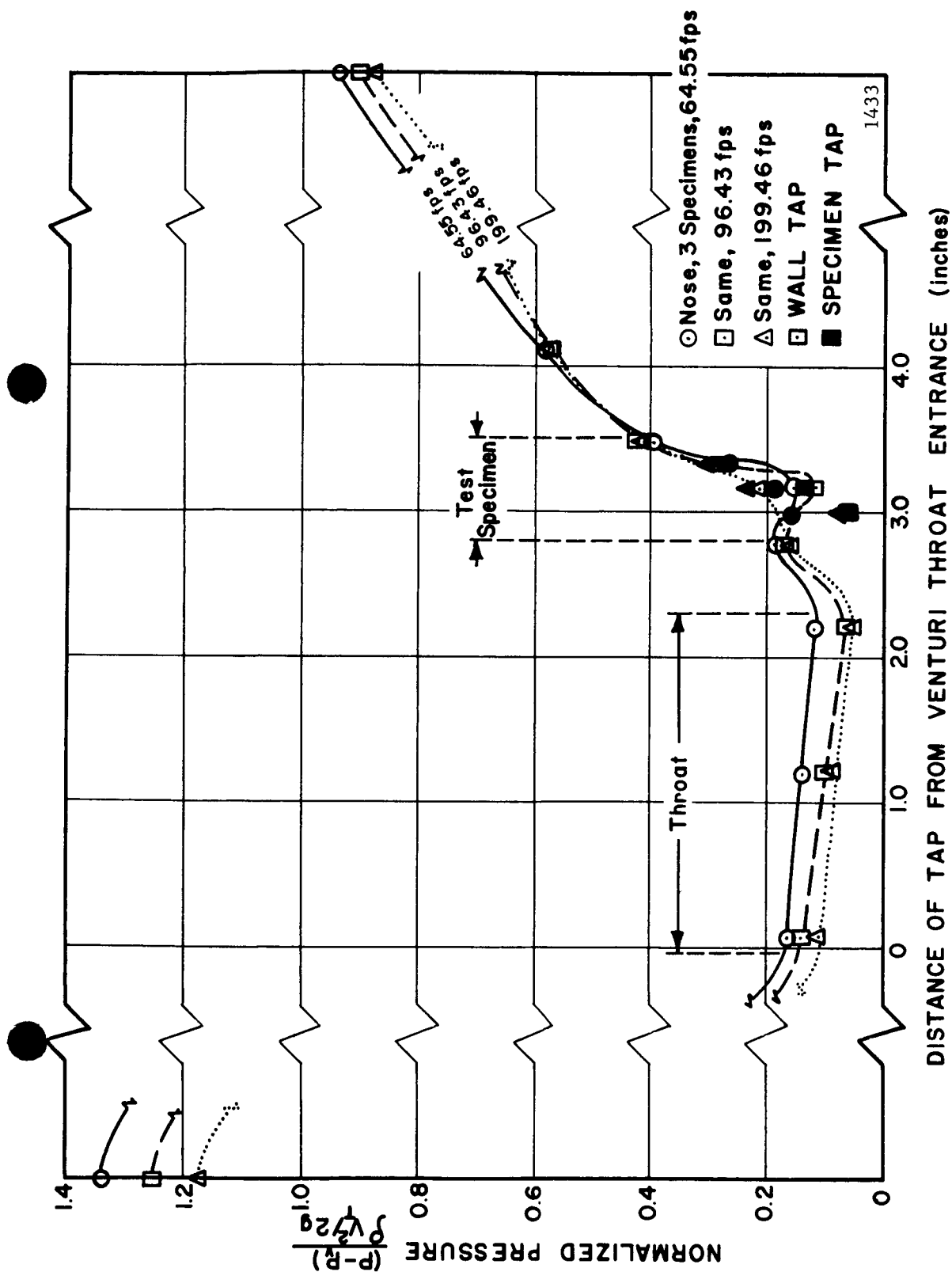


Fig. 18. Normalized Pressure Profile for Cavitation to Nose, 3 Specimens, in Water, at Various Velocities.

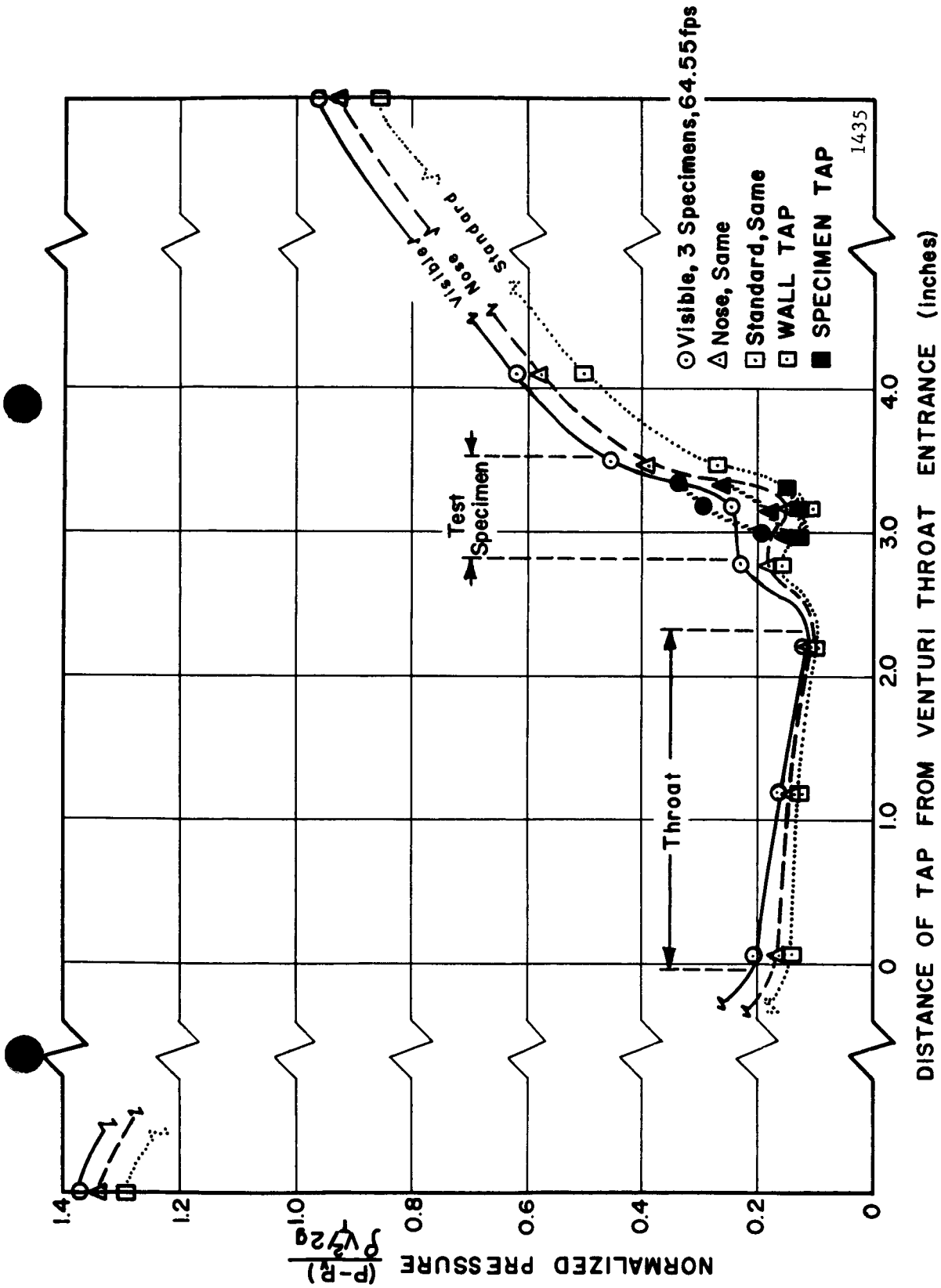


Fig. 20. Normalized Pressure Profile for 64.5 ft/sec., 3 Specimens, in Water, at Various Cavitation Conditions.

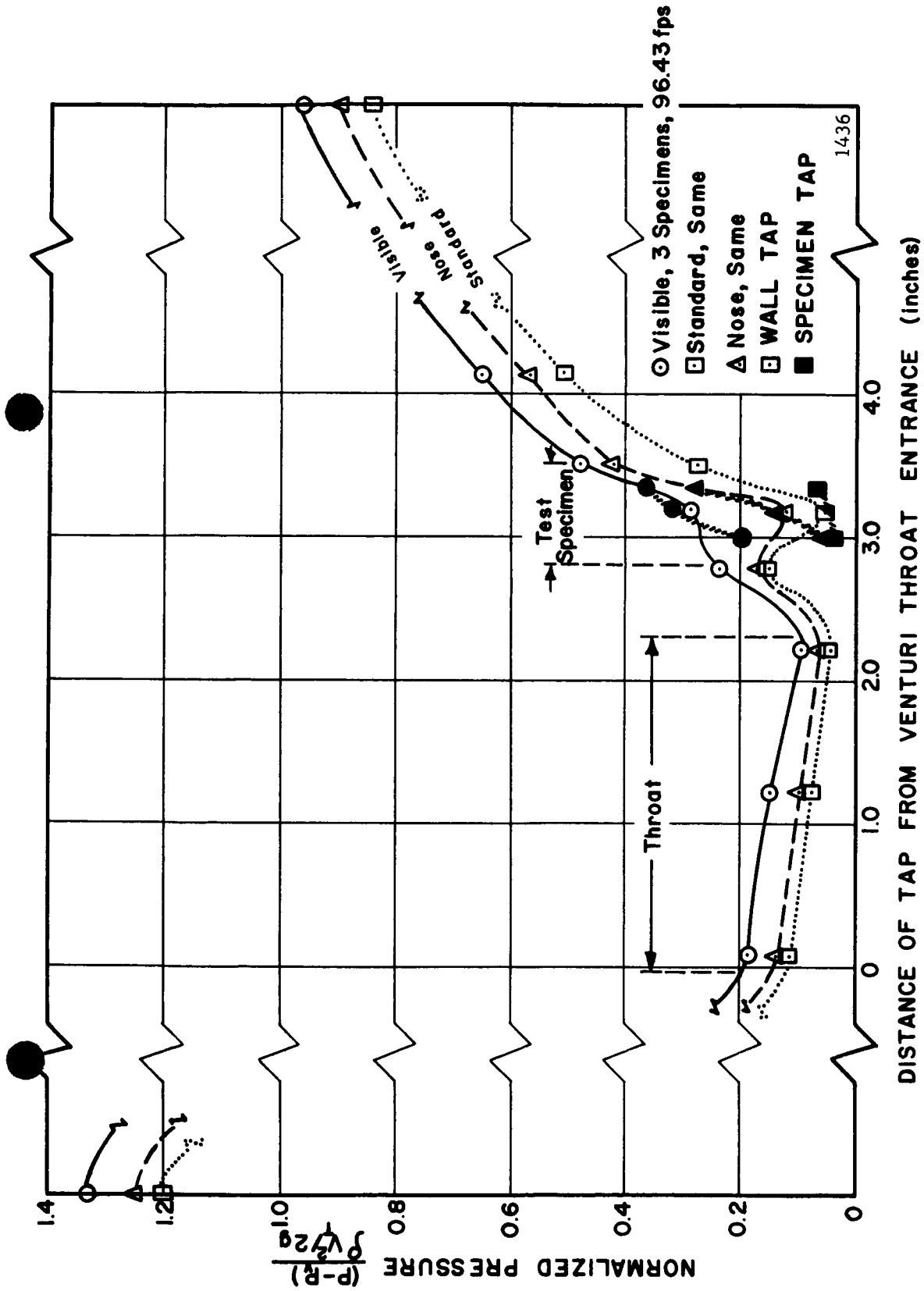


Fig. 21. Normalized Pressure Profile for 96.4 ft/sec., 3 Specimens, in Water, at Various Cavitation Conditions.

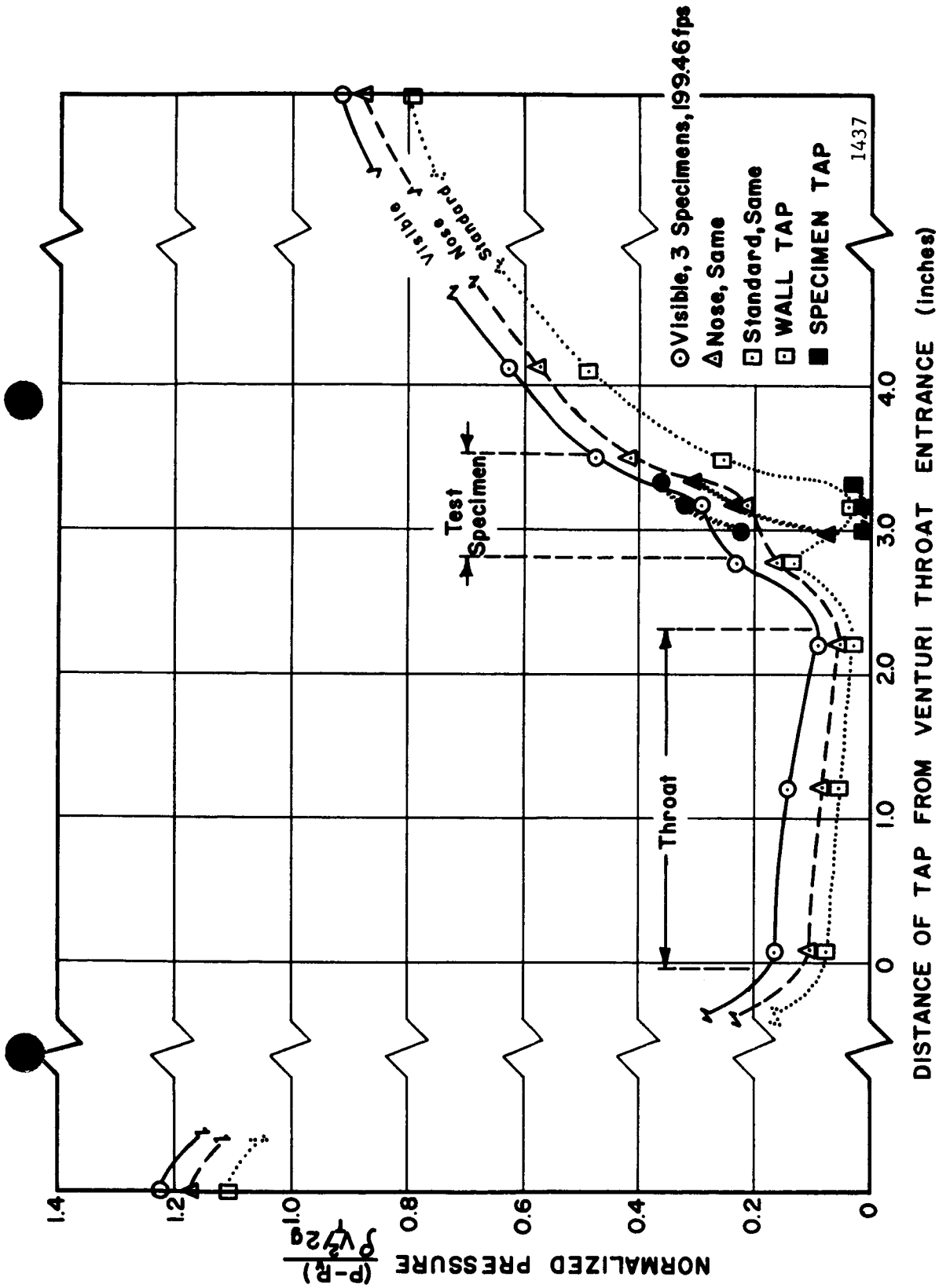
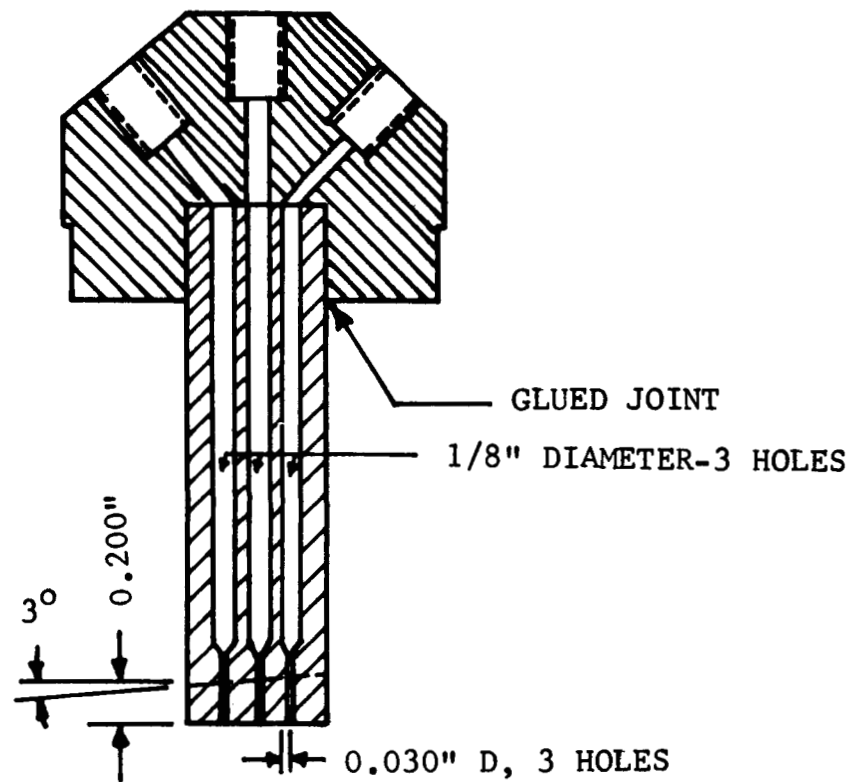


Fig. 22. Normalized Pressure Profile for 199.5 ft/sec., 3 Specimens, in Water, at Various Cavitation Conditions.



SECTION A-A

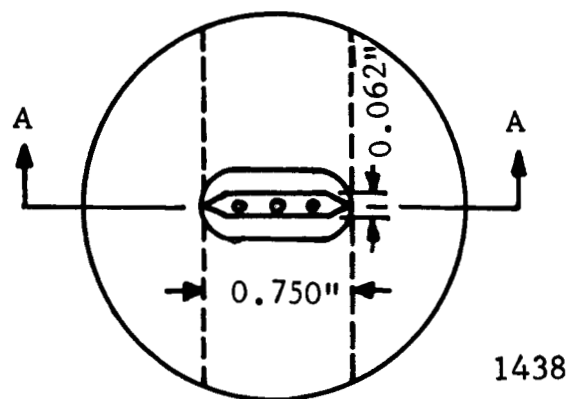


Fig. 23. Drawing of Plexiglas Holder-Specimen Combination for Measuring Pressures on the Specimen Face.

From the pressure profiles (Figures 13-22) it can be seen that the pressures on the specimen surface are slightly lower than the wall pressures measured at the same axial location. For the more developed cavitation conditions the pressure on the wall adjacent to the nose of the specimen is apparently increased by the flow pattern around the specimen, presumably causing an increased kinetic component in the tap reading. It can also be seen quite clearly that the pressure gradient on the surface of the specimens is very substantial for the less developed cavitation conditions and less so for the more fully developed conditions, where the entire surface of the specimen is under pressure not too greatly in excess of vapor pressure.

The normalized profiles for different velocities are almost identical (Figures 13, 14, 17, 18 and 19). Hence, the actual pressures on the surface of the test specimens are relatively higher for the higher velocity cases, and this difference becomes substantial in terms of actual pressure for the less developed cavitation conditions. Actual pressure values are given in the next section under velocity effects, which illustrate this very clearly.

4.3.2 Experimental Results

a. Water Tests

The effect of velocity upon normalized* mean depth of penetration at 50 and 100 hours duration (where comparisons are available from

*Normalized to the maximum mean depth of penetration data point for the particular set of comparative data. Hence, damage magnitude comparisons between different materials are not possible from these curves.

the present data) are shown for water in Figures 24 and 25. Figure 24 shows the copper and brass data for "Standard Cavitation." It is noted that velocity has very little effect between 64 and 97 ft./sec., but fairly substantial effect between 97 and 200 ft./sec., for which latter range, the average damage velocity exponent is about 1.5.* Generally speaking, the overall effect is somewhat greater for the brasses than the coppers. For the highest velocity (200 ft./sec.), the pressure gradient on the surface of the specimens is greater than for the others; so that the downstream end of the specimen is exposed to a higher pressure above vapor pressure by a factor of 2 to 3 than for the two lower velocities, for which two the pressure above vapor pressure is almost the same. Thus, the bubbles collapsing on the surface of the specimens are exposed to a greater driving force for collapse, thus causing greater damage in the 200 ft./sec. runs. However, the effect on the pressures of varying the velocity over this range is much less than might be expected, and hence the effect of velocity on damage is also fairly small. Table 7 shows typical sets of data for both water and mercury. It is noted that the effect of velocity on pressure for the mercury data is also quite small, as was the damage variation with velocity. An exception is the downstream tap position for the "wet" mercury high-velocity run. The pronounced difference in pressure profiles between "dry" and "wet" mercury is not explainable at present. However, the more rapid pressure recovery in the "wet" mercury may be related to the higher damage rates observed.

*Assuming the relation: $\text{Damage} = \text{Constant} \times \text{Velocity}^n$, where n is the damage velocity exponent.

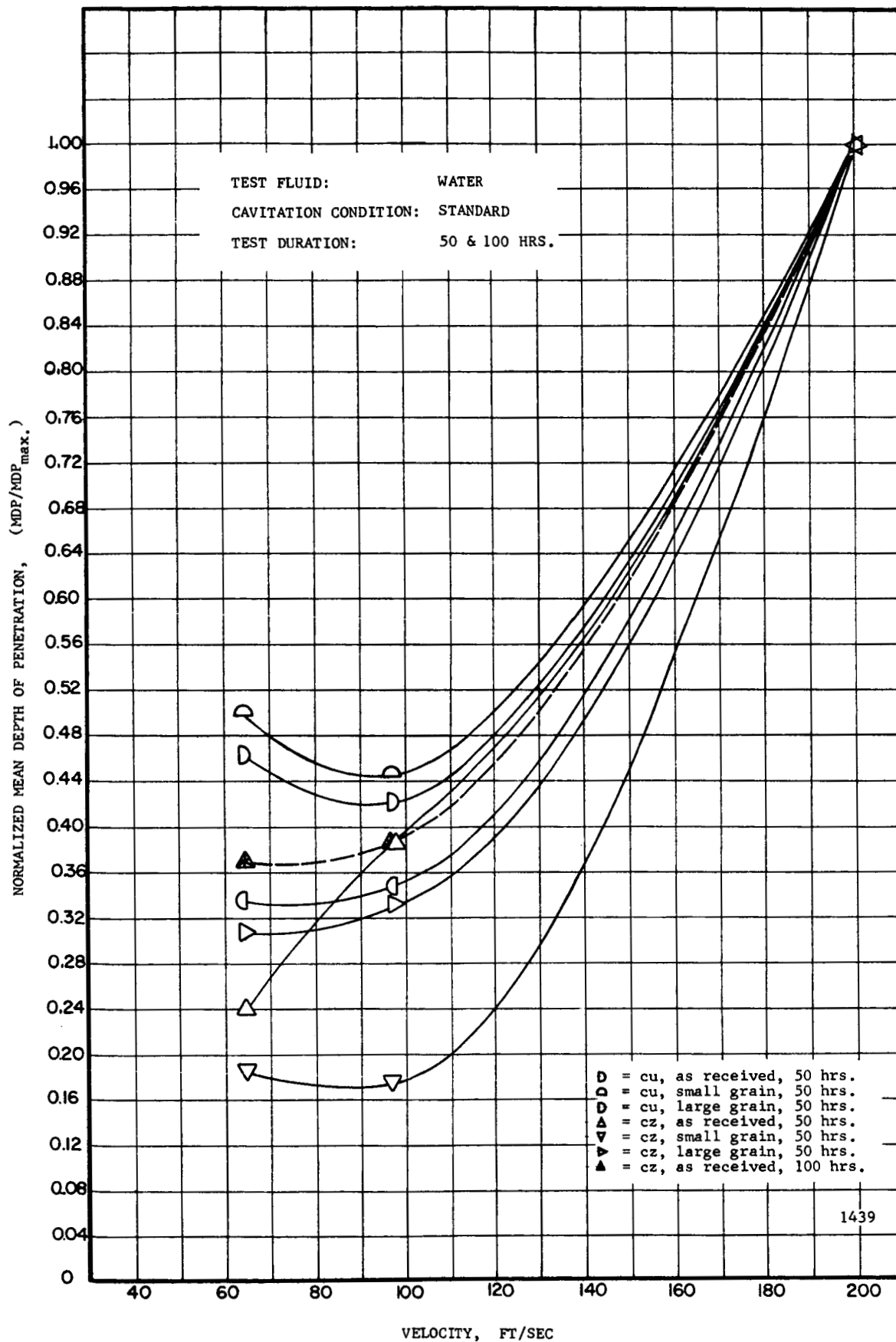


Fig. 24. $(MDP)/(MDP_{max})$ versus Velocity for Standard Cavitation in Water for Copper and Brasses.

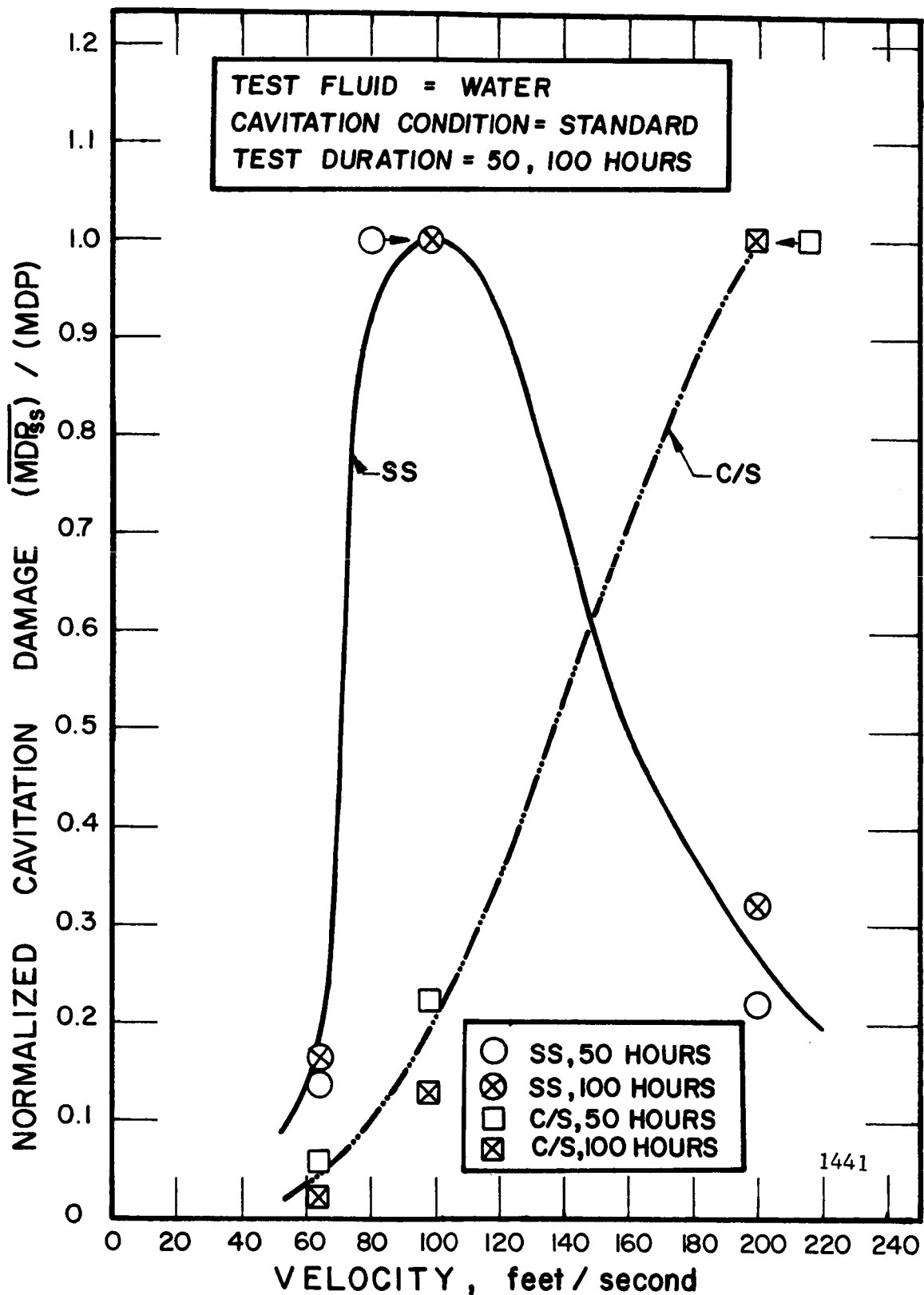


Fig. 25. $(MDP)/(MDP_{max})$ versus Velocity for Standard Cavitation in Water for Stainless Steel and Carbon Steel.

TABLE 7

ACTUAL PRESSURE ABOVE VAPOR PRESSURE ON TEST SPECIMEN SURFACE
FOR STANDARD CAVITATION IN MERCURY AND WATER¹⁵

Fluid	Velocity Ft./Sec.	No. of Specs.	Spec. Tap No.	Pressure (psi)		
				Run No. 1	Run No. 2	Run No. 3
Water 54°F.	64	3	1	3.9	4.4	3.0
			2	4.2	4.5	3.4
			3	4.6	5.0	3.9
Water 54°F.	97	3	1	2.6	2.6	2.4
			2	3.4	2.9	2.9
			3	4.9	4.3	3.3
Water 75°F.	200	3	1	4.0	3.9	3.5
			2	5.5	5.2	5.2
			3	11.7	7.1	6.2
"Dry" Mercury 75°F.	23	3	1	3.5	4.7	3.6
			2	9.2	11.0	10.0
			3	15.1	16.0	15.2
"Dry" Mercury 88°F.	34	3	1	5.3	7.0	6.5
			2	11.5	17.5	13.8
			3	19.1	29.3	25.5
"Dry" Mercury 120°F.	46	3	1	12.1	9.1	8.7
			2	9.4	9.8	8.2
			3	14.7	16.3	16.6
"Wet" Mercury 75°F.	23	3	1	9.7	11.1	9.7
			2	15.5	15.8	15.4
			3	21.6	22.1	21.5
"Wet" Mercury 88°F.	34	3	1	3.3	3.1	3.0
			2	11.4	12.2	11.0
			3	31.1	31.3	29.3
"Wet" Mercury 115°F.	46	3	1	8.3	3.5	4.8
			2	20.6	16.0	15.0
			3	59.8	30.5	51.8

No data is yet available for these materials at other cavitation conditions. However, it is expected that the increase of damage with velocity should be greater for "Cavitation to Nose" or "Visible Initiation," since the pressure across the specimen would then be higher and more dependent upon velocity. By the same token, it is presumed that the velocity effect would be much less for a more fully developed cavitation condition as "Cavitation to Back." The pressure profiles in Figures 20, 21, and 22 for water and Figures 15 and 16 for mercury demonstrate the above suppositions very clearly. It can be seen that the pressure gradient on the surface of the test specimens is very severe for "Visible Initiation" and "Cavitation to Nose" and very low for "Standard Cavitation" and "Cavitation to Back." Comparing five Figures 15, 16, 20, 21 and 22, it is also noted that the absolute magnitude of the pressure gradient on the surface of the test specimens increases with velocity, for any cavitation condition, since, for a given cavitation condition, the normalized gradients are not particularly velocity-sensitive.

Figure 25 shows for stainless steel and carbon steel comparisons corresponding to Figure 24 for the brasses, etc. The carbon steel curve is quite similar to that for the brasses especially, except that the effect in the lower velocity range is greater. The overall velocity exponent for this curve is about 3. The curve for stainless steel is greatly different in that the maximum damage occurs at 97 ft./sec., and the damage decreases considerably for 200 ft./sec. It is believed that the explanation for such unexpected behavior, which, as will be noted, also occurs for mercury in some cases, involves the interplay between

the increased collapse pressure due to increased velocity and detailed flow-structure changes lumped under the term "scale effects." Presumably material properties are also involved, since they affect the relative importance of different damage mechanisms.

b. Mercury Tests

The velocity effects with mercury for "Standard Cavitation" are shown in Figure 26 for stainless steel and Cb - 1Zr alloy, both after 50 and 100 hours in those cases for which data is available. In addition, a curve for stainless steel for "Cavitation to Back" is included.

The effect of a velocity change over the range from 24 to 64 ft./sec. at "Standard Cavitation" for stainless steel is not significant. As noted, the 50 hour curve shows a minimum at 34 ft./sec. and the 100 hour curve a maximum at the same point. However, the differences are not large enough to be considered significant in view of the limited data. Cb - 1Zr shows about a 2:1 increase of damage for an increase of velocity from 34 to 48 ft./sec., corresponding to a velocity exponent of about 2 over this range. Again, the data is considered too limited to be significant. For "Cavitation to Back" a decrease in damage by a factor of about 4 is shown for a velocity increase from 34 to 64 ft./sec.

On the whole, it is felt that no consistent trend of damage with velocity is indicated by this rather limited data for the well-developed cavitation conditions. Since static pressure in the region of the test specimens (Figures 13 and 14) is not particularly velocity-dependent, the general result is as expected.

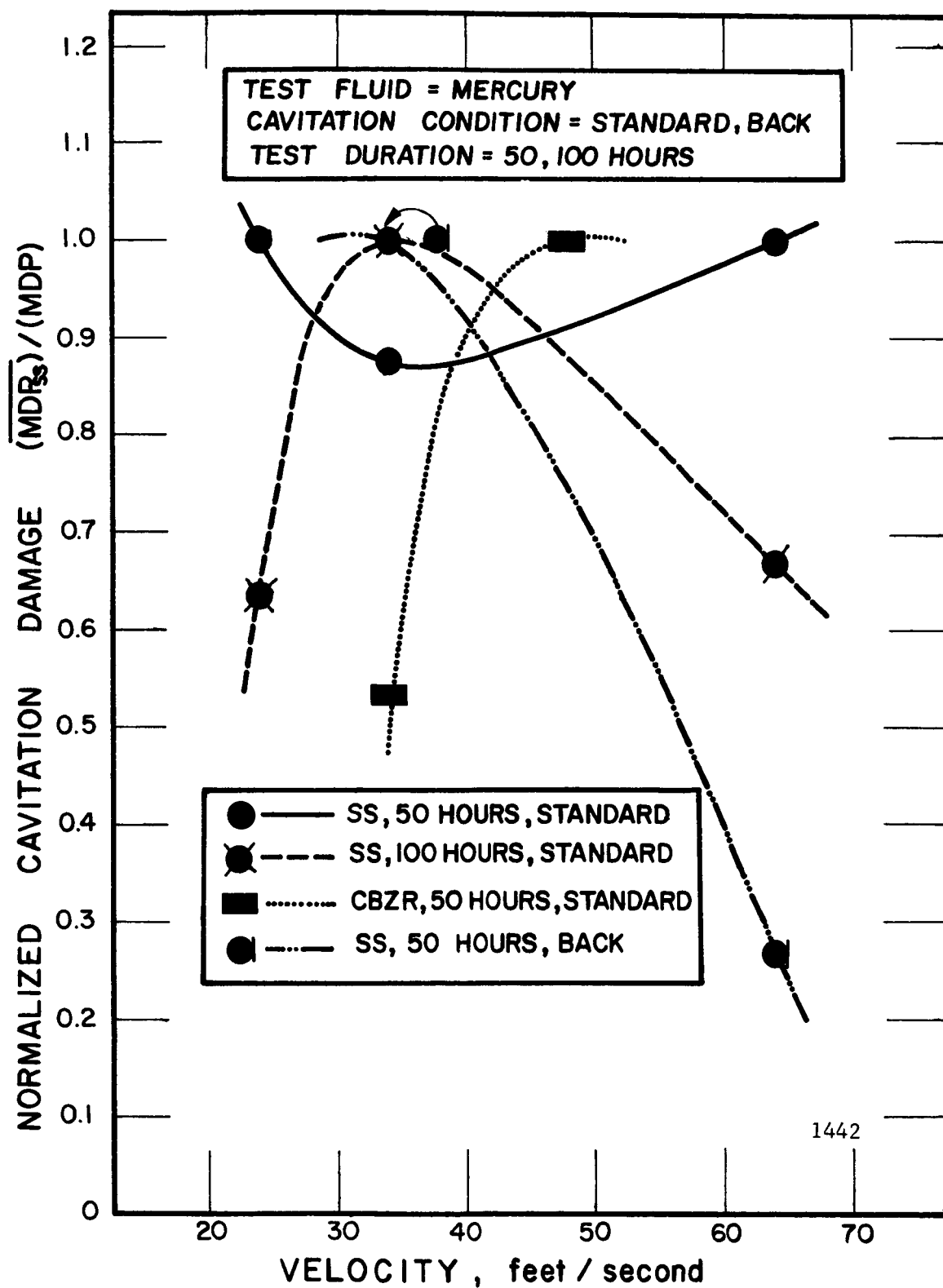


Fig. 26. $(MDP)/(MDP_{max})$ versus Velocity for Standard and Back Cavitation in Mercury for Stainless Steel and Columbian-1% Zirconium.

The velocity effect in mercury for the less-developed cavitation conditions of "Cavitation to Nose" and "Visible Initiation" are shown in Figure 27 for those cases where the data exists. Figure 13 shows the corresponding pressure profile for "Visible Initiation" in the lower velocity range. Since the normalized pressure above vapor pressure is well above zero over the test specimen, the actual pressure varies substantially with velocity. Thus, the driving force causing bubble collapse is highly velocity-dependent for these cavitation conditions, so that it would be expected that damage would increase strongly with velocity. Examination of the curve for "Cavitation to Nose" indicates that this is the case with a velocity exponent as averaged over the different materials of about 2.2. The single-point data for "Visible Initiation," while still showing an increase of damage with velocity, is apparently less velocity-dependent. Since the overall damage for this condition is much less, and hence the experimental precision much poorer, this point should not be considered as particularly significant compared to the "Nose Cavitation" points.

The present data, both for mercury and water, gives no good indication (with the possible exception of Figure 27) of the existence of a threshold velocity. It seems more likely that for this type of facility there will be some damage even for quite small velocities as long as cavitation itself occurs.

4.4 Degree of Cavitation Effects

4.4.1 General Anticipations

As previously discussed in greater detail,³ varying the degree of cavitation from initiation toward the more fully-developed conditions

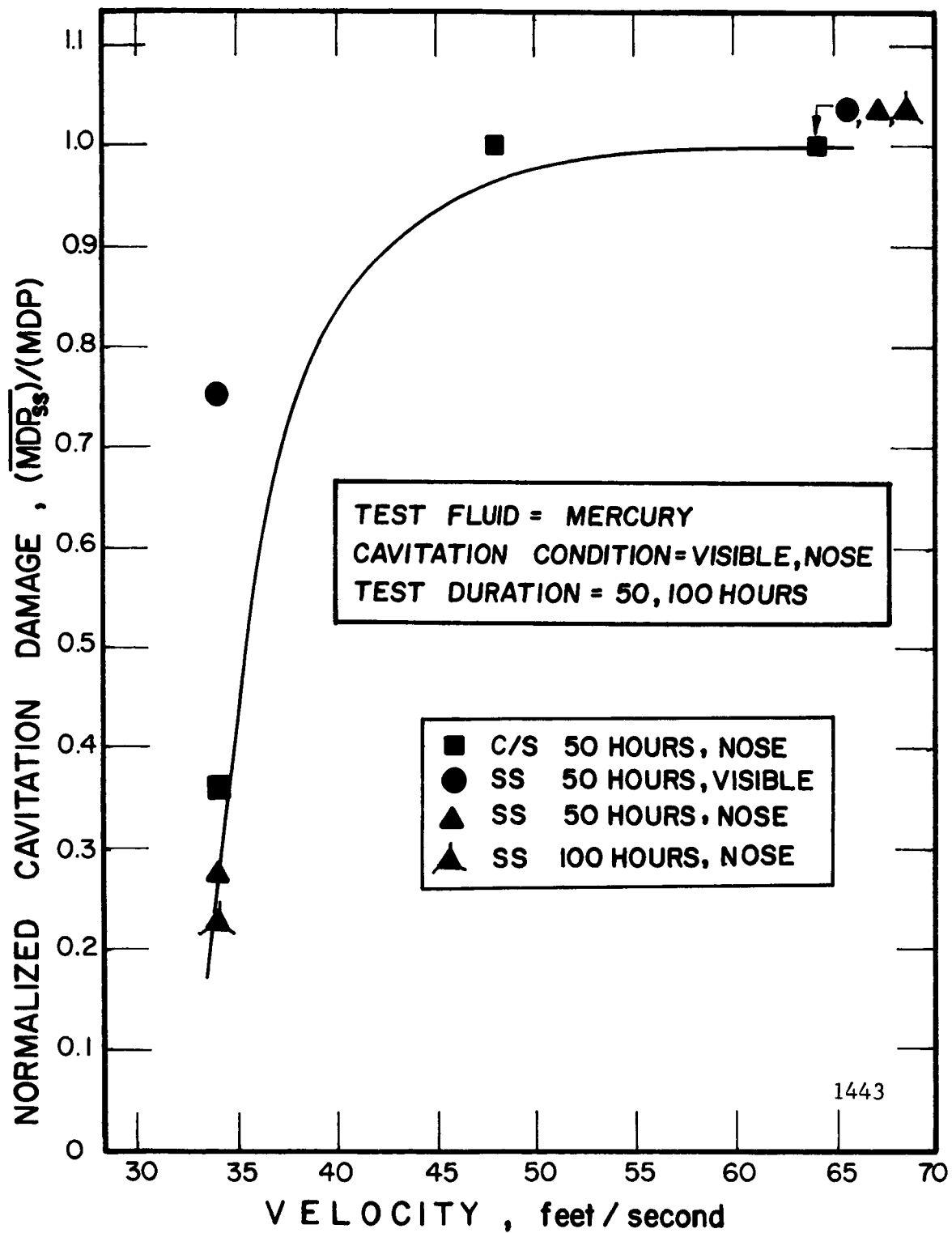


Fig. 27. $(MDP)/(MDP_{max})$ versus Velocity for Visible and Nose Cavitation in Mercury for Stainless and Carbon Steel.

(at fixed velocity) has two primary effects relative to damage:

- i) The average normalized static pressure adjacent to the specimens, causing bubble collapse decreases;
- ii) The number of bubbles in the vicinity of the test specimens increases. However, as the number of bubbles increases, the energy available per bubble to cause damage decreases. This is true even though many of the bubbles may be the result of local cavitation caused by the specimens themselves. Thus, it would be expected that damage would increase from very little as cavitation condition was increased from initiation, would pass through a maximum, and then decrease as the bubbles became of insufficient energy to cause damage. Representative axial pressure profiles are presented in Figures 15, 16, 20, 21 and 22.

As has been previously discussed,¹ the situation may be represented by a plot as shown schematically in Figure 28, showing a hypothesized bubble energy spectrum, i.e., $n(E)$ = (number of bubbles of energy E) vs. E . As shown in the figure, as the cavitation degree moves toward fully-developed ("First Mark Cavitation"), the number of bubbles increases, but the average energy per bubble decreases.

4.4.2 Experimental Results

The experimental results relating degree of cavitation to damage are summarized in Figure 29. Separate curves are shown for the following distinct conditions:

- i) Three-specimen venturi in water (copper and brass specimens)
- ii) Two-specimen venturi in water (stainless steel)

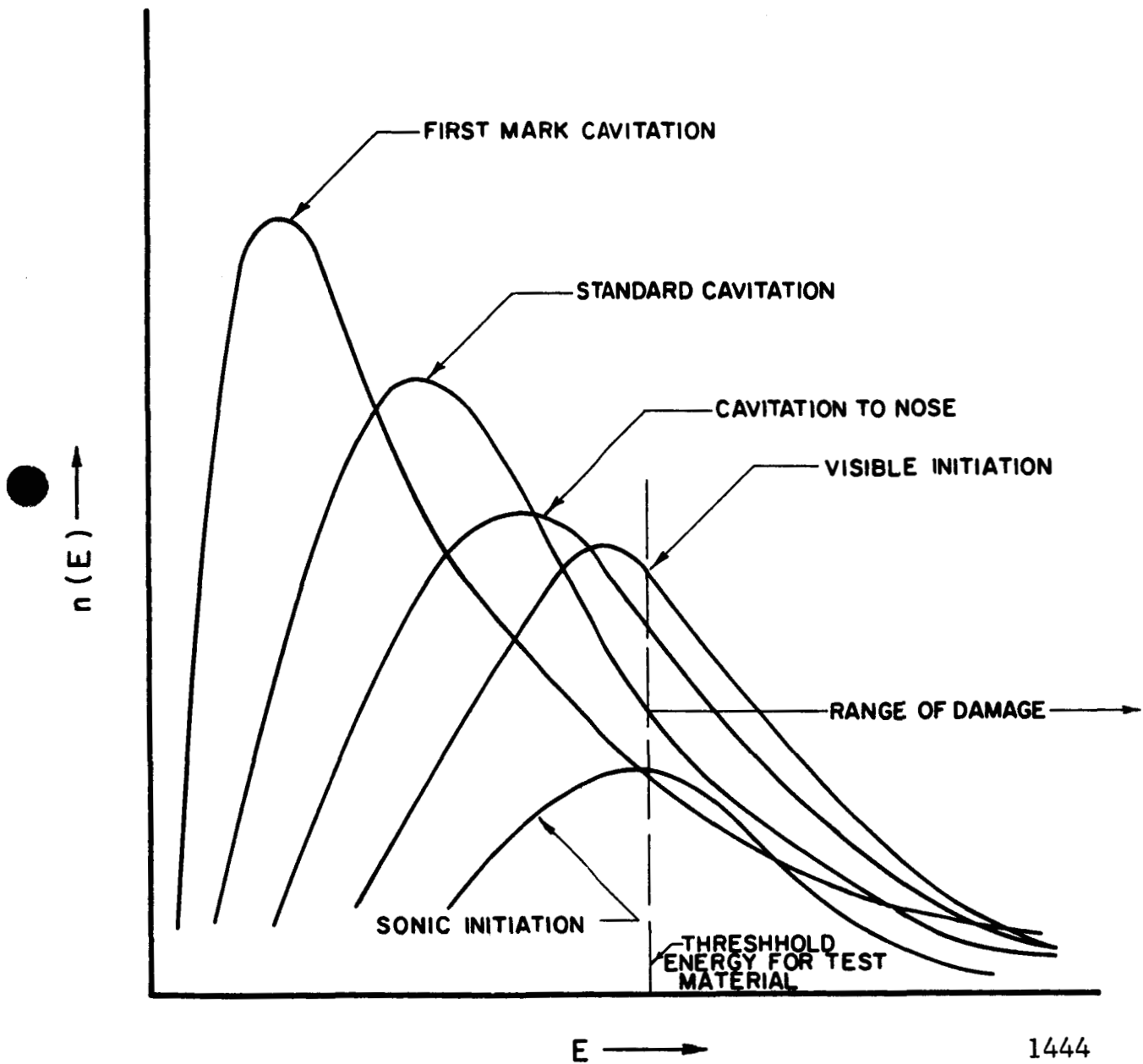


Fig. 28 Hypothesized bubble energy spectra for various cavitation conditions at a constant velocity, for a given material. Presumably, curves at higher velocity are generally similar, but at higher $n(E)$ and E . The quantity $n(E)$ = number of bubbles from those "in vicinity" of damage specimen which deliver an energy quantum E to the surface of the specimen, and E = energy delivered by an individual bubble to the surface of the specimen.

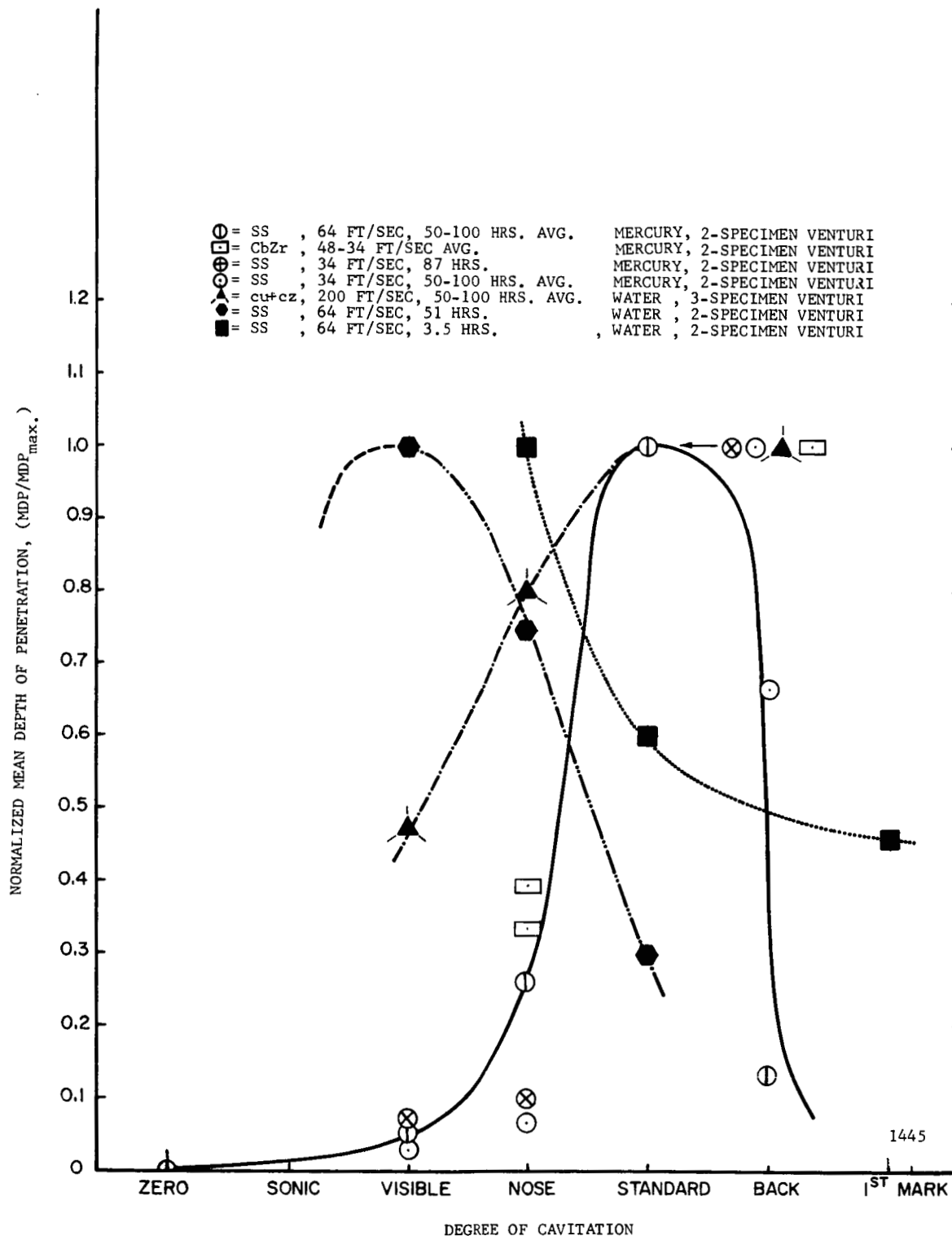


Fig. 29. $(MDP)/(MDP_{max})$ versus Cavitation Condition for Various Materials in Mercury and Water.

- iii) Two-specimen venturi in mercury--included are points for two materials (stainless steel and Cb - 12r) and two velocities (34 and 64 ft./sec.)

The number of specimens in the venturi, i.e., whether a two- or three-specimen venturi is used (designs of which have been previously described), is important because of the change in flow pattern and pressure profile in the vicinity of the specimens, as discussed below. The durations for which the comparisons are made are generally of the order of 50 to 100 hours and are appropriately labeled on the curve sheet.

a. Overall Trend

The overall trend is as expected, i.e., for all cases the damage passes through a maximum as the degree of cavitation is increased from zero, approaching very low values for either extreme, i.e., initiation or fully-developed ("First Mark Cavitation").

b. Two-Specimen vs. Three-Specimen Venturi

The comparison between two-specimen and three-specimen venturis with regard to damage effects is available only for water, and must be made across materials, i.e., sets of copper and brass data only are available for the three-specimen unit, and only stainless steel data for the two-specimen type. It appears that the most damaging condition for the two-specimen venturi is close to "Visible Initiation," and for the three-specimen type it is close to "Standard Cavitation." At present, the corresponding pressure profiles in water are only available for "Standard Cavitation" showing the effects of number of specimens at three fixed velocities. These are presented in Figures 30, 31 and 32.

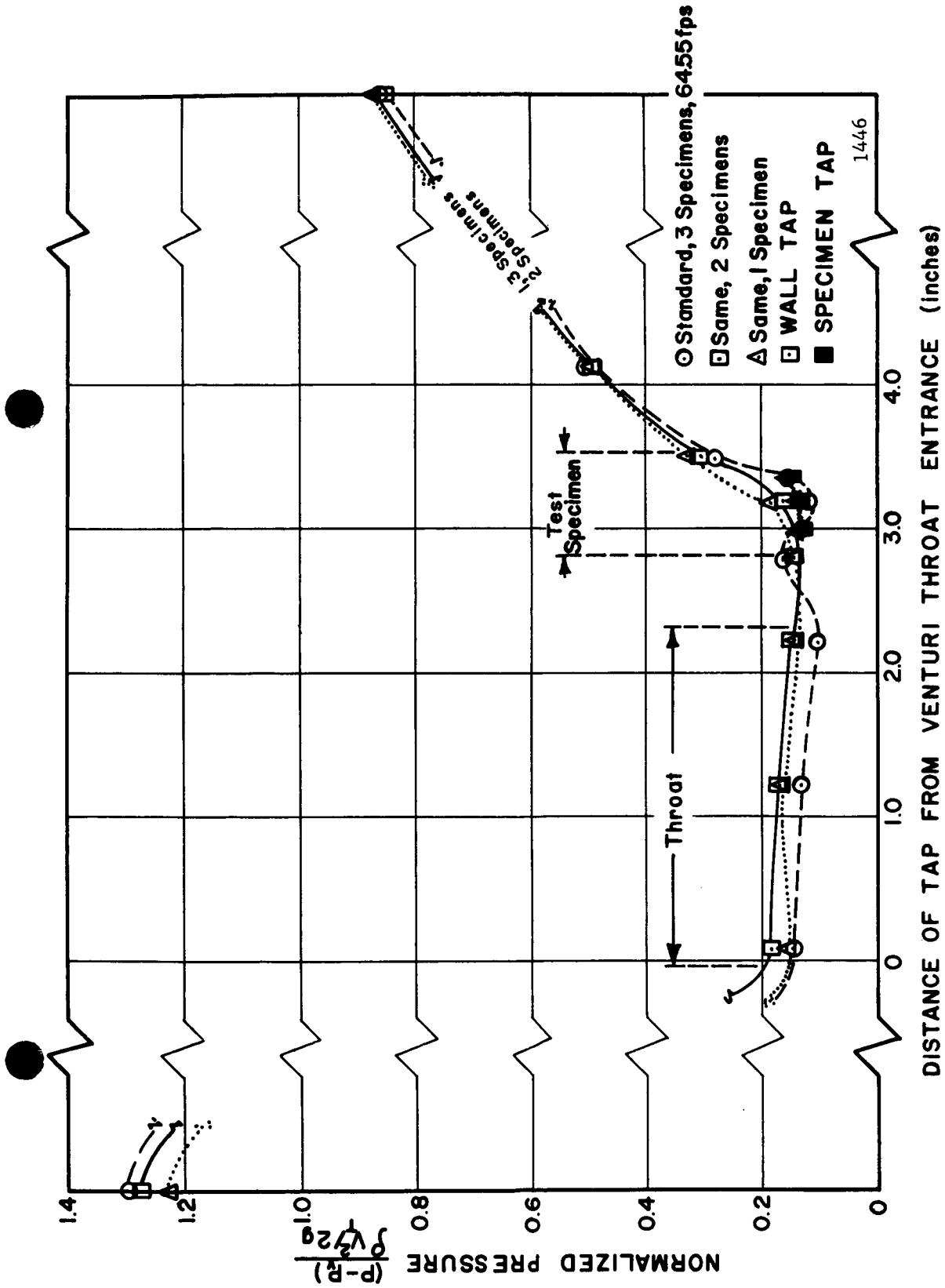


Fig. 30. Normalized Pressure Profile for Velocity of 64.5 ft/sec., for Standard Cavitation in Water, 1, 2 and 3 Specimens.

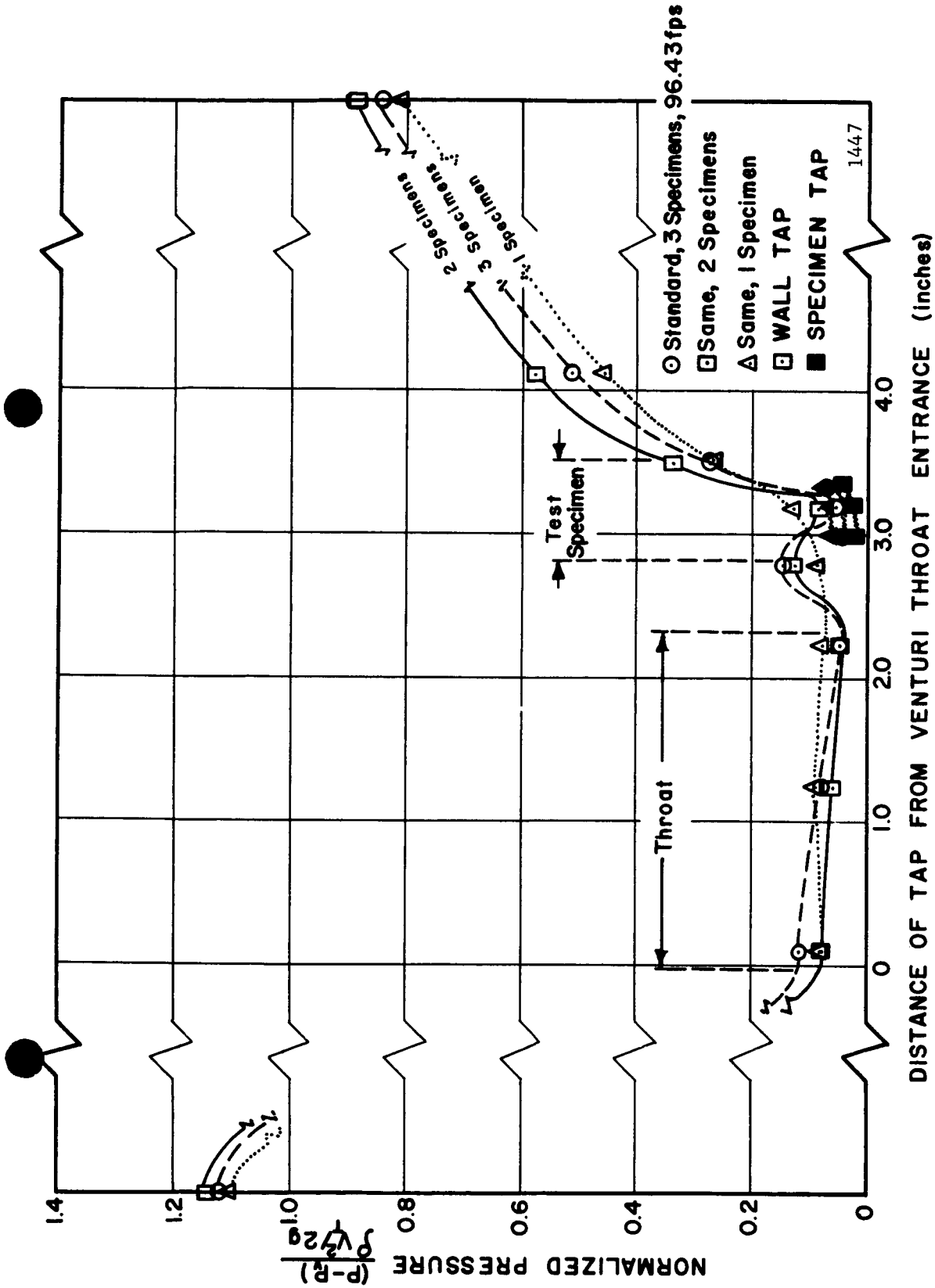


Fig. 31. Normalized Pressure Profile for Velocity of 96.4 ft/sec., for Standard Cavitation in Water, 1, 2 and 3 Specimens.

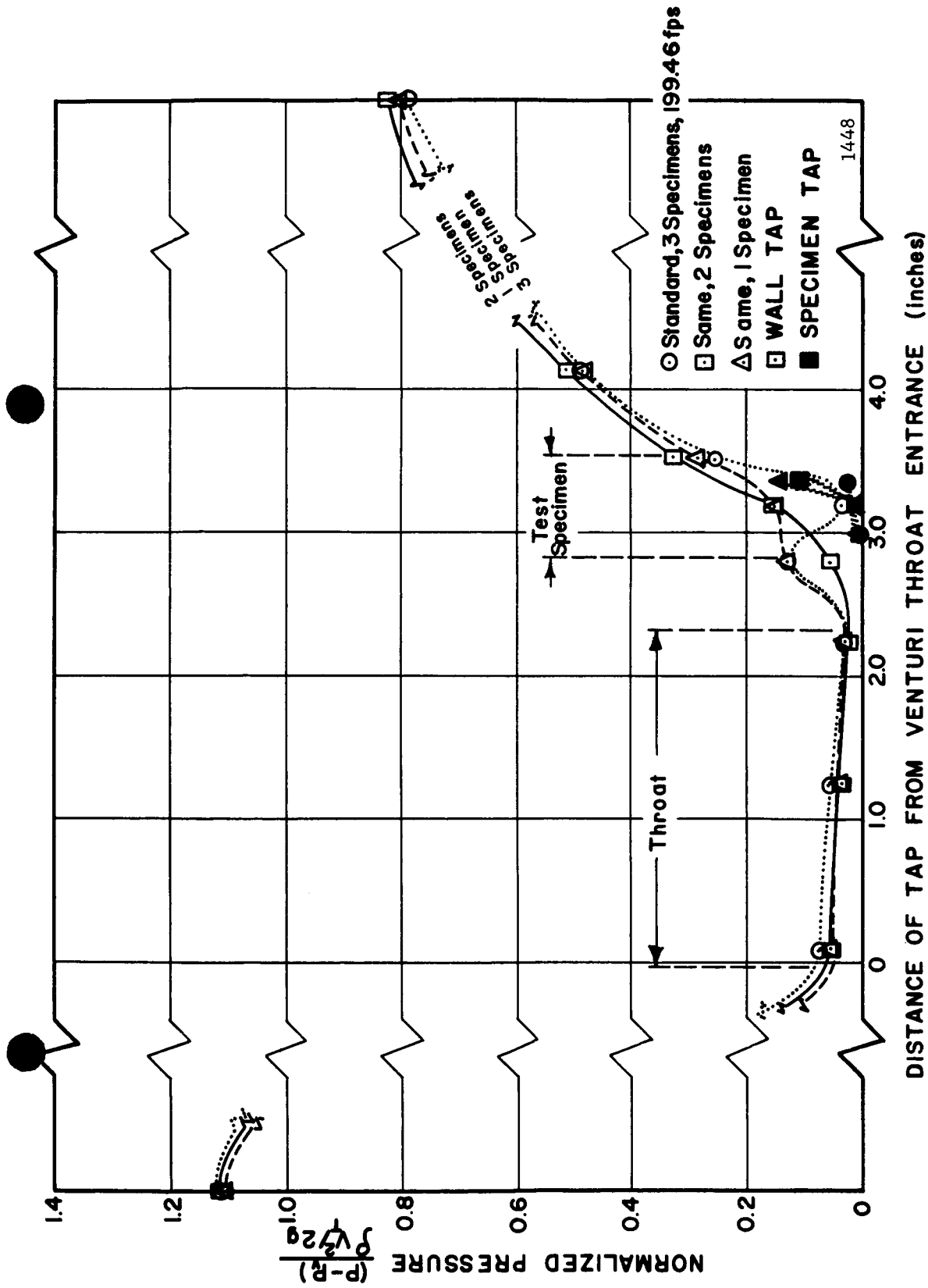


Fig. 32. Normalized Pressure Profile for Velocity of 199.5 ft./sec., for Standard Cavitation in Water, 1, 2 and 3 Specimens.

The difference between the two-specimen and three-specimen venturis for mercury at two velocities are shown in Figures 33, 34, 35 and 36. An examination of the corresponding pressure profiles in mercury shows that in general the magnitude of the actual pressures on the specimen surface is greater when the number of test specimens in the venturi is increased. Thus, the mean pressure for "Standard Cavitation" for the three-specimen venturi is similar to that for a less developed cavitation condition as "Cavitation to Nose" or "Visible Initiation" for a two-specimen unit, as required by the damage results previously discussed (Figure 29). However, the same comparison for the corresponding profiles in water shows little effect at the two lower velocities, but shows that the pressure gradient and pressures on the surface of the test specimens are greater for the two-specimen venturi than for the three-specimen venturi for 200 ft./sec.

As mentioned previously, although the same terms are used to describe the cavitation conditions for both types of venturis, the corresponding flow patterns are not identical. Detailed visual descriptions and cross correlations between mercury and water conditions are given in the Appendix.

c. Mercury vs. Water

The only presently available comparison between mercury and water is for the two-specimen venturi with stainless steel. For mercury, Cb - 1Zr is also available for the two-specimen venturi, while it is available only for water in the three-specimen venturi. In mercury, it yields results very similar to those of stainless steel, so that these two are lumped into a single curve.

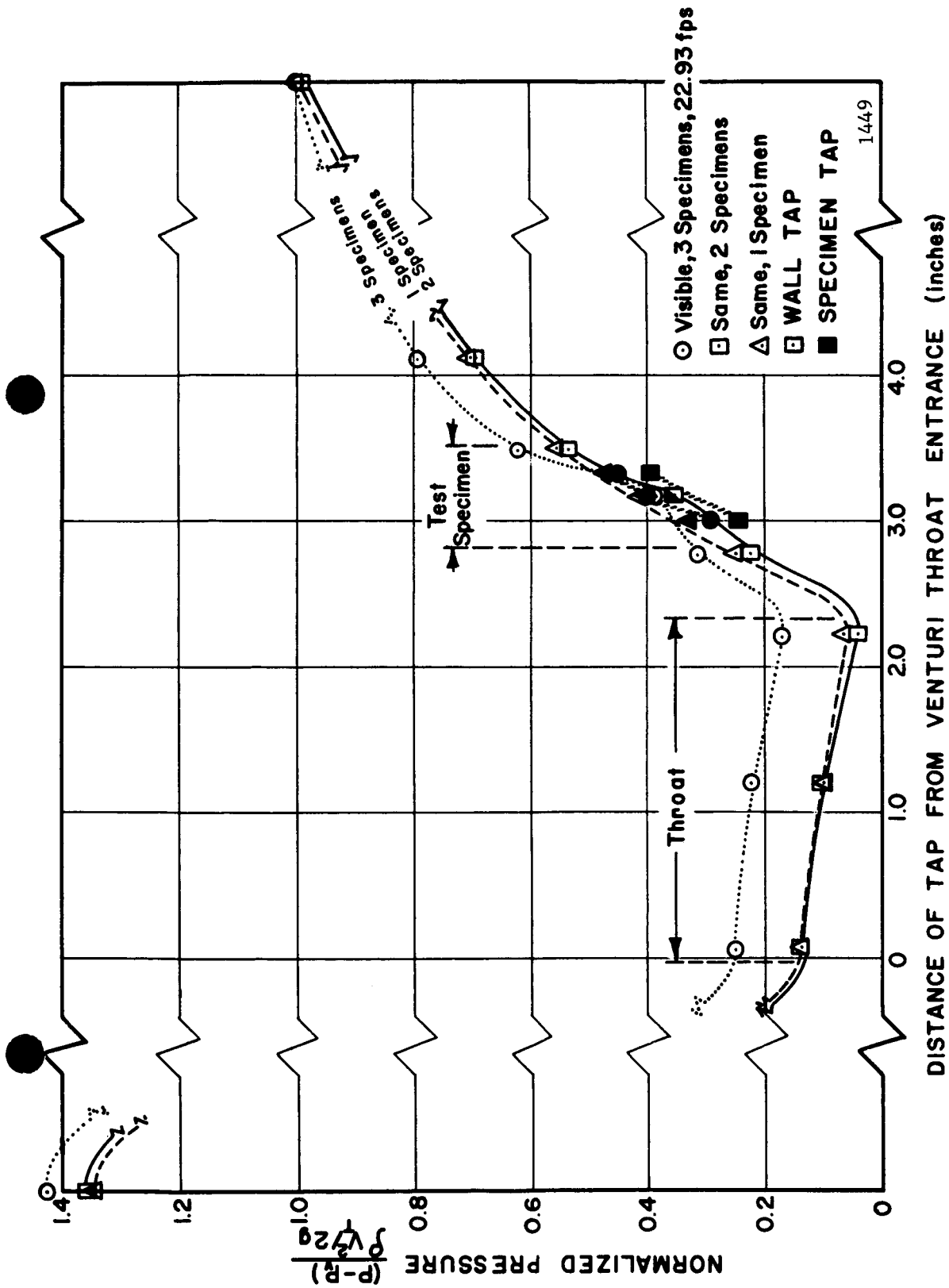


Fig. 33. Normalized Pressure Profile for Velocity of 22.9 ft/sec., for Visible Initiation in Mercury, 1, 2 and 3 Specimens.

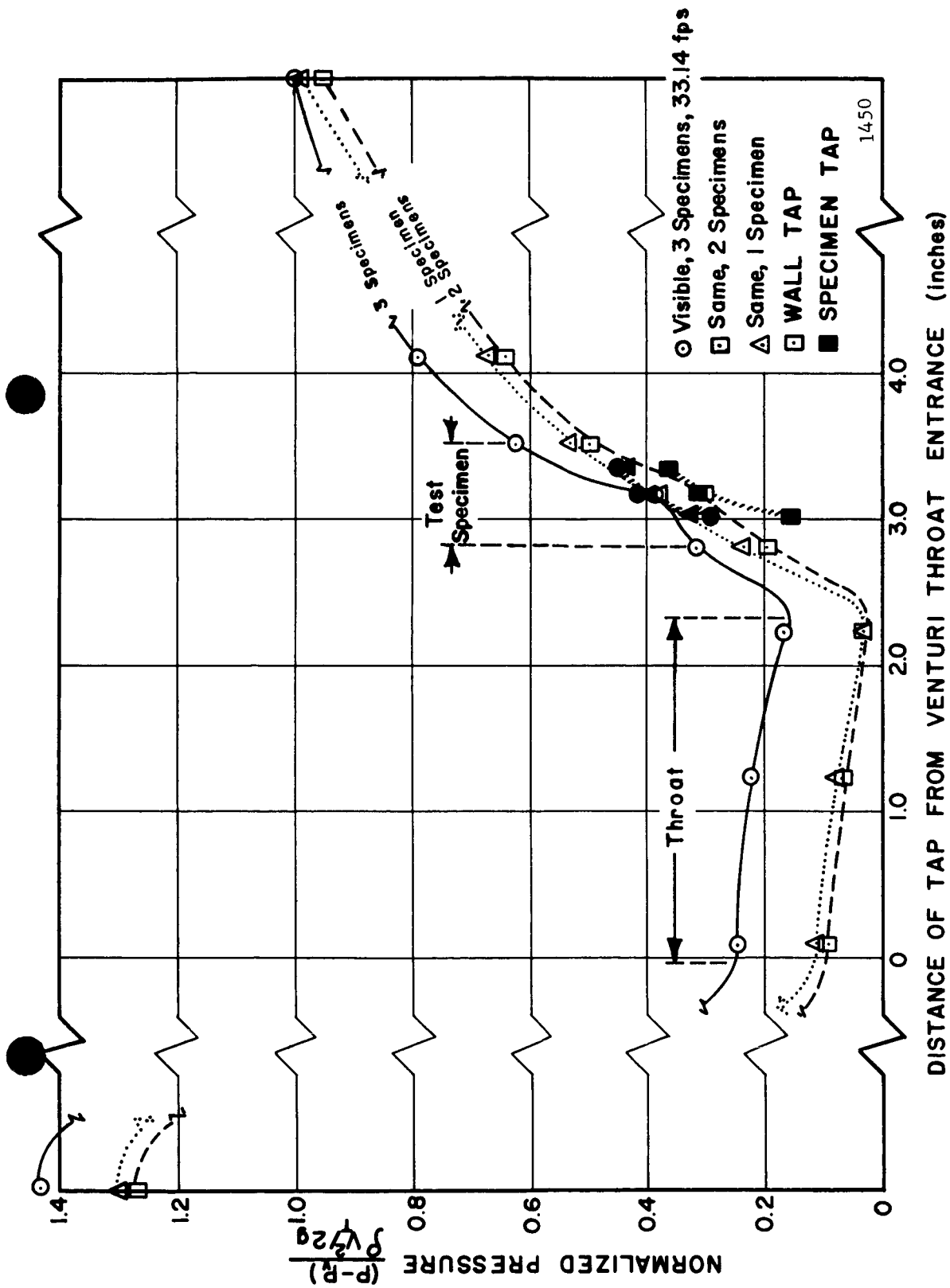


Fig. 34. Normalized Pressure Profile for Velocity of 33.1 ft/sec., for Visible Initiation in Mercury, 1, 2 and 3 Specimens.

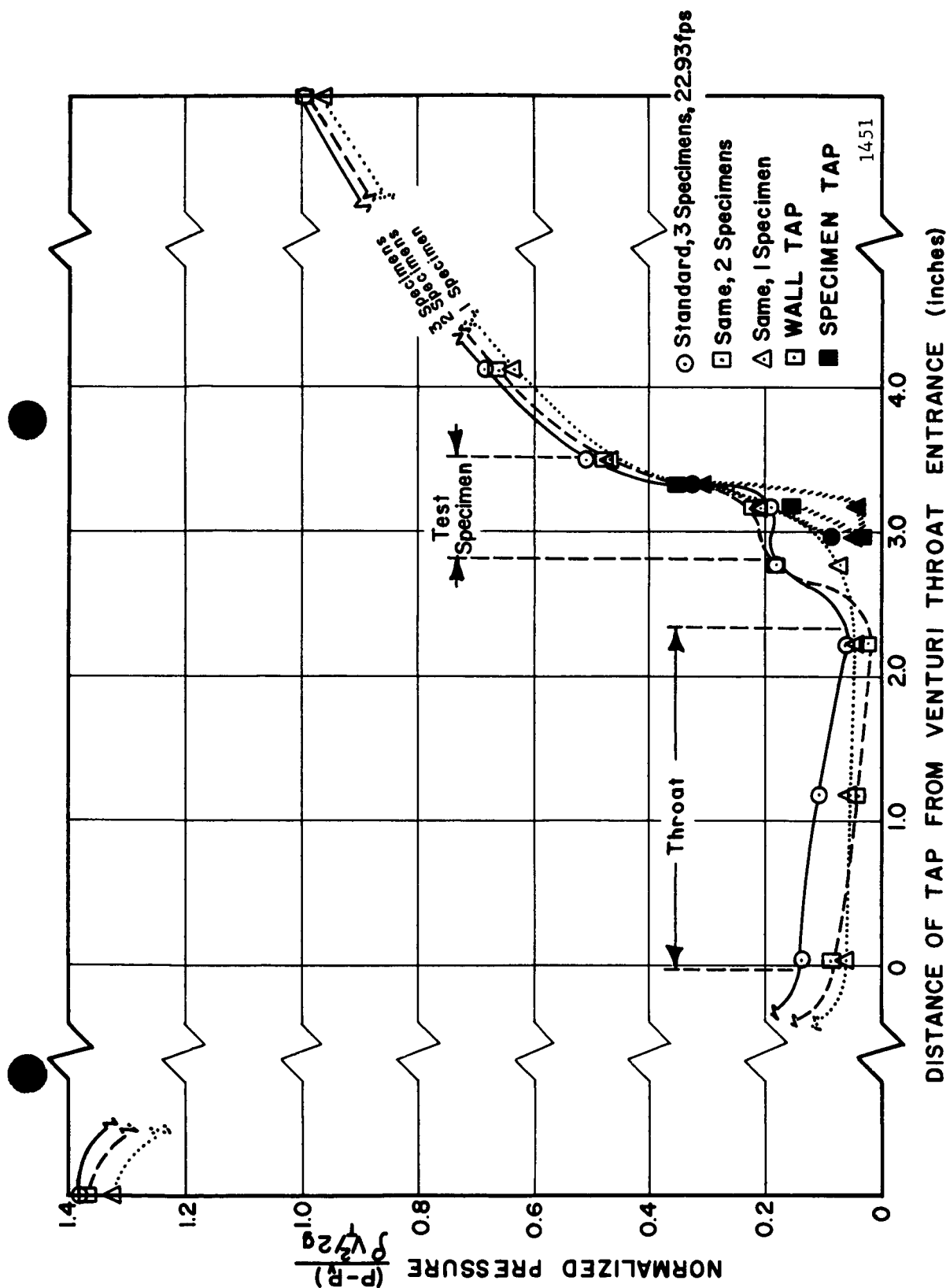


Fig. 35. Normalized Pressure Profile for Velocity of 22.9 ft/sec.,
for Standard Cavitation in Mercury, 1, 2 and 3 Specimens.

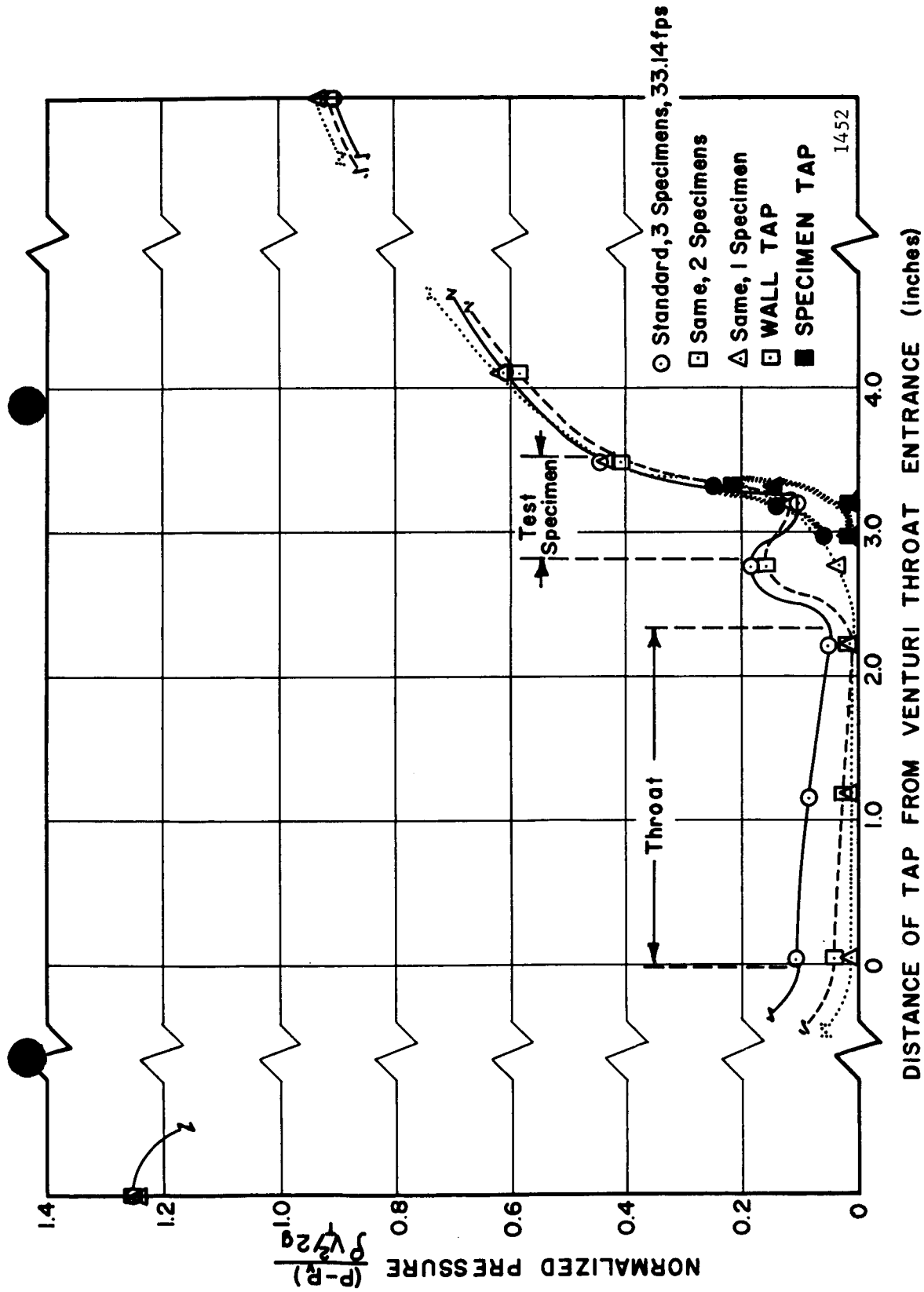


Fig. 36. Normalized Pressure Profile for Velocity of 33.1 ft/sec., for Standard Cavitation in Mercury, 1, 2 and 3 Specimens.

It is noted from Figure 29 that the maximum damage occurs with a less-developed cavitation condition for water than for mercury. An examination of comparable mercury at 33 ft./sec. and water at 97 ft./sec. pressure profiles, Figures 16 and 21 respectively, shows that the pressure gradient on the surface of the test specimens for "Standard Cavitation" in mercury is very similar to that for "Cavitation to Nose" in water, and that for "Cavitation to Back" in mercury to that for "Standard Cavitation" in water. Hence, the pressure profiles are consistent with the damage data, in this respect. This difference in behavior between mercury and water has been discussed previously¹ when less comprehensive data was available. New damage data has been consistent with the old, and the explanation can now be given.

Since the cavitation conditions are set visually, it was not certain that a given visual setting of the apparent end of the cavitation cloud in mercury, where only activity in the boundary layer can be viewed, would produce pressure profiles similar to those from the setting of apparently the same cloud termination position in water, where an averaged view through the stream is obtained. However, since the comparable pressure profiles for mercury and water, Figures 16 and 21 respectively, where the visual setting of the termination of the cavitation cloud is at the middle of the specimen (being "Standard Cavitation" for mercury and "Cavitation to Nose" for water as explained in the Appendix), show substantially the same pressure profile on the surface of the specimens, it appears that the visual settings of the termination point in mercury do correspond to those in water. Other measurements on the void fraction in the venturi in mercury¹¹ have shown that

the visual setting does indeed correspond with the centerline termination of the cavitation cloud in the venturi, thus further confirming the visual settings in mercury.

5.0 CONCLUSIONS

Many conclusions are drawn throughout the body of the report. However, those which are of greatest importance are believed to be the following:

- i) Tests with pure copper and 70/30 brass, each under three heat-treat conditions, affords a group of relatively non-corrodible materials in water which have a broad range of mechanical properties. The extreme variation in tensile strength is by a factor of about 3, and that in strain energy to failure about 9. For this group of materials in general, as strength properties increase, ductility and strain energy to failure decrease.

Since the mean depths of penetration induced by cavitation for all these materials does not differ substantially, it is apparent that high strength and low strain energy, or vice-versa, represent combinations of properties giving substantially equal resistance to cavitation damage. Hence, it is apparent that no single property can in general satisfactorily correlate cavitation damage. Rather a grouping of properties, involving at least a representative strength property, and an energy property is required.

The above conclusions are further reinforced by the facts that:

- a. Steels and refractory metals which were tested show increasing resistance to cavitation damage as either strength or

strain energy is increased. However, for the materials of these types which were tested, these properties increase together. The best curve to represent mean depth of penetration for these materials versus, e.g., strain energy, is very substantially different from that for the coppers and brasses, and also differs depending on whether the test fluid is water or mercury.

- b. Compared to steels, e.g., plexiglas is very immune from cavitation damage in water (in the present tests), but very subject to damage in mercury. Hence, damage correlating parameters must in some way consider coupling parameters between fluid and material as well as simply material parameters. The same conclusion can be drawn from the differences in behavior of steels and refractories between water and mercury mentioned under (a) above.
- ii) In the cavitating venturi arrangement used in the present tests, the mean depth of penetration rate shows an initial hump before significant damage has been suffered, and hence, before there can be significant flow perturbation. Hence, this must be a result of material surface properties and behavior as perhaps the early removal of inclusions or other "weak spots," or the incurrance of substantial surface cold-work early in the test. One or several subsequent humps in the rate curves occur after substantial damage exists to a degree which is capable of significant flow perturbation. The first of these "secondary" humps is apparently comparable to the hump already observed by

other investigators in the rate curve from either magnetostriction or rotating disc apparatuses. However, as opposed to the observations from the magnetostriction type facility, the present rate curves (from the venturi facilities) show no indication of becoming asymptotic to a fixed value.

- iii) Quantity of damage with mercury as test fluid is very sensitive to "effective" vapor pressure. It was found that mercury containing a trace of water was an order of 10 times more damaging to stainless steel than was substantially dry mercury. It is believed that the significant difference is that of vapor pressure, which can affect substantially bubble nucleation growth, and collapse. This conclusion is reinforced by the fact that a damage test with austenitic stainless steel in "dry" mercury at 500°F proved about as damaging as "wet" mercury at room temperature, and hence much more damaging than "dry" mercury at room temperature. Since the mechanical properties of austenitic stainless steel are not very greatly affected by a temperature of 500°F, it is felt that the significant change is that of vapor pressure. The vapor pressure of 500°F mercury is of the same order as that of room temperature water (and hence of room temperature "wet" mercury), whereas the vapor pressure of room temperature "dry" mercury is substantially nil.
- iv) A pin-type cavitation specimen held in the cavitating region of the venturi diffusor normal to the stream has been developed, upon which damage is incurred orders of magnitude more rapidly than upon the "conventional" plate-type specimens used hitherto. Such a specimen design would constitute a very accelerated

cavitation device, especially with "wet" mercury. In addition, it emphasizes the fact that combined vortex and translatory flows (as with the pin-type specimen) are very damaging compared with substantially translatory flow (as with the plate-type specimen). This observation also is of course verified by turbomachinery tests, or by the rotating-disc type of cavitation damage facility. It points up the possibility of modeling a given turbomachinery flow in a cavitating venturi by suitably adjusting the pressure gradient, vorticity, and velocity.

- v) Quantity of damage is not nearly so dependent upon velocity in the cavitating venturi as in other types of cavitation tests which have been reported. However, the dependence is greatest for the less fully-developed cavitation conditions, since, for these, the dependence of static pressure in the vicinity of the test specimens is the greatest.
- vi) The dependence of damage upon degree of cavitation is such that it reaches a maximum for an intermediate cavitation condition, becoming very small for either extreme, i.e., initiation or fully-developed. This observation is explained on the basis of the interplay between the number of bubbles in the vicinity of the test specimens (which increases as the cavitation becomes more fully developed) and the static pressure, which provides the driving force for collapse, and which decreases as the cavitation becomes more developed.

The maximum damage occurs for mercury for the same actual cavitation condition as defined by pressure profiles as for

water. Its relation to degree of cavitation depends also upon the number of test specimens in the venturi (since the flow pattern is so affected).

6.0 APPENDIX

The degree of cavitation terminology has somewhat different significance for mercury than for water. In the two-specimen mercury venturi,* cavitation initiates at the throat outlet for all velocities used thus far, and the degree of cavitation applied to the mercury tests describes the extent of the cavitation cloud starting at the throat outlet and extending downstream to the point indicated, i.e., "Cavitation to Nose," etc., are self-explanatory. However, in the case of the three-specimen venturis used with water, the cavitation cloud initiates on the nose of the specimens and extends downstream to some point arbitrarily labeled in terms of the degree of cavitation terminology previously established for the two-specimen venturis. The first visible manifestation of cavitation occurs on the nose of the test specimen, and thus the term Visible Initiation was applied in this case. Then succeeding degrees of cavitation followed the old progression, thus not signifying the termination point on the specimen, as previously. The following are the definitions of the degrees of cavitation as used in this investigation:

Mercury (2-Specimen Venturi)

Visible Initiation - continuous ring of cavitation at the throat outlet, about 1/8" long.

*No three-specimen venturi has been used in the mercury damage tests.

- Cavitation to Nose - cavitation cloud extends from throat outlet to termination at the nose of the specimen.
- Standard Cavitation - cavitation cloud extends from throat outlet to termination at the middle of the specimen.
- Cavitation to Back - cavitation cloud extends from throat outlet to termination at the rear of the specimen.

Water (3-Specimen Venturi)

- Visible Initiation - cavitation cloud extends from nose of specimen to a point downstream on specimen; about 1/8" long.
- Cavitation to Nose - cavitation cloud extends from nose of specimen to termination at the middle of the specimen.
- Standard Cavitation - cavitation cloud extends from nose of specimen to termination at the rear of the specimen.

From the pressure profile data in this report the correspondence between water and mercury from a standpoint of degree of cavitation should more graphically have been made as follows:

<u>Mercury Condition</u>	corresponds to	<u>Water Condition</u>
Cavitation to Nose	--	Visible Initiation
Standard Cavitation	--	Cavitation to Nose
Cavitation to Back	--	Standard Cavitation

This would result in the pressure gradients on the surfaces and the termination points on the surfaces being the same for corresponding conditions from water to mercury.

- Cavitation to Nose - cavitation cloud extends from throat outlet to termination at the nose of the specimen.
- Standard Cavitation - cavitation cloud extends from throat outlet to termination at the middle of the specimen.
- Cavitation to Back - cavitation cloud extends from throat outlet to termination at the rear of the specimen.

Water (3-Specimen Venturi)

- Visible Initiation - cavitation cloud extends from nose of specimen to a point downstream on specimen; about 1/8" long.
- Cavitation to Nose - cavitation cloud extends from nose of specimen to termination at the middle of the specimen.
- Standard Cavitation - cavitation cloud extends from nose of specimen to termination at the rear of the specimen.

From the pressure profile data in this report the correspondence between water and mercury from a standpoint of degree of cavitation should more graphically have been made as follows:

<u>Mercury Condition</u>	corresponds to	<u>Water Condition</u>
Cavitation to Nose	--	Visible Initiation
Standard Cavitation	--	Cavitation to Nose
Cavitation to Back	--	Standard Cavitation

This would result in the pressure gradients on the surfaces and the termination points on the surfaces being the same for corresponding conditions from water to mercury.

12. "Investigation of Local Fluid Flow Conditions in Cavitating Venturi Damage Tests," M. John Robinson, Thesis Investigation, Progress Report No. 1, Nuclear Engineering Department, The University of Michigan (Aug., 1964).
13. Pamphlet by United States Steel, USS 304 LN Stainless Steel, Pamphlet ADUCO 03135A-61.
14. "Cavitation Damage on Thin Foils Using an Ultrasonic Cavitation System," H. G. Olson, Thesis Investigation, Progress Report, Nuclear Engineering Department, The University of Michigan (Sept., 1964).
15. "Local Fluid Flow Conditions in Cavitating Mercury and Water Systems," M. John Robinson, Thesis Investigation, Progress Report No. 2, Nuclear Engineering Department, The University of Michigan (Sept., 1964).